

Low-order outcomes and clustered designs: combining design and analysis for causal inference under network interference

Matthew Eichhorn^{*†} Samir Khan^{*‡} Johan Ugander[‡] Christina Lee Yu[†]

July 15, 2024

Abstract

Variance reduction for causal inference in the presence of network interference is often achieved through either outcome modeling, which is typically analyzed under unit-randomized Bernoulli designs, or clustered experimental designs, which are typically analyzed without strong parametric assumptions. In this work, we study the intersection of these two approaches and consider the problem of estimation in low-order outcome models using data from a general experimental design. Our contributions are threefold. First, we present an estimator of the total treatment effect (also called the global average treatment effect) in low-order outcome models when the data are collected under general experimental designs, generalizing previous results for Bernoulli designs. We refer to this estimator as the pseudoinverse estimator and give bounds on its bias and variance in terms of properties of the experimental design. Second, we evaluate these bounds for the case of cluster randomized designs with both Bernoulli and complete randomization. For clustered Bernoulli randomization, we find that our estimator is always unbiased and that its variance scales like the smaller of the variance obtained from a low-order assumption and the variance obtained from cluster randomization, showing that combining these variance reduction strategies is preferable to using either individually. For clustered complete randomization, we find a notable bias-variance trade-off mediated by specific features of the clustering. Third, when choosing a clustered experimental design, our bounds can be used to select a clustering from a set of candidate clusterings. Across a range of graphs and clustering algorithms, we show that our method consistently selects clusterings that perform well on a range of response models, suggesting that our bounds are useful to practitioners.

1 Introduction

Standard methods for estimating causal effects from randomized experiments typically rely on the stable-unit treatment value assumption (SUTVA), which ensures that a unit’s outcome depends only on its treatment, and not the treatments of other units. A recent line of work has revisited this assumption and developed methods for estimating treatment effects while allowing for interference between units. One common approach in this line of work is to model the interference through an exposure mapping [Aronow and Samii, 2017], and then construct experimental designs that mitigate the impact of the interference [Ugander et al., 2013, Eckles et al., 2017, Holtz et al., 2024, Karrer et al., 2021, Li et al., 2022]. Another common approach is to specify a parametric outcome model that captures the interference, and then estimate causal effects as functions of the model

^{*}Equal contribution. Please direct correspondence to meichhorn@cornell.edu and samirk@stanford.edu.

[†]Cornell University, Center for Applied Math and Department of Operations Research and Information Engineering

[‡]Stanford University, Department of Statistics and Department of Management Science and Engineering

parameters [Toulis and Kao, 2013, Cai et al., 2015, Basse and Airoidi, 2018b, Chin, 2019, Cortez-Rodriguez et al., 2023]. In this paper we focus on the intersection of these two approaches, the analysis of estimators based on well-specified outcome models with data collected from complex experimental designs, which has received comparatively less attention in the literature.

We assume the interference has a network structure, in which an underlying graph dictates the extent of the spillovers in treatment. We take as a starting point the work of Cortez et al. [2022], Cortez-Rodriguez et al. [2023] introducing the low-order interaction model for network interference, which requires that if a unit’s outcome depends on the treatment status of neighbors, it does so in a way that is linear in the treatment status of only small subsets of neighbors. Cortez-Rodriguez et al. [2023] study the problem of estimating the parameters of this model using data collected under Bernoulli designs, in which each unit i is assigned to treatment independently with probability p_i . We go beyond their setting and study the problem of estimating the parameters of a low-order interaction model using data collected under graph cluster randomized (GCR) designs [Ugander et al., 2013]. These designs partition the units into clusters based on the underlying interference graph, and then assign treatments at the cluster level rather than the individual level. This increases the probability of a unit and its neighbors being treated together, which reduces the variance of treatment effect estimators under a neighborhood exposure assumption.

Our setting raises a number of questions both narrow and broad. How do we estimate the model parameters from cluster-randomized data? What are the bias and variance properties of the resulting estimators? If we are in the position of designing the cluster-randomized experiment, how should we select the clustering? More generally, is there value in using both a complex outcome model and a complex experimental design, or is using either one alone sufficient to handle interference effectively? In this paper, we answer all of these questions by developing a general theory for estimation in the low-order interaction model using data collected from an arbitrary experimental design, and then instantiating this theory for the case of graph cluster randomized (GCR) designs under both Bernoulli and complete randomization.

1.1 Summary Of Results

As mentioned above, we present both general theory on estimation under arbitrary experimental designs as well as specific results for GCR designs; we summarize each of these in turn.

Pseudoinverse estimators. We introduce an estimator of the total treatment effect (or global average treatment effect) in the low-order outcome model of Cortez-Rodriguez et al. [2023] that uses data collected under arbitrary experimental designs, which we refer to as the pseudoinverse estimator. We give bounds on the bias and variance of this estimator in terms of the experimental design, and these bounds can be evaluated even with only sampling access to the design. As a first application, we use these bounds to extend the results of Cortez-Rodriguez et al. [2023] to completely randomized designs.

Bernoulli GCR designs. Next, we compute bounds on the bias and variance of the pseudoinverse estimators for Bernoulli randomized GCR designs. We find that the pseudoinverse estimator is unbiased and that the variance scales like the lesser of the variance obtained using a GCR design with a naïve estimator and the variance obtained using a low-order outcome model with a naïve design. This scaling demonstrates a subtle interplay between design and estimator that has not been previously observed in the literature. As an application, we show that the scaling of the vari-

Design	Bias	Variance	
		$\beta = 1$ (low-order)	$\beta = d_{\max}$ (full-order)
Bern(p)	0 (unbiased)	$O(\text{poly}(d_{\max})/n)$	$O(\exp(d_{\max})/n)$
Comp(k)	$O(\#\{i : d_i = n\}/n)$	$O(\text{poly}(d_{\max})/n)$	—
GCR _{Bern} (\mathcal{C}, p)	0 (unbiased)	$O(\text{poly}(d_{\max}, \kappa)/n)$	$O(\text{poly}(d_{\max}) \exp(\kappa)/n)$
GCR _{Comp} (\mathcal{C}, k_c)	$O(\#\{i : \mathcal{C}(\mathcal{N}_i) = m\}/n)$	$O(\text{poly}(d_{\max}, \kappa)/n)$	—

Table 1: Summary of our theoretical results on the bias and variance of our proposed estimator, with results from prior work shaded in light gray. See Section 2 for details on notation. The key points are that our estimator is unbiased when Bernoulli randomizing but potentially biased when completely randomizing, has variance polynomial in both κ and d_{\max} when assuming a low-order model and cluster randomizing, and has the same variance behavior when completely randomizing as when Bernoulli randomizing.

ance of an appropriate pseudoinverse estimator in this setting is more favorable than the scaling of the variance of the Horvitz–Thompson estimator derived by Ugander et al. [2013].

Complete GCR designs. In settings with a small number of clusters, it is preferable to completely randomize cluster treatments rather than Bernoulli randomize, since this avoids the possibility of having no treated or no control units. We derive the pseudoinverse estimator for this setting and show that, unlike in the Bernoulli case, it exhibits a bias-variance trade-off that is mediated by properties of the clustering. The relevant feature of the clustering is the number of nodes that have an in-neighbor in every cluster; as the number of such nodes increases, the variance decreases at the cost of increased bias. This bias-variance trade-off is unusual in that it is not controlled by a parameter of the estimator but by the experimental design itself.

Design of clustered experiments. Finally, we consider the practical problem of designing an experiment when we know the pseudoinverse estimator will be used for the downstream analysis. We propose selecting a clustering for a GCR experiment by minimizing an upper bound on the mean-squared-error formed by combining our bias and variance bounds. Such a choice has favorable behavior in simulation across a range of response models, graphs, and clustering algorithms.

A summary of our theoretical results is shown in Table 1, with results from prior work shaded in light gray. In this table, we see that:

- (i) our estimator is unbiased when treatments are Bernoulli randomized but potentially biased when treatments are completely randomized;
- (ii) cluster randomization together with a low-order assumption replaces an exponential dependence on κ in the variance of our estimator with a polynomial dependence on κ (relative to cluster randomization without a low-order model) and polynomial factors of d_{\max} in the variance of our estimator with polynomial factors of κ , which are always smaller (relative to low-order modeling without cluster randomization);

(iii) results on the variance of our estimator under Bernoulli randomization can be extended to complete randomization as well.

As a whole, our work both develops the foundation for analysis of the low-order model under arbitrary experimental designs and provides a detailed example of such an analysis for graph cluster randomized designs.

1.2 Related Work

The problem of causal estimation under fully general interference is known to be intractable [Basse and Airoldi, 2018a], and so the literature contains many different assumptions that aim to make the problem more tractable. In this section, we survey several strands of work that either make similar assumptions to ours or study similar problems.

Neighborhood exposure mappings. Exposure mappings, first introduced by Aronow and Samii [2017] but closely related to earlier work on “effective treatments” [Manski, 2013], specify exactly which treatment assignments impact the outcome of a unit. We follow much of the existing network interference literature in making a neighborhood exposure mapping assumption [Ugander et al., 2013, Eckles et al., 2017, Sussman and Airoldi, 2017, Chin, 2019, Bargagli-Stoffi et al., 2020], in which the outcome of an individual depends only on the treatment assignments within their local neighborhood in an interference graph. More specifically, we make what is known as a neighborhood treatment response assumption, in which an individual responds to global treatment the same way they would to all of their neighbors being treated (see Assumption 1 for an exact statement). This differs from other work making a fractional neighborhood treatment response assumption, in which an individual responds as they would to global treatment once a certain fraction of their neighbors are treated, such as Eckles et al. [2017] or Holtz and Aral [2020].

Graph structure assumptions. Even under a neighborhood exposure assumption, the set of possible outcomes is exponential in the size of the neighborhood, meaning that naïvely running a Bernoulli design and using the Horvitz–Thompson estimator [Horvitz and Thompson, 1952] will lead to a variance that scales with the maximum degree in the interference graph. As such, it is standard in the network interference setting to assume that this maximum degree is bounded [Ugander et al., 2013, Ugander and Yin, 2023, Cortez-Rodriguez et al., 2023], an assumption we make in most of our bounds as well.

Going beyond Bernoulli designs, one approach to variance reduction is to use a graph cluster randomized design [Ugander et al., 2013], which lowers the variance of the Horvitz–Thompson estimator under appropriate assumptions on the clustering and graph. For example, the results of Ugander et al. [2013] assume that the graph satisfies κ -restricted growth, meaning that the neighborhoods of a node increase in size by at most a multiplicative factor of κ as their width increases. Thus a node has at most d_{\max} nodes in its neighborhood, at most $d_{\max}\kappa$ nodes in its 2-neighborhood, and so on. When analyzing graph cluster randomized designs in Section 5, we will also make such κ -restricted growth assumptions. We remark that the κ -restricted growth assumption is closely related to certain assumptions made by Leung [2022a]. In particular, κ -restricted growth implies the exponential growth rate condition given in (18) of Leung [2022a] with $C = d_{\max}$ and $\beta = \log \kappa$, and Leung [2022a] show that this condition (together with appropriate corresponding conditions on the interference) is sufficient to obtain a central limit theorem for their proposed estimator. The common idea between Ugander et al. [2013], Leung [2022a], and the

present work is to use growth rate conditions to control the size of neighborhoods in the graph, and thus bound the amount of interference.

Lastly, in a different kind of assumption on the graph structure, Li and Wager [2022] assume the graph is sampled from a graphon, and derive asymptotics under this assumption. Such assumptions are not necessary in our work since we do not work in a large sample limit, but deriving central limit theorems for our estimators under such assumptions is a promising area for future work.

Outcome model assumptions. Rather than positing assumptions on the graph structure and constructing experimental designs to exploit them, another line of work instead makes assumptions on the structure of the potential outcomes that go beyond the neighborhood exposure assumption.

A common paradigm across much of this work is to assume that the potential outcomes are linear in an individual’s own treatment and some simple statistics of the treatment assignments of their neighbors such as the number or proportion of treated neighbors [Toulis and Kao, 2013, Gui et al., 2015, Parker et al., 2017, Holtz et al., 2024], or linear in engineered features of the treatment assignments [Chin, 2019, Han and Ugander, 2023]. In all of this work, the number of model parameters is less than the number of individuals, and so standard regression-based techniques for parameter estimation are applicable.

In contrast, the recent work by Yu et al. [2022], Cortez et al. [2022], Cortez-Rodriguez et al. [2023] that we build on also assumes a parametric model for the potential outcomes, but allows the number of model parameters to potentially exceed the number of observations, making regression-based estimators infeasible. That work instead assumes that the order of interactions present between units is bounded, enabling parameter estimation and allowing for variance bounds that scale polynomially in the graph degree (rather than exponentially). This setting, in which the potential outcome functions are confined to a function space without rendering the problem fully parametric, is also the setting of Harshaw et al. [2022], who propose the so-called Riesz estimators. Indeed, Cortez-Rodriguez et al. [2023] show that their estimator is an example of a Riesz estimator.

Monotonicity assumptions. When deriving our bounds, we will sometimes rely on monotonicity assumptions, which ensure that the sign of the treatment effect is the same for all individuals (see Assumptions 4 and 5 for precise statements). These assumptions are natural in the network interference setting, where we expect that if a treatment has a positive effect on one unit, that same positive effect will spillover to the unit’s neighbors, and are also common in the literature. For example, Eckles et al. [2017] use such an assumption to prove bias reduction results that are generalized by Holtz et al. [2024] under similar monotonicity assumptions. Such assumptions can also be used to facilitate estimation, as in Choi [2017], or to facilitate experimental design, as in Pouget-Abadie et al. [2018].

Design of clustered experiments. In Section 7.2 we show how our bounds can be used to inform the choice of clustering in a graph cluster randomized experiment. The problem of designing the clustering in a GCR experiment has also been considered by Leung [2022b], who calculate the optimal number of square clusters in a spatial experiment as a function of the rate of decay of the interference. This spatial decay model is also studied by Leung [2023], who give results on the number of clusters that should be used for a particular downstream estimator that drops certain units on the boundaries of the clusters.

For the more general problem of optimizing over the space of all clusterings, Viviano et al. [2023]

develop an algorithm for constructing a clustering to minimize an upper bound on the mean-squared-error in a GCR experiment. The key difference between our work and theirs is the choice of estimator: Viviano et al. [2023] study a modification of the difference-in-means estimator that is a sum of independent terms, and thus more straightforward to analyze. In contrast, because it assumes and exploits a low-order outcome model, our estimator is a sum of dependent terms, and much of our effort focuses on controlling this dependence. Understanding the differences between the clusterings preferred by the bound of Viviano et al. [2023] and the clusterings preferred by our bounds is an interesting future direction that would further explore the relationship between designs and estimators for causal inference under interference.

Finally, in a different vein, Candogan et al. [2023] consider correlating the treatment assignments between clusters to achieve nearly equal numbers of treated and control units. We do not consider such designs in this work, but our methods and bounds extend readily, and could be used to obtain new results for such correlated designs.

2 Set-up and Notation

In this section we introduce our notation, the class of outcome models we consider, the target estimand, and the experimental designs of interest to us.

We consider a population of n individuals, denoted $[n]$, each of whom is assigned a binary treatment $z_i \in \{0, 1\}$. We interpret $z_i = 0$ as an assignment of i to the control group and $z_i = 1$ as an assignment of i to the treatment group. We collect these treatments into vector $\mathbf{z} = (z_1, \dots, z_n)$. After the treatments have been assigned, we measure outcomes Y_i , which may depend on the treatment assignments of other individuals due to interference. Thus each Y_i can be naturally encoded as a function $Y_i: \{0, 1\}^n \rightarrow \mathbb{R}$. We assume a design-based framework in which these functions Y_i are deterministic, so that the only randomness in the problem is in the distribution of \mathbf{z} . As such, all expectations we take are with respect to the distribution \mathbf{z} , which is specified where necessary.

2.1 Low-order Outcome Models

We now turn to our outcome model of interest, which is the low-order model of Cortez-Rodriguez et al. [2023]. This model is characterized by two assumptions, which we introduce below. For the remainder of the paper, we will always assume that Assumption 1 and 2 hold without explicit statement.

For the first assumption, we will suppose that the interference can be modeled by a directed graph G in which the edge (j, i) indicates that the treatment of individual j has an effect on the outcome of individual i . For individual i , we let \mathcal{N}_i represent the in-neighborhood of i in this graph (which includes individual i itself, since the treatment of individual i certainly affects its outcome).

Assumption 1 (Neighborhood interference). If treatment vectors \mathbf{z} and \mathbf{z}' are such that $z_j = z'_j$ for all $j \in \mathcal{N}_i$, then $Y_i(\mathbf{z}) = Y_i(\mathbf{z}')$.

Assumption 1 corresponds to a common choice of exposure mapping [Aronow and Samii, 2017] that is often referred to as *neighborhood interference*. Our bounds are often stated in terms of the degrees $d_i = |\mathcal{N}_i|$ of these in-neighborhoods. In particular, we use $d_{\max} = \max_i d_i$ to denote the maximum degree, which we assume to be a fixed constant that does not depend on n .

Using Assumption 1 along with the fact that each $z_i \in \{0, 1\}$, we can (without loss of generality) represent Y_i as a polynomial,

$$\begin{aligned} Y_i(\mathbf{z}) &= \sum_{T \subseteq \mathcal{N}_i} a_{i,T} \mathbb{I}(z_j = 1 \text{ for all } j \in T, z_j = 0 \text{ for all } j \notin T) \\ &= \sum_{T \subseteq \mathcal{N}_i} a_{i,T} \prod_{j \in T} z_j \prod_{j' \in \mathcal{N}_i \setminus T} (1 - z_{j'}). \end{aligned} \quad (1)$$

Here, $a_{i,T}$ is a parameter that captures the contribution to i 's outcome when the individuals in T within its neighborhood are treated and the individuals in $\mathcal{N}_i \setminus T$ are not treated.

Following Cortez-Rodriguez et al. [2023], we reparametrize this polynomial representation of Y_i in terms of the additive treatment effect on individual i from each subset of their neighborhood that is completely treated, regardless of the treatment assignments of its other neighbors. This corresponds to writing

$$Y_i(\mathbf{z}) = \sum_{S \subseteq \mathcal{N}_i} c_{i,S} \mathbb{I}(z_j = 1 \text{ for all } j \in S) = \sum_{S \subseteq \mathcal{N}_i} c_{i,S} \prod_{j \in S} z_j, \quad (2)$$

and is a transformation of (1) to the monomial polynomial basis, with the exact mapping between coefficients given by

$$c_{i,S} = \sum_{T \subseteq S} (-1)^{|S \setminus T|} \cdot a_{i,T}.$$

With this representation of Y_i in hand, we introduce our next assumption, which is the central assumption of the low-order model.

Assumption 2 (Order- β interactions). We have $c_{i,S} = 0$ whenever $|S| > \beta$.

In Assumption 2, we assume that only sufficiently small subsets of an individual's neighborhood can have an additive effect on their outcome. The parameter β represents the maximum possible size of such a subset and so, under this assumption, the outcome model (2) simplifies to

$$Y_i(\mathbf{z}) = \sum_{\substack{S \subseteq \mathcal{N}_i \\ |S| \leq \beta}} c_{i,S} \prod_{j \in S} z_j =: \sum_{S \in \mathcal{S}_i^\beta} c_{i,S} \prod_{j \in S} z_j. \quad (3)$$

Here we write \mathcal{S}_i^β to represent the set of all subsets of \mathcal{N}_i with size at most β . Note that the empty set always belongs to \mathcal{S}_i^β and its corresponding coefficient $c_{i,\emptyset}$ is the observed outcome under global control, i.e., $c_{i,\emptyset} = Y_i(\mathbf{0})$.

The parameter β controls the complexity of the model: $\beta = 1$ corresponds to a heterogeneous linear potential outcomes model [Yu et al., 2022], and $\beta = d_{\max}$ corresponds to fully general network interference.

In what follows, we let $\tilde{\mathbf{z}}_i$ be the vector indexed by $S \in \mathcal{S}_i^\beta$ (in some canonical order with \emptyset in the first position) with entries $(\tilde{\mathbf{z}}_i)_S = \prod_{j \in S} z_j$. We similarly collect the model coefficients $c_{i,S}$ into a vector \mathbf{c}_i , where $(\mathbf{c}_i)_S = c_{i,S}$. In this notation, we have that

$$Y_i(\mathbf{z}) = \langle \tilde{\mathbf{z}}_i, \mathbf{c}_i \rangle.$$

Throughout the paper, we use both $\langle v, w \rangle$ and $v^\top w$ to denote the standard Euclidean inner product of v and w .

2.2 Total Treatment Effect

Our causal estimand of interest is the *total treatment effect* (otherwise referred to as the *global average treatment effect* or GATE),

$$\text{TTE} = \frac{1}{n} \sum_{i=1}^n \left(Y_i(\mathbf{1}) - Y_i(\mathbf{0}) \right),$$

the average difference between an individual’s outcome under global treatment and their outcome under global control. Under Assumptions 1 and 2, we can use the representation of Y_i given in (3) to express the total treatment effect in terms of the coefficients $c_{i,S}$:

$$\text{TTE} = \frac{1}{n} \sum_{i=1}^n \sum_{\substack{S \in \mathcal{S}_i^\beta \\ S \neq \emptyset}} c_{i,S} = \frac{1}{n} \sum_{i=1}^n \langle \theta_i, \mathbf{c}_i \rangle, \quad (4)$$

where we define $\theta_i = [0 \ 1 \ \dots \ 1]^\top$ to be the length- $|\mathcal{S}_i^\beta|$ column vector with 0 in its first entry (corresponding to $S = \emptyset$) and 1 in all other entries.

Some of our bounds require further assumptions on the \mathbf{c}_i . The first of these is a standard boundedness assumption, which is analogous to an assumption on the boundedness of $Y_i(\mathbf{0})$ and $Y_i(\mathbf{1})$ in a standard potential outcomes model without interference.

Assumption 3 (Bounded outcomes). We have $\|\mathbf{c}_i\|_2 \leq B$ for all $i \in [n]$.

Next, our analysis sometimes leverages one of the following monotonicity assumptions in the treatment effects.

Assumption 4 (Weak monotonicity). The sign of $\langle \mathbf{c}_i, \theta_i \rangle$ is constant across i .

Assumption 5 (Strong monotonicity). The sign of $c_{i,S}$ is constant across all i and $S \subseteq \mathcal{S}_i^\beta$.

Assumption 4 requires that the sign of the effect of the treatment is the same for each individual. That is, the treatment does not help some individuals and harm others. This assumption is used to establish our main variance bound for our estimator (Theorem 2). In contrast, the stronger Assumption 5 requires that the sign of the effect of each treated subset on an individual is the same for each subset and individual, which implies Assumption 4, and also precludes the possibility of “cancellation” between interference effects. This will be crucial for our analysis of the correlation structure of the entries of $\tilde{\mathbf{z}}_i$ under completely randomized designs (Lemma 5). As discussed in Section 1.2, such monotonicity assumptions are common in the interference literature.

We remark that although we focus on the TTE in this work, we expect that our results extend to other causal estimands, such as the direct or indirect effects of Hu et al. [2022], that can be written as linear combinations of the \mathbf{c}_i . That is to say, our results do not rely at all on the particular form of θ_i —if we were interested in $\langle v, \mathbf{c}_i \rangle$ for some other vector v , our analysis would go through identically with θ_i replaced by v , and we would obtain similar estimators and bounds.

2.3 Experimental Designs

The designs that we consider in this paper can be characterized by two features: whether treatment is assigned at the individual level or the cluster level, and whether the treatments are Bernoulli

		Randomization Mechanism	
		Bernoulli	Complete
Treatment Granularity	Unit	$\mathbf{z} \sim \text{Bern}(p)$	$\mathbf{z} \sim \text{Comp}(k)$
	Cluster	$\mathbf{z} \sim \text{GCR}_{\text{Bern}}(\mathcal{C}, p)$	$\mathbf{z} \sim \text{GCR}_{\text{Comp}}(\mathcal{C}, k_c)$

Table 2: Notation for each of the four designs we consider. Note that the designs in the first row can be recovered from the designs in the second row by setting \mathcal{C} to be the singleton clustering.

randomized or completely randomized. We now describe these in greater detail and introduce appropriate notation. To unify notation between the individually randomized and cluster randomized cases, we introduce a set of $m \leq n$ random treatment decisions $\mathbf{w} \in \{0, 1\}^m$ and write the unit-level treatments z_i as a function of \mathbf{w} .

Treatment Granularity. The level at which treatments are assigned.

- Under *unit randomization*, we have $m = n$ and $z_i = w_i$ for each $i \in [n]$, so that each unit is assigned to treatment or control individually.
- Under *graph cluster randomization* (GCR), we first fix a clustering \mathcal{C} of the individuals, which partitions the units into a set of m clusters $\mathcal{C} = \{C_1, \dots, C_m\}$ with each $C_j \subseteq [n]$. Then, we set $z_i = w_{\mathcal{C}(i)}$ where $\mathcal{C}(i)$ is the cluster containing individual i . That is, a unit inherits the treatment of the cluster that contains it.

Randomization Mechanism. The joint distribution of the entries of \mathbf{w} . We again consider two possibilities:

- In a *Bernoulli randomization* (abbreviated “Bern”), the treatment decisions w_j are independent $\text{Bern}(p)$ for some marginal treatment probability p .
- In a *completely randomized design* (abbreviated “Comp”), a uniform random subset $S \subseteq [m]$ with $|S| = k$ (for some $0 < k < m$) is selected, and we set $w_j = \mathbb{I}(j \in S)$ for each $j \in [m]$. Equivalently, we sample the k treated entries of \mathbf{w} without replacement from $[m]$.

Fixing both of these attributes gives four possible randomized designs. Throughout the paper, we shorthand these designs using the notation in Table 2.

2.4 Estimators

We focus mainly on two estimators: the first is the pseudoinverse estimator for low-order outcome models, which we introduce in Section 3. The second, which we take as a baseline over which we improve, is the Horvitz-Thompson estimator [Horvitz and Thompson, 1952], which is an inverse-probability-weighted estimator for the total treatment effect given by

$$\widehat{\text{TTE}}_{\text{HT}} = \frac{1}{n} \sum_{i=1}^n Y_i(\mathbf{z}) \left[\frac{\mathbb{I}(\bigcap_{j \in \mathcal{N}_i} z_j = 1)}{\Pr(\bigcap_{j \in \mathcal{N}_i} z_j = 1)} - \frac{\mathbb{I}(\bigcap_{j \in \mathcal{N}_i} z_j = 0)}{\Pr(\bigcap_{j \in \mathcal{N}_i} z_j = 0)} \right]. \quad (5)$$

This estimator is unbiased whenever Assumption 1 (neighborhood interference) is satisfied, although

may have prohibitively large variance when the exposure probabilities $\Pr(\bigcap_{j \in \mathcal{N}_i} z_j = 1)$ are small [Ugander et al., 2013].

3 The Pseudoinverse Estimator

In this section, we introduce the *pseudoinverse estimator* for the TTE, which depends on the order parameter β as well as the β^{th} -moments of the design. For a particular choice of design and order, the resulting estimator targets the TTE in an order- β model using data collected under the specified design, thus generalizing the estimator of Cortez-Rodriguez et al. [2023] beyond unit-randomized designs. We also provide bounds on the bias and variance of this estimator for general experimental designs, and in later sections we will specialize these results to particular experimental designs.

We motivate this estimator through the lens of least squares regression and establish some preliminary properties about its bias and variance.

3.1 Deriving the Pseudoinverse Estimator

Recall from Section 2.2 that, in an order- β outcome model, the total treatment effect is a linear combination of the effect coefficients $c_{i,S}$. Thus, to estimate the TTE, it is natural to consider an approach employing good estimators for each \mathbf{c}_i , which we can then extend by linearity to a good estimator for the TTE. We restrict our attention to estimating \mathbf{c}_i for an arbitrary $i \in [n]$. To motivate our estimator for \mathbf{c}_i , we consider a hypothetical setting where we can independently carry out our randomized experiment R times, and reason analogously to the motivation given in Section 4.1 of Cortez-Rodriguez et al. [2023].

In each replication, $r \in [R]$, we sample a treatment vector \mathbf{z}^r according to the randomized design, which induces the vector $\tilde{\mathbf{z}}_i^r$ indicating the complete treatment of each subset $S \in \mathcal{S}_i^\beta$. We also observe the outcome $Y_i(\mathbf{z}^r)$ of unit i . From this information, we can write the linear system

$$\underbrace{\begin{bmatrix} Y_i(\mathbf{z}^1) \\ Y_i(\mathbf{z}^2) \\ \vdots \\ Y_i(\mathbf{z}^R) \end{bmatrix}}_{\mathbf{Y}_i^R} = \underbrace{\begin{bmatrix} -(\tilde{\mathbf{z}}_i^1)^\top & - \\ -(\tilde{\mathbf{z}}_i^2)^\top & - \\ \vdots & \vdots \\ -(\tilde{\mathbf{z}}_i^R)^\top & - \end{bmatrix}}_{\tilde{\mathbf{Z}}_i^R} \begin{bmatrix} | \\ | \\ | \\ | \end{bmatrix} \mathbf{c}_i.$$

Suppose that we multiply both sides of this system by $\frac{1}{R}(\tilde{\mathbf{Z}}_i^R)^\top$. Then, by the strong law of large numbers, the left side would be

$$\frac{1}{R}(\tilde{\mathbf{Z}}_i^R)^\top \mathbf{Y}_i^R = \frac{1}{R} \sum_{r=1}^R Y_i(\mathbf{z}^r) \tilde{\mathbf{z}}_i^r \xrightarrow{a.s.} \mathbb{E}_{\mathbf{z}} [Y_i(\mathbf{z}) \tilde{\mathbf{z}}_i]$$

Similarly the right side would be

$$\left(\frac{1}{R}(\tilde{\mathbf{Z}}_i^R)^\top \tilde{\mathbf{Z}}_i^R \right)_{S,T} = \frac{1}{R} \sum_{i=1}^R (\tilde{\mathbf{z}}_i^r)_S (\tilde{\mathbf{z}}_i^r)_T \xrightarrow{a.s.} \mathbb{E} [(\tilde{\mathbf{z}}_i \tilde{\mathbf{z}}_i^\top)_{S,T}],$$

for each $S, T \in \mathcal{S}_i^\beta$, which we abbreviate by the notation

$$\frac{1}{R}(\tilde{\mathbf{Z}}_i^R)^\top \tilde{\mathbf{Z}}_i^R \xrightarrow{a.s.} \mathbb{E} [\tilde{\mathbf{z}}_i \tilde{\mathbf{z}}_i^\top].$$

Thus, in the limit as $R \rightarrow \infty$, we arrive at the equation

$$\mathbb{E} [Y_i(\mathbf{z})\tilde{\mathbf{z}}_i] = \mathbb{E} [\tilde{\mathbf{z}}_i\tilde{\mathbf{z}}_i^\top] \mathbf{c}_i. \quad (6)$$

The matrix $\mathbb{E} [\tilde{\mathbf{z}}_i\tilde{\mathbf{z}}_i^\top]$ has entries that are functions only of the experimental design. As such, we refer to it as the *design matrix*, and often denote it by M_i . Note that the design matrix is not data-dependent and can be computed by the practitioner given the exact distribution of \mathbf{z} , or approximated to arbitrary precision given sampling access to the distribution of \mathbf{z} (see Appendix E for details). From here, we consider two possibilities.

Case 1: First, suppose that the design matrix is invertible, as was shown for unit randomized designs by Cortez-Rodriguez et al. [2023]. Then we can rearrange (6) to solve for \mathbf{c}_i :

$$\mathbf{c}_i = \mathbb{E} [\tilde{\mathbf{z}}_i\tilde{\mathbf{z}}_i^\top]^{-1} \mathbb{E} [Y_i(\mathbf{z})\tilde{\mathbf{z}}_i].$$

By approximating this latter expectation by its experimental realization, we obtain the estimator

$$\hat{\mathbf{c}}_i := Y_i(\mathbf{z}) \mathbb{E} [\tilde{\mathbf{z}}_i\tilde{\mathbf{z}}_i^\top]^{-1} \tilde{\mathbf{z}}_i,$$

which is unbiased by linearity. The core ideas in this case —deriving a system of unbiasedness equations whose solution identifies an estimator— are akin to those of Harshaw et al. [2022], and we expect that our estimator coincides with the Riesz estimator whenever the design matrix is invertible just as it does for Bernoulli designs [Cortez-Rodriguez et al., 2023].

Case 2: Alternatively, suppose that the design matrix is not invertible. This can be the case in cluster-randomized designs, as the rank of the design matrix is limited to the number of subsets of at most β clusters, which can be significantly smaller than $|\mathcal{S}_i^\beta|$. In this case, the system of equations given by (6) is underdetermined, and we can use the Moore-Penrose pseudoinverse to obtain the minimum ℓ^2 -norm solution

$$\hat{\mathbf{c}}_i = \mathbb{E} [\tilde{\mathbf{z}}_i\tilde{\mathbf{z}}_i^\top]^\dagger \mathbb{E} [Y_i(\mathbf{z})\tilde{\mathbf{z}}_i].$$

Using the same reasoning as in Case 1, we obtain an estimator \mathbf{c}_i by replacing the second expectation by the single observation:

$$\hat{\mathbf{c}}_i := Y_i(\mathbf{z}) \mathbb{E} [\tilde{\mathbf{z}}_i\tilde{\mathbf{z}}_i^\top]^\dagger \tilde{\mathbf{z}}_i.$$

Note that this estimator subsumes the estimator from Case 1, so we utilize this form throughout the rest of the paper.

Now, substituting the estimated $\hat{\mathbf{c}}_i$ for each i into (4), we obtain an estimator for the total treatment effect:

$$\widehat{\text{TTE}} := \frac{1}{n} \sum_{i=1}^n \sum_{\substack{S \in \mathcal{S}_i^\beta \\ S \neq \emptyset}} (\hat{\mathbf{c}}_i)_S = \frac{1}{n} \sum_{i=1}^n \langle \theta_i, \hat{\mathbf{c}}_i \rangle = \frac{1}{n} \sum_{i=1}^n Y_i(\mathbf{z}) \langle \mathbb{E} [\tilde{\mathbf{z}}_i\tilde{\mathbf{z}}_i^\top]^\dagger \theta_i, \tilde{\mathbf{z}}_i \rangle, \quad (7)$$

where θ_i is the vector with $(\theta_i)_\emptyset = 0$ and with all other entries $(\theta_i)_S = 1$. We refer to (7) as the *pseudoinverse estimator* for the TTE.

We remark that the form of this estimator was identified by Cortez-Rodriguez et al. [2023] for the invertible case, but not evaluated or analyzed for any design other than unit-level Bernoulli randomization. In contrast, we handle both the invertible and non-invertible cases and derive new results for more complex designs in both cases.

3.2 Bias

In this section, we present bounds on the bias of $\widehat{\text{TTE}}$ as a function of the experimental design and use these bounds to identify conditions under which $\widehat{\text{TTE}}$ is unbiased. Our analysis of the bias leads to the following theorem. Proofs from this section appear in Appendix A.

Theorem 1. *The bias of $\widehat{\text{TTE}}$ satisfies the following:*

(a) *the exact bias is*

$$\mathbb{E}[\widehat{\text{TTE}}] - \text{TTE} = \frac{1}{n} \sum_{i=1}^n \mathbf{c}_i^\top (M_i^\dagger M_i - I) \theta_i, \quad (8)$$

where $M_i = \mathbb{E}[\tilde{\mathbf{z}}_i \tilde{\mathbf{z}}_i^\top]$;

(b) *if Assumption 3 holds, so that $\|\mathbf{c}_i\|_2 \leq B$, we have the bias upper bound*

$$|\mathbb{E}[\widehat{\text{TTE}}] - \text{TTE}| \leq \frac{B}{n} \sum_{i=1}^n \|(M_i^\dagger M_i - I) \theta_i\|_2; \quad (9)$$

(c) *if θ_i lies in the column space of $\mathbb{E}[\tilde{\mathbf{z}}_i \tilde{\mathbf{z}}_i^\top]$ for each $i \in [n]$, then $\mathbb{E}[\widehat{\text{TTE}}] = \text{TTE}$.*

Theorem 1(a) is obtained by direct algebra and Theorem 1(b) follows from the Cauchy–Schwarz inequality. The right-hand side of (9) is essentially a measure of the extent to which $M_i^\dagger M_i$ fails to be invertible in the direction of θ_i . As such, if θ_i lies in the column space of M_i , the definition of the Moore–Penrose pseudoinverse ensures that $M_i^\dagger M_i \theta_i = \theta_i$, and the contribution of unit i to the bound (9) is zero. This observation leads to Theorem 1(c), which identifies a condition under which $\widehat{\text{TTE}}$ is unbiased.

Thus, for a given design, we can verify the unbiasedness of the pseudoinverse estimator by checking a linear algebraic condition. Note that a sufficient (but not necessary, see Section 5) condition for unbiasedness is the invertibility of the design matrix, which ensures that the column space spans $\mathbb{R}^{|\mathcal{S}_i^\beta|}$. In general, we find that this unbiasedness condition is satisfied for Bernoulli randomized designs, but not for completely randomized designs.

When $\widehat{\text{TTE}}$ is biased, it is not an instance of the Riesz estimator defined by Harshaw et al. [2022], since the Riesz estimator is always unbiased. In the case of completely randomized designs, this is because the positivity condition necessary for the unbiasedness of the Riesz estimator is not satisfied.

3.3 Variance

We now present a generic bound that identifies functions of the experimental design and interference graph that control the variance of $\widehat{\text{TTE}}$.

At a high level, our approach to understanding the variance of $\widehat{\text{TTE}}$ is to first write

$$\text{var}(\widehat{\text{TTE}}) = \frac{1}{n^2} \sum_{i,j=1}^n \text{cov}(\theta_i^\top \widehat{\mathbf{c}}_i, \theta_j^\top \widehat{\mathbf{c}}_j) = \frac{1}{n^2} \sum_{i,j=1}^n \theta_i^\top \text{cov}(\widehat{\mathbf{c}}_i, \widehat{\mathbf{c}}_j) \theta_j,$$

and then distinguish two possibilities. If $\theta_i^\top \text{cov}(\widehat{\mathbf{c}}_i, \widehat{\mathbf{c}}_j) \theta_j \leq 0$, then we can drop that covariance term and obtain an upper bound on the variance. This will be the case if, for instance, $\widehat{\mathbf{c}}_i$ is independent

of $\widehat{\mathbf{c}}_j$, which occurs when the treatments of all of the neighbors of unit i are independent of the treatments of all of the neighbors of unit j . In this case, we will in fact have $\theta_i^\top \text{cov}(\widehat{\mathbf{c}}_i, \widehat{\mathbf{c}}_j)\theta_j = 0$. Otherwise, we must control the quadratic form $\theta_i^\top \text{cov}(\widehat{\mathbf{c}}_i, \widehat{\mathbf{c}}_j)\theta_j$, which we do by separating out the contributions of the two units to the quadratic form.

This approach leads to the following theorem.

Theorem 2. *Suppose that Assumption 3 holds, so that $\|\mathbf{c}_i\|_2 \leq B$, and that Assumption 4 holds, so that the sign of $\langle \mathbf{c}_i, \theta_i \rangle$ is constant across i . Then,*

$$\text{var}(\widehat{\text{TTE}}) \leq \frac{B^2}{n^2} \sum_{i,j=1}^n \gamma_i \gamma_j \cdot \mathbb{I}(\theta_i^\top \text{cov}(\widehat{\mathbf{c}}_i, \widehat{\mathbf{c}}_j)\theta_j > 0) \leq \frac{B^2}{n^2} \sum_{i,j=1}^n \gamma_i \gamma_j \cdot \mathbb{I}(\bar{\mathbf{z}}_i \not\perp \bar{\mathbf{z}}_j), \quad (10)$$

where $\gamma_i = \sqrt{|\mathcal{S}_i^\beta| \cdot \theta_i^\top \mathbb{E}[\bar{\mathbf{z}}_i \bar{\mathbf{z}}_i^\top] \dagger \theta_i}$.

Paralleling the discussion above, the bound of Theorem 2 has two components. The first component is the discrete $\mathbb{I}(\theta_i^\top \text{cov}(\widehat{\mathbf{c}}_i, \widehat{\mathbf{c}}_j)\theta_j > 0)$, which tracks which terms contribute positively to the variance. As mentioned above and shown in Theorem 2, this term can be further bounded by $\mathbb{I}(\bar{\mathbf{z}}_i \not\perp \bar{\mathbf{z}}_j)$, and this independence condition is both more interpretable and easier to check. Unfortunately, this independence condition is too loose when analyzing completely randomized designs as we do in this work, and so we present both forms of the bound in Theorem 2.

The second component is the continuous term $\gamma_i \gamma_j$, which captures the contributions of units i and j to the variance. Based on this, the quantity γ_i is a natural proxy for the contribution of unit i to the variance of the pseudoinverse estimator under a particular design and interference graph. To better understand γ_i , note that it depends on the quadratic form $\theta_i^\top \mathbb{E}[\bar{\mathbf{z}}_i \bar{\mathbf{z}}_i^\top] \dagger \theta_i$, which is a sum of certain entries of $\mathbb{E}[\bar{\mathbf{z}}_i \bar{\mathbf{z}}_i^\top] \dagger$. These entries will be small when the entries of $\mathbb{E}[\bar{\mathbf{z}}_i \bar{\mathbf{z}}_i^\top]$ are large, and so γ_i will be small when the treatments within \mathcal{N}_i are correlated. Thus, Theorem 2 can be thought of as a quantitative form of the intuition that correlating the treatments of adjacent nodes in the interference graph reduces the variance of treatment effect estimates.

We remark that the bound of Theorem 2 can be understood as a bound on the worst-case variance over all outcome models with $\|\mathbf{c}_i\|_2 \leq B$, and so can be used to select a clustering that is likely to have moderate variance under any such model. We explore this approach in Section 7.2 and find that it has good properties in practice. As an extension, both the bound of Theorem 2 and thus the practice of cluster selection can be refined based on more precise domain knowledge of \mathbf{c}_i .

The results of this section provide a framework for understanding the behavior of the pseudoinverse estimator under arbitrary experimental designs. In the next three sections, we will instantiate this framework for several different designs. First, in Section 4 we will consider unit-randomized designs, recover the results of Cortez-Rodriguez et al. [2023], and provide novel results for the pseudoinverse estimator under completely randomized treatment assignment using Theorems 1 and 2.

Then, in Sections 5 and 6, we will turn to our main focus in this work: cluster-randomized designs with Bernoulli and complete randomization. Again using Theorems 1 and 2, we obtain results on the bias and variance of the pseudoinverse estimator under each of these designs, thus providing a complete characterization of estimation in the low-order model with cluster randomized data and demonstrating the value of the results of this section.

Throughout these sections, we will analytically evaluate bias and variance bounds by deriving the form of M_i and M_i^\dagger and then bounding the relevant quantities. We emphasize that the value of our

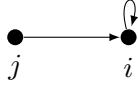


Figure 1: Illustration of a toy example in which unit i has a single neighbor, so that $\mathcal{N}_i = \{i, j\}$.

bounds is in no way limited to the setting where such analytical calculations are feasible. These calculations are necessary to give theoretical results, but our bounds can be evaluated numerically given nothing more than sampling access to the distribution. This sampling access can be used to estimate $\mathbb{E}[\tilde{\mathbf{z}}_i \tilde{\mathbf{z}}_i^\top]$, which can be pseudoinverted numerically, and then all bounds can be computed efficiently. This means, for example, that our bounds can be used to select a clustering (as we demonstrate in Section 7.2) for designs even more complex than those we consider here, like those of Ugander and Yin [2023] or Candogan et al. [2023].

4 Unit Randomized Designs

In this section, we use unit-level Bernoulli randomization and unit-level complete randomization as basic examples to demonstrate the machinery of Theorems 1 and 2. Since the pseudoinverse estimator separately estimates the causal effects of each individual, we can restrict our focus to one particular $i \in [n]$ and then extend our results by linearity.

As a running example, we suppose that i has an in-neighborhood that includes one other individual, so that $\mathcal{N}_i = \{i, j\}$. This example is illustrated in Figure 1. In this case, if the underlying potential outcomes model has order $\beta = 1$, we have that $\mathcal{S}_i^1 := \{\emptyset, \{i\}, \{j\}\}$. If $\beta = 2$, then we instead have that $\mathcal{S}_i^2 := \{\emptyset, \{i\}, \{j\}, \{i, j\}\}$.

4.1 Bern(p) Design

In a Bern(p) design, each individual is assigned to treatment with probability p , and these decisions are mutually independent. In this section, we derive the form of the design matrix and pseudoinverse estimator for the Bern(p) design, and show that we recover the estimator of Cortez-Rodriguez et al. [2023] in this case. Similarly, we also show that the results of Section 3 can be used to recover the theoretical results of Cortez-Rodriguez et al. [2023].

Recall that the entries of the design matrix are indexed by sets $S, T \in \mathcal{S}_i^\beta$, with

$$\left[\mathbb{E} [\tilde{\mathbf{z}}_i \tilde{\mathbf{z}}_i^\top] \right]_{S,T} = \Pr \left(\bigcap_{j \in S \cup T} z_j = 1 \right).$$

The mutual independence of the treatments allows us to simplify this probability to the exponential $p^{|S \cup T|}$. In the example of Figure 1 with $\beta = 2$, we obtain an invertible design matrix, which is shown below along with its (pseudo)inverse.

$$\mathbb{E} [\tilde{\mathbf{z}}_i \tilde{\mathbf{z}}_i^\top] = \begin{matrix} & \emptyset & \{i\} & \{j\} & \{i,j\} \\ \emptyset & \begin{bmatrix} 1 & p & p & p^2 \\ p & p & p^2 & p^2 \\ p & p^2 & p & p^2 \\ p^2 & p^2 & p^2 & p^2 \end{bmatrix} \end{matrix} \quad \mathbb{E} [\tilde{\mathbf{z}}_i \tilde{\mathbf{z}}_i^\top]^\dagger = \frac{1}{p^2(1-p)^2} \begin{bmatrix} p^2 & -p^2 & -p^2 & p^2 \\ -p^2 & p & -p & -p \\ -p^2 & -p & p & -p \\ p^2 & -p & -p & 1 \end{bmatrix}.$$

In general, the entries of the (pseudo)inverse have the form:

$$\left[\mathbb{E} [\tilde{\mathbf{z}}_i \tilde{\mathbf{z}}_i^\top]^\dagger \right]_{S,T} = \left(\frac{-1}{p} \right)^{|S|+|T|} \sum_{\substack{U \in \mathcal{S}_i^\beta \\ (S \cup T) \subseteq U}} \left(\frac{p}{1-p} \right)^{|U|}, \quad (11)$$

which can be substituted into (7) to obtain the estimator

$$\widehat{\text{TTE}} = \frac{1}{n} \sum_{i=1}^n Y_i(z) \sum_{S \in \mathcal{S}_i^\beta} \left(\prod_{j \in S} \frac{z_j - p}{p} - \prod_{j \in S} \frac{z_j - p}{p-1} \right). \quad (12)$$

This agrees with the SNIPE estimator of Cortez-Rodriguez et al. [2023] when the treatment probabilities p_i of that work, which can vary by unit, are set uniformly to $p_i = p$.

We next turn to the properties of $\widehat{\text{TTE}}$ for this design. Since this family of design matrices is always invertible (this is shown in Lemma 1 of Cortez-Rodriguez et al. [2023]), our Theorem 1(c) implies that $\widehat{\text{TTE}}$ is unbiased. To obtain a variance bound using Theorem 2, we must determine when $\tilde{\mathbf{z}}_i \not\perp \tilde{\mathbf{z}}_j$ and bound γ_i . We can check that the former occurs when $\mathcal{N}_i \cap \mathcal{N}_j \neq \emptyset$, i.e., when units i and j share a neighbor. To bound γ_i , we use the form of the entries of the pseudoinverse computed in (11) and obtain the following bound.

Lemma 1. *Suppose that $p \leq 1/2$ and $\mathbf{z} \sim \text{Bern}(p)$. Then, for a node of degree d_i ,*

$$\gamma_i^2 \leq \begin{cases} 4d_i^\beta \cdot p^{-d_i} & d_i \leq \beta, \\ 16d_i^{2\beta} \cdot p^{-\beta} & d_i > \beta. \end{cases} \quad (13)$$

This lemma sheds light on the basic value of low-order modeling: when a node i has degree $d_i > \beta$, it still contributes terms of order $p^{-\beta}$ to the variance, rather than p^{-d_i} . Combining Lemma 1 with the observation above and Theorem 2, we obtain the following bound on the variance.

Corollary 1. *Suppose that $\mathbf{z} \sim \text{Bern}(p)$ for some $p \leq \frac{1}{2}$, that Assumption 2 holds for some $\beta \leq d_{\max}$, and that Assumption 3 holds for some B . Then,*

$$\text{var}(\widehat{\text{TTE}}) = O\left(\frac{B^2 d_{\max}^{2\beta+2}}{np^\beta}\right). \quad (14)$$

It is instructive to compare (14) to Theorem 1 of Cortez-Rodriguez et al. [2023], which, in our notation, shows that

$$\text{var}(\widehat{\text{TTE}}) = O\left(\frac{B^2 d_{\max}^{\beta+2}}{np^\beta}\right) \quad (15)$$

We see that (14) and (15) exhibit the same scaling in n and B , as well as the same $O(p^{-\beta})$ dependence. The dependence on $d_{\max}^{2\beta+2}$ in (14) is slightly looser than the dependence of (15) on $d_{\max}^{\beta+2}$; this is a consequence of the fact that our analysis is a special case of our results for general designs, while the analysis of Cortez-Rodriguez et al. [2023] is tailored to unit-randomized Bernoulli designs. Crucially, our bounds retain a polynomial dependence on d_{\max} , and highlight the key point that the variance scales with $p^{-\beta}$ rather than $p^{-d_{\max}}$. Thus we see that our general pseudoinverse framework, and the corresponding variance bound theory, largely recovers the results of Cortez-Rodriguez et al. [2023].

4.2 Comp(k) Design

In a Comp(k) design (or a *completely randomized unit design*), the treatment assignments of individuals are correlated to ensure that a fixed number of units are treated. Specifically, under this design, a uniform random subset of k individuals are assigned to treatment, with the remaining individuals assigned to control. Each time an individual i is assigned to treatment, this uses up one of the k treatment allotments and reduces the conditional treatment probability of all other individuals. With this in mind, we obtain the following formula for the entries of the design matrix:

$$\left[\mathbb{E} [\tilde{\mathbf{z}}_i \tilde{\mathbf{z}}_i^\top] \right]_{S,T} = \Pr \left(\bigcap_{j \in S \cup T} z_j = 1 \right) = \prod_{\ell=0}^{|S \cup T|-1} \frac{k-\ell}{n-\ell}.$$

Analysis of these design matrices in full generality is challenging, so we restrict our attention to the $\beta = 1$ case, which is already sufficient to illustrate many interesting phenomena. We emphasize that this assumption is only meant to facilitate exact calculation and analysis—all of the results of Section 3 hold for all values of β , and the bias and variance bounds can be computed by numerically pseudoinverting the design matrices.

Continuing with our running example illustrated in Figure 1, if $\beta = 1$, the design matrix $\mathbb{E} [\tilde{\mathbf{z}}_i \tilde{\mathbf{z}}_i^\top]$ for an individual i with $\mathcal{N}_i = \{i, j\}$ has the form:

$$\mathbb{E} [\tilde{\mathbf{z}}_i \tilde{\mathbf{z}}_i^\top] = \begin{matrix} & \emptyset & \{i\} & \{j\} \\ \emptyset & \begin{bmatrix} 1 & \frac{k}{n} & \frac{k}{n} \end{bmatrix} & \\ \{i\} & \begin{bmatrix} \frac{k}{n} & \frac{k}{n} & \frac{k(k-1)}{n(n-1)} \end{bmatrix} & \\ \{j\} & \begin{bmatrix} \frac{k}{n} & \frac{k(k-1)}{n(n-1)} & \frac{k}{n} \end{bmatrix} & \end{matrix}.$$

Note that the entries in this matrix are functions not only of the treatment level k but also of n . The following lemma shows that the design matrix for complete randomization, unlike Bernoulli randomization, need not be invertible. The proof of this lemma, along with all other results from this section, appears in Appendix B.

Lemma 2. *Suppose that $\mathbf{z} \sim \text{Comp}(k)$ and Assumption 2 holds with $\beta = 1$. Then, the design matrix for unit i has determinant*

$$\det \left(\mathbb{E} [\tilde{\mathbf{z}}_i \tilde{\mathbf{z}}_i^\top] \right) = \frac{k^{d_i} \cdot (n-k)^{d_i} \cdot (n-d_i)}{n^{(d_i+1)} \cdot (n-1)^{d_i}}.$$

Lemma 2 shows that the design matrix will fail to be invertible whenever unit i has graph degree n . This will be the case when the outcome of unit i is affected by the treatments of every other unit. Although this is unlikely to occur in real-world networks, this invertibility issue will become more relevant in the case of cluster-randomized designs, which we discuss in Section 6. In that setting, we will see that the analog of this condition is an individual having a neighbor in each cluster, which may be inevitable when the number of clusters is small.

In light of Lemma 2, we compute the pseudoinverse of the design matrix for individuals with $d_i < n$ by taking the standard matrix inverse. For individuals with $d_i = n$, we compute the pseudoinverse by making an ansatz for the form of the pseudoinverse and then verifying the defining properties of the Moore–Penrose pseudoinverse. Combining these cases gives the following form for $\widehat{\text{TTE}}$.

Lemma 3. *Suppose that $\mathbf{z} \sim \text{Comp}(k)$ and that Assumption 2 holds with $\beta = 1$. Then, the pseudoinverse estimator for the total treatment effect is given by:*

$$\widehat{\text{TTE}} = \frac{1}{n} \sum_{i=1}^n Y_i(\mathbf{z}) \cdot \begin{cases} \frac{n^2(n-1)}{k(n-k)(n-d_i)} \sum_{j \in \mathcal{N}_i} (z_j - \frac{k}{n}) & d_i < n, \\ \frac{nk^2}{(k^2+n)^2} \sum_{j \in \mathcal{N}_i} (z_j + \frac{1}{k}) & d_i = n. \end{cases}$$

The proof of this lemma includes a derivation of the explicit formulas for the requisite (pseudo)inverse matrices.

4.2.1 Bias

To reason about the bias of this pseudoinverse estimator, we make use of Theorem 1. Any individual $i \in [n]$ with $d_i < n$ has an invertible design matrix, so they do not contribute any bias to the estimator. The remaining individuals have a non-invertible design matrix. The null space of these matrices has dimension 1, suggesting that θ_i may still lie in the column space and ensure unbiasedness. The following example demonstrates that this need not be the case, and can be generalized to show that this is never the case.

Example 1. *In the setting of Figure 1 with $k = 1$ and $n = 2$ (meaning exactly one of i, j is randomly selected for treatment), the design matrix given above simplifies to*

$$\mathbb{E} [\tilde{\mathbf{z}}_1 \tilde{\mathbf{z}}_1^\top] = \begin{bmatrix} 1 & \frac{1}{2} & \frac{1}{2} \\ \frac{1}{2} & \frac{1}{2} & 0 \\ \frac{1}{2} & 0 & \frac{1}{2} \end{bmatrix}.$$

The column space of this matrix is spanned by its first two columns (note that the third column is the first minus the second). The vector $\theta_1 = [0 \ 1 \ 1]^\top$ does not lie in the column space; the only vectors in the column space with 0 in their first entry are the scalar multiples of $[0 \ -1 \ 1]^\top$.

In fact, for any i with $d_i = n$, θ_i will always lie outside of the column space of the design matrix, meaning they will all incur some bias. We quantify this bias in the following lemma, which provides both an exact expression and a bound on the bias based on Theorem 1.

Lemma 4. *Suppose that $\mathbf{z} \sim \text{Comp}(k)$ and that Assumption 2 holds with $\beta = 1$. Then:*

(a) the exact bias of $\widehat{\text{TTE}}$ is

$$\mathbb{E}[\widehat{\text{TTE}}] - \text{TTE} = \frac{1}{k^2 + n} \sum_{i=1}^n \mathbb{I}(d_i = n) \cdot \left(k \cdot c_{i,\emptyset} - \sum_{j=1}^n c_{i,j} \right);$$

(b) if Assumption 3 holds, $\|\mathbf{c}_i\|_2 \leq B, \forall i$, the bias of $\widehat{\text{TTE}}$ satisfies the bound

$$|\mathbb{E}[\widehat{\text{TTE}}] - \text{TTE}| \leq \frac{\#\{i : d_i = n\}}{n} \cdot \frac{B}{k/n};$$

(c) if $d_i < n$ for all $i \in [n]$, then $\widehat{\text{TTE}}$ is unbiased.

As mentioned above, we typically expect to have no units with $d_i = n$ and thus no bias in $\widehat{\text{TTE}}$.

4.2.2 Variance

To apply Theorem 2 to completely randomized unit designs, we must do two things: identify when $\theta_i \text{cov}(\widehat{\mathbf{c}}_i, \widehat{\mathbf{c}}_j) \theta_j$ is negative and compute γ_i .

For the first of these, consider two units i and j . If the neighborhoods of units i and j are disjoint, then the entries of $\tilde{\mathbf{z}}_i$ will be distinct from the entries of $\tilde{\mathbf{z}}_j$. This means that all of the entries of $\tilde{\mathbf{z}}_i$ will be negatively correlated with the entries of $\tilde{\mathbf{z}}_j$, since

$$\text{cov}(z_i, z_j) = \frac{k(k-1)}{n(n-1)} - \frac{k^2}{n^2} = -\frac{k(n-k)}{n^2(n-1)} < 0$$

under complete randomization. It is thus natural to expect that $\theta_i \text{cov}(\widehat{\mathbf{c}}_i, \widehat{\mathbf{c}}_j) \theta_j$ will be negative in this case, and we verify this in the following lemma.

Lemma 5. *Suppose that $\mathbf{z} \sim \text{Comp}(k)$, Assumption 2 hold with $\beta = 1$, and Assumption 5 holds, so that the sign of $c_{i,\mathcal{S}}$ is constant. Then, for two units $i, j \in [n]$ with $\mathcal{N}_i \cap \mathcal{N}_j = \emptyset$, we have*

$$\text{cov}(\theta_i^\top \widehat{\mathbf{c}}_i, \theta_j^\top \widehat{\mathbf{c}}_j) < 0.$$

The next step is to compute $\gamma_i = \sqrt{|\mathcal{S}_i^\beta| \cdot \theta_i^\top \mathbb{E}[\tilde{\mathbf{z}}_i \tilde{\mathbf{z}}_i^\top] \dagger \theta_i}$. Since we assume that $\beta = 1$, we have $|\mathcal{S}_i^\beta| = d_i + 1$, leaving only the task of computing the quadratic form. As the form of the design matrix pseudoinverse differs when $d_i < n$ versus when $d_i = n$, our calculation also distinguishes these cases, as seen in the following lemma.

Lemma 6. *Suppose that $\mathbf{z} \sim \text{Comp}(k)$ and that Assumption 2 holds with $\beta = 1$. Then*

$$\gamma_i^2 = \begin{cases} \frac{(d_i+1)d_i(n-1)}{(k/n)(1-k/n)(n-d_i)} & d_i < n, \\ \frac{(n+1)n^2k^2}{(k^2+n)^2} & d_i = n. \end{cases}$$

We see from Lemma 6 that the value of γ_i^2 increases monotonically with d_i for $d_i < n$, but then decreases at $d_i = n$. Indeed, for $d_i = n-1$, we have $\gamma_i^2 = n(n-1)^2 / ((k/n)(1-k/n))$, while the value of γ_i for $d_i = n$ can be written as $(n+1)n^2 / (k+n/k)^2$. The numerators of both expressions are

of order n^3 , but the denominator of the latter expression is much larger (in particular it is greater than 1, unlike $k/n(1 - k/n)$). Thus, the value of γ_i for $d_i = n$ will typically be much smaller.

Since these units with $d_i = n$ control the scale of the bias, there is a bias-variance trade-off mediated by the number of units with $d_i = n$: when there are no units with $d_i = n$, the mean-squared error is simply the variance, while when there are many units with $d_i = n$, the mean-squared error is dominated by the bias.

Finally, combining our two lemmas with Theorem 2, we obtain the following result on the variance of $\widehat{\text{TTE}}$ under completely randomized designs when $\beta = 1$.

Corollary 2. *Suppose that $\mathbf{z} \sim \text{Comp}(k)$, $d_{\max} < n$, Assumption 2 holds with $\beta = 1$, Assumption 3 holds for some B , Assumption 5 holds, and that $k/n < 1/2$. Then*

$$\text{var}(\widehat{\text{TTE}}) \leq O\left(\frac{B^2}{n} \cdot \frac{d_{\max}^4}{k/n} \cdot \frac{n}{n - d_{\max}}\right).$$

Note that the assumption that $d_{\max} < n$ ensures that all nodes fall into the first case of Lemma 6. This assumption is relatively benign in this case. When we consider completely randomized cluster designs in Section 6, we show that the analog of this assumption, that a node is not exposed to every cluster, is not realistic; our careful analysis of this second case will uncover a novel bias-variance trade-off for these designs.

Corollary 2 establishes that the variance of $\widehat{\text{TTE}}$ is polynomial in d_{\max} , rather than exponential, for completely randomized unit designs when $\beta = 1$, thus generalizing the $\beta = 1$ case of the variance bound of Cortez-Rodriguez et al. [2023] to the completely randomized setting. More generally, this section and its results show how our framework can be used to obtain bounds on the variance of the pseudoinverse estimator under arbitrary designs. In the sequel, we continue to apply the same framework to study the pseudoinverse estimator under clustered designs.

5 $\text{GCR}_{\text{Bern}}(\mathcal{C}, p)$ Design

Thus far we have introduced the pseudoinverse estimator, given generic bounds on its bias and variance, and instantiated these bounds in simple examples. With this preparation, we are ready to turn to our main focus in this work: analyzing the pseudoinverse estimator for GCR designs. In this section, we focus on the Bernoulli randomized case (i.e., the $\text{GCR}_{\text{Bern}}(\mathcal{C}, p)$ design of Table 2) and treat the completely randomized case (i.e., the $\text{GCR}_{\text{Comp}}(\mathcal{C}, k_c)$ design of Table 2) in the sequel, Section 6. We find that for $\text{GCR}_{\text{Bern}}(\mathcal{C}, p)$ designs the pseudoinverse estimator is always unbiased, and exhibits a “best-of-both-worlds” variance structure that scales with the stronger of the low-order assumption and the graph structure assumptions. The key technical ingredient for this result is to relate the design matrices in the clustered case to the design matrices in the unit randomized case using rank-decomposition properties of the Moore–Penrose pseudoinverse.

We begin with some notation. As in Section 2.3, a clustering \mathcal{C} partitions the individuals $[n]$ into m disjoint clusters $\{C_1, \dots, C_m\}$. We can view \mathcal{C} as a map $[n] \rightarrow [m]$, where $\mathcal{C}(i)$ is the cluster containing node i , and we extend this notation to define $\mathcal{C}(S) := \{\mathcal{C}(i) : i \in S\}$. In particular, $\mathcal{C}(\mathcal{N}_i)$ denotes the set of clusters that include at least one neighbor of i . Throughout this section, we will use standard uppercase letters (S, T, U) to denote sets of *individuals* and calligraphic letters ($\mathcal{S}, \mathcal{T}, \mathcal{U}$) to denote sets of *clusters*. Recall also from Section 2.3 that GCR designs assign a treatment

decision $w_{C_j} \in \{0, 1\}$ to cluster $j \in [m]$. Then, the treatment assignments of an individual $i \in [n]$ are inherited from their cluster, so that $z_i = w_{C(i)}$.

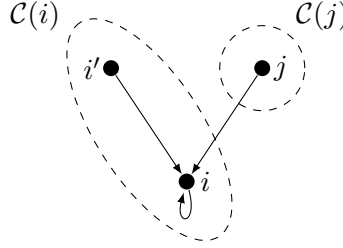
5.1 Reducing Clusters to Units

With this notation in hand, we see that the design matrices for GCR designs are highly structured. Given any $S, T \in \mathcal{S}_i^\beta$, we have

$$\left[\mathbb{E}[\tilde{\mathbf{z}}_i, \tilde{\mathbf{z}}_i^\top] \right]_{S, T} = \Pr \left(\bigcap_{j \in S \cup T} z_j = 1 \right) = \Pr \left(\bigcap_{C \in \mathcal{C}(S \cup T)} w_C = 1 \right).$$

The entries of this matrix only depend on which clusters intersect with S and T : given $S, S', T, T' \in \mathcal{S}_i^\beta$ with $\mathcal{C}(S) = \mathcal{C}(S')$ and $\mathcal{C}(T) = \mathcal{C}(T')$, we have that $\left[\mathbb{E}[\tilde{\mathbf{z}}_i, \tilde{\mathbf{z}}_i^\top] \right]_{S, T} = \left[\mathbb{E}[\tilde{\mathbf{z}}_i, \tilde{\mathbf{z}}_i^\top] \right]_{S', T'}$. As a result the design matrix has a block structure, illustrated in the following example.

Example 2. Consider the neighborhood $\mathcal{N}_i = \{i, i', j\}$ in an interference graph with $\beta = 2$. Suppose that the graph has been clustered so that $\mathcal{C}(i) = \mathcal{C}(i') \neq \mathcal{C}(j)$.



The design matrix for a $\text{GCR}_{\text{Bern}}(\mathcal{C}, p)$ design for this instance is shown below. Note the ordering of the rows and columns of this matrix.

$$\mathbb{E}[\tilde{\mathbf{z}}_i \tilde{\mathbf{z}}_i^\top] = \begin{array}{c} \begin{array}{c} \emptyset \\ \{i\} \\ \{i'\} \\ \{i, i'\} \\ \{j\} \\ \{i, j\} \\ \{i', j\} \end{array} \begin{array}{c} \left[\begin{array}{c|c|c|c|c|c|c} \emptyset & \{i\} & \{i'\} & \{i, i'\} & \{j\} & \{i, j\} & \{i', j\} \\ \hline 1 & p & p & p & p & p^2 & p^2 \\ \hline p & p & p & p & p^2 & p^2 & p^2 \\ \hline p & p & p & p & p^2 & p^2 & p^2 \\ \hline p & p & p & p & p^2 & p^2 & p^2 \\ \hline p & p^2 & p^2 & p^2 & p & p^2 & p^2 \\ \hline p^2 & p^2 & p^2 & p^2 & p^2 & p^2 & p^2 \\ \hline p^2 & p^2 & p^2 & p^2 & p^2 & p^2 & p^2 \end{array} \right] \end{array} \end{array} \left. \begin{array}{l} \vphantom{\begin{array}{c} \emptyset \\ \{i\} \\ \{i'\} \\ \{i, i'\} \\ \{j\} \\ \{i, j\} \\ \{i', j\} \end{array}} \right\} \begin{array}{l} M_i^\beta(\emptyset) = 1 \\ M_i^\beta(\{\mathcal{C}(i)\}) = 3 \\ M_i^\beta(\{\mathcal{C}(j)\}) = 1 \\ M_i^\beta(\{\mathcal{C}(i), \mathcal{C}(j)\}) = 2 \end{array}$$

The blocks in the design matrix in Example 2 are delineated by dashed lines and correspond to subsets of clusters in $\mathcal{C}(\mathcal{N}_i)$ with size at most β . We'll use \mathcal{C}_i^β to denote all such subsets of clusters. The width of the block corresponding to a subset $\mathcal{S} \subseteq \mathcal{C}(\mathcal{N}_i)$ is the number of subsets $S \in \mathcal{S}_i^\beta$ with $\mathcal{C}(S) = \mathcal{S}$, which we denote by $M_i^\beta(\mathcal{S})$. One can calculate $M_i^\beta(\mathcal{S})$ for $\mathcal{S} = \{C_{j_1}, \dots, C_{j_\ell}\}$ with the

Quantity	# units, n	neighborhood, \mathcal{N}_i	degree, d_i
Cluster analog	# clusters, m	cluster neighborhood, $\mathcal{C}(\mathcal{N}_i)$	cluster degree, $ \mathcal{C}(\mathcal{N}_i) $

Table 3: The notational analogy between the cluster-randomized setting and the unit-randomized setting. The clusters play the role of the units and all other notation follows in parallel.

formula

$$M_i^\beta(\mathcal{S}) = \sum_{\substack{a_1, \dots, a_\ell \\ a_1 + \dots + a_\ell \leq \beta \\ a_1, \dots, a_\ell \geq 1}} \prod_{k=1}^{\ell} \binom{|\mathcal{C}_{j_k} \cap \mathcal{N}_i|}{a_j}.$$

The entries within the block indexed by $\mathcal{S}, \mathcal{T} \in \mathcal{C}_i^\beta$ correspond to the entries in a $\text{Bern}(p)$ design where individual i has one neighbor for each of its neighboring clusters (compare this example to the one from Section 4.1).

Let $\tilde{\mathbf{w}}_i$ be the analog of $\tilde{\mathbf{z}}_i$ for the cluster treatment decisions. That is, $\tilde{\mathbf{w}}_i$ is a $\{0, 1\}$ -vector indexed by \mathcal{C}_i^β with $[\tilde{\mathbf{w}}_i]_{\mathcal{S}} = \prod_{C \in \mathcal{S}} w_C$. This notation allows us to obtain the following form for the design matrix for GCR designs.

Lemma 7. *Fix a clustering \mathcal{C} of $[n]$ with $|\mathcal{C}| = m$ and an individual $i \in [n]$. Then, if the design of \mathbf{z} assigns treatment at the cluster level with cluster treatment indicators $\mathbf{w} \in \{0, 1\}^m$, the pseudoinverse of the design matrix has entries*

$$\left[\mathbb{E} [\tilde{\mathbf{z}}_i \tilde{\mathbf{z}}_i^\top]^\dagger \right]_{S,T} = \frac{1}{M_i^\beta(\mathcal{C}(S)) \cdot M_i^\beta(\mathcal{C}(T))} \cdot \left[\mathbb{E} [\tilde{\mathbf{w}}_i \tilde{\mathbf{w}}_i^\top]^\dagger \right]_{\mathcal{C}(S), \mathcal{C}(T)}.$$

for each $S, T \in \mathcal{S}_i^\beta$.

This lemma tells us that the entries within each block of this cluster design matrix are normalized entries of the unit-randomized design matrix corresponding to \mathbf{w} . The normalization factors correspond to the sizes of each matrix block. A proof of this lemma is given in Appendix C and proceeds by factoring the design matrix based on the block structure to obtain a rank decomposition, and then using the fact that $(AB)^\dagger = B^\dagger A^\dagger$ when AB is a rank decomposition. In light of this lemma, we can recast the analysis of cluster-randomized designs as the analysis of a unit-randomized design in which clusters play the roles of units. This analogy is made precise in Table 3, which shows how notation in one setting corresponds to notation in the other.

Now, recall that the $\text{GCR}_{\text{Bern}}(\mathcal{C}, p)$ design assigns each cluster to treatment with probability p , mutually independent of the decisions of other clusters. In this case, $\mathbb{E} [\tilde{\mathbf{w}}_i \tilde{\mathbf{w}}_i^\top]$ has the structure of a $\text{Bern}(p)$ design matrix, as in (11). Substituting (11) into Lemma 7, we find that the entries of the GCR_{Bern} design matrix have the form

$$\left[\mathbb{E} [\tilde{\mathbf{z}}_i \tilde{\mathbf{z}}_i^\top]^\dagger \right]_{S,T} = \frac{\left(\frac{-1}{p}\right)^{|\mathcal{C}(S)|+|\mathcal{C}(T)|}}{M_i^\beta(\mathcal{C}(S)) \cdot M_i^\beta(\mathcal{C}(T))} \sum_{\substack{U \in \mathcal{C}_i^\beta \\ \mathcal{C}(S \cup T) \subseteq U}} \left(\frac{p}{1-p}\right)^{|U|}. \quad (16)$$

Finally, with (16) in hand, we obtain the form of $\widehat{\mathbf{TTE}}$ for the GCR_{Bern} design.

Lemma 8. Fix a clustering \mathcal{C} and suppose that $\mathbf{z} \sim \text{GCR}_{\text{Bern}}(\mathcal{C}, p)$. Then, the pseudoinverse estimator for the TTE is

$$\widehat{\text{TTE}} = \frac{1}{n} \sum_{i=1}^n Y_i(\mathbf{z}) \sum_{\mathcal{U} \in \mathcal{C}_i^\beta} \left(\prod_{\mathcal{C} \in \mathcal{U}} \frac{w_{\mathcal{C}} - p}{p} - \prod_{\mathcal{C} \in \mathcal{U}} \frac{w_{\mathcal{C}} - p}{p - 1} \right). \quad (17)$$

Note that this expression for $\widehat{\text{TTE}}$ is essentially a cluster analog of the expression for $\widehat{\text{TTE}}$ under a Bernoulli design given in (12). Having characterized the form of the design matrices and estimator, we are now in a position to discuss the bias and variance of $\widehat{\text{TTE}}$.

5.2 Bias

We can verify that the condition of Theorem 1(c) is satisfied for the GCR_{Bern} design, and so $\widehat{\text{TTE}}$ is unbiased. We record this fact in the following lemma, whose proof appears in Appendix C.

Lemma 9. Fix a clustering \mathcal{C} and suppose that $\mathbf{z} \sim \text{GCR}_{\text{Bern}}(\mathcal{C}, p)$. Then the pseudoinverse estimator $\widehat{\text{TTE}}$ of (17) is unbiased, so that $\mathbb{E}[\widehat{\text{TTE}}] = \text{TTE}$.

5.3 Variance

Next we consider the variance of the pseudoinverse estimator for GCR_{Bern} designs.

5.3.1 Improvement on Horvitz–Thompson

Before applying Theorem 2 to analyze the variance, we give a preliminary result showing that the variance of $\widehat{\text{TTE}}$ always improves on the variance of the Horvitz–Thompson estimator defined in (5) (which assumes a neighborhood exposure model as in Assumption 1), suggesting that we should always prefer the pseudoinverse to the Horvitz–Thompson estimator when using a $\text{GCR}(\mathcal{C}, p)$ design.

Theorem 3. Fix a clustering \mathcal{C} and suppose that $\mathbf{z} \sim \text{GCR}(\mathcal{C}, p)$ with $p \leq \frac{1}{2}$ and that Assumption 5 holds, so that each $c_{i,S}$ has the same sign. Then, writing $\widehat{\text{TTE}}$ for the pseudoinverse estimator and $\widehat{\text{TTE}}_{\text{HT}}$ for Horvitz–Thompson estimator, we have

$$\text{var} \left(\widehat{\text{TTE}} \right) \leq \text{var} \left(\widehat{\text{TTE}}_{\text{HT}} \right).$$

A proof of this theorem, which relies on the explicit form of the Horvitz–Thompson estimator, can be found in Appendix C. It is not surprising that the pseudoinverse estimator has a lower variance than the Horvitz–Thompson estimator since it exploits the β -order interactions structure of the potential outcomes. The Horvitz–Thompson estimator, in contrast, does not exploit this structure, leading to higher variance (but with the advantage of being unbiased for a larger class of outcome models).

5.3.2 Quantitative Variance Bounds

We now more precisely characterize the variance structure of the pseudoinverse estimator in terms of the experimental design. To do this, we first specialize Theorem 2 to the setting of cluster

randomization without any assumption on the clustering structure or β ; then, we present a series of more concrete variance bounds under more particular assumptions.

We begin with some high-level intuition for our results. The main observation is that both the low-order assumption and the cluster-randomized design aim to reduce variance by reducing the “effective degree” of a node. Without either assumption, the variance of an estimator of the TTE typically scales like p^{-d_i} . In comparison, the variance of the pseudoinverse estimator under an order β assumption scales like $p^{-\beta}$, and the variance of the Horvitz–Thompson estimator under cluster-randomization scales like $p^{-|\mathcal{C}(\mathcal{N}_i)|}$ (recall from Table 3 that $|\mathcal{C}(\mathcal{N}_i)|$ is the analog of d_i for cluster randomization). Our main theoretical result of this section shows that using the pseudoinverse estimator together with cluster randomization offers the best of both worlds: when $\beta > |\mathcal{C}(\mathcal{N}_i)|$, the node i contributes to the variance like it would under cluster randomization, and when $\beta \leq |\mathcal{C}(\mathcal{N}_i)|$, the node i contributes to the variance like it would under the low-order assumption.

As before our analysis has two pieces: identifying when $\tilde{\mathbf{z}}_i \perp \tilde{\mathbf{z}}_j$ in a cluster randomized design and bounding γ_i . Both of these can be done by applying the analogy of Table 3 to the discussion of Section 4.1. For identifying when $\tilde{\mathbf{z}}_i \perp \tilde{\mathbf{z}}_j$, the condition that $\mathcal{N}_i \cap \mathcal{N}_j = \emptyset$ is replaced by an analogous condition on cluster neighborhoods, given in the next lemma.

Lemma 10. *If $\mathbf{z} \sim \text{GCR}(\mathcal{C}, p)$ and $\mathcal{C}(\mathcal{N}_i) \cap \mathcal{C}(\mathcal{N}_j) = \emptyset$, then $\tilde{\mathbf{z}}_i \perp \tilde{\mathbf{z}}_j$.*

That is, if there is no cluster containing both a neighbor of node i and a neighbor of node j , then $\tilde{\mathbf{z}}_i$ is independent of $\tilde{\mathbf{z}}_j$. This lemma follows from the fact that $\tilde{\mathbf{z}}_i$ is a function of the treatments of the clusters represented among the neighbors of node i , and so if there is no cluster represented in both \mathcal{N}_i and \mathcal{N}_j , then $\tilde{\mathbf{z}}_i$ and $\tilde{\mathbf{z}}_j$ are functions of disjoint sets of independent random variables.

Next, the bound on γ_i for the GCR_{Bern} design is analogous to the bound of Lemma 1, with some subtlety in which factors of d_i are translated to factors of $|\mathcal{C}(\mathcal{N}_i)|$ and which are not.

Lemma 11. *Suppose that $p \leq 1/2$ and $\mathbf{z} \sim \text{GCR}_{\text{Bern}}(\mathcal{C}, p)$. Then, for a node of degree d_i ,*

$$\gamma_i^2 \leq \begin{cases} 4d_i^\beta \cdot p^{-|\mathcal{C}(\mathcal{N}_i)|} & |\mathcal{C}(\mathcal{N}_i)| < \beta, \\ 16d_i^\beta \cdot |\mathcal{C}(\mathcal{N}_i)|^\beta p^{-\beta} & |\mathcal{C}(\mathcal{N}_i)| \geq \beta. \end{cases} \quad (18)$$

This bound elucidates the interplay between the order β assumption and the cluster randomization. When $|\mathcal{C}(\mathcal{N}_i)| < \beta$, we find that γ_i scales like $p^{-|\mathcal{C}(\mathcal{N}_i)|}$, like it would under cluster randomization. When $|\mathcal{C}(\mathcal{N}_i)| \geq \beta$, we find that γ_i scales like $p^{-\beta}$, like it would under the order β assumption.

By specifying particular clusterings and order assumptions, we can derive several concrete corollaries of these two lemmas. In all of them, we assume that $\mathbf{z} \sim \text{GCR}_{\text{Bern}}(\mathcal{C}, p)$.

First, if we consider the case where each unit is its own cluster, which is equivalent to unit randomization, we can recover the variance bound from Corollary 1.

Next, we consider the case of a 3-net clustering of a graph G with restricted growth coefficient κ while also assuming that $\beta = 1$. This setting has two important features. First, since $|\mathcal{C}(\mathcal{N}_i)|$ is always at least 1, our bound on γ_i is especially simple in this case. Second, Ugander et al. [2013] show in their Proposition 4.2 that $|\mathcal{C}(\mathcal{N}_i)| \leq \kappa^3$, allowing us to control the number of pairs of units that do not satisfy the condition of Lemma 10. Note that we also have the bound $|\mathcal{C}(\mathcal{N}_i)| \leq d_{\max}$, and so our results here can be slightly strengthened by replacing factors of κ^3 by $\min(\kappa^3, d_{\max})$; we state the result in terms of κ^3 for simplicity and consistency with prior literature. An empirical

study of the relative sizes of d_{\max} and κ in real-world social networks can be found in Ugander and Yin [2023]. In practice, the exact variance of $\widehat{\text{TTE}}$ under different designs will depend on the unit-level values of d_i and neighborhood sizes, rather than the worst-case bounds in terms of d_{\max} and κ used in our theory. Together, these lead to the following variance bound.

Corollary 3 (3-net clusterings of restricted growth graphs with $\beta = 1$). *Suppose that Assumption 2 holds with $\beta = 1$, and that Assumption 3 holds so that $\|\mathbf{c}_i\|_2 \leq B$. Suppose further that the interference graph G has restricted growth coefficient κ . If the clustering \mathcal{C} is a 3-net of G and each cluster has at most N units, then $\text{var}(\widehat{\text{TTE}}) = O(d_{\max}^2 \kappa^6 N B^2 p^{-1}/n)$.*

Crucially, the bound of Corollary 3 is polynomial in κ , rather than exponential in κ like variance bounds for cluster randomization without a low-order assumption [Ugander et al., 2013]. On the other hand, without cluster randomization, the factors of κ in Corollary 3 would be replaced by factors of d_{\max} , and the bound would scale with d_{\max}^4 . Thus we see from Corollary 3 how the low-order assumption and cluster randomized design collaborate to give more favorable variance properties than either would alone.

Finally, we consider the case of an arbitrary clustering of G without any conditions on the restricted growth coefficient (since restricted growth assumptions are only informative when the clustering is a 3-net). We assume that $\beta = 2$, so that now there is a genuine trade-off between the low-order assumption and the clustering (as opposed to $\beta = 1$, when the low-order assumption is always stronger). We obtain a variance bound that depends on the quality of the clustering:

Corollary 4 (Arbitrary clusterings with $\beta = 2$). *Suppose that Assumption 3 holds so that $\|\mathbf{c}_i\|_2 \leq B$, and that each cluster has at most N units. Then*

$$\text{var}(\widehat{\text{TTE}}) = O\left(\frac{B^2 N}{n} \left(\frac{n_1}{n} \cdot d_{\max}^4 p^{-3/2} + \frac{n_{>1}}{n} d_{\max}^6 p^{-2}\right)\right),$$

where $n_1 = |\{i : \mathcal{C}(\mathcal{N}_i) = 1\}|$ is the number of nodes for which \mathcal{N}_i is contained in a single cluster, and $n_{>1} = n - n_1$.

An interesting feature of Corollary 4 is that it captures the effect of the clustering quality on the variance through the n_1/n and $n_{>1}/n$ terms. When n_1/n is large, most units are adjacent to only one cluster and thus have high exposure probabilities, limiting their contribution to the variance. When $n_{>1}/n$ is large, most units are adjacent to multiple clusters, and we must control their contribution to the variance through the $\beta = 2$ assumption. The $\beta = 2$ assumption leads to larger exponents on d_{\max} and p^{-1} , and so this result underscores the value of choosing a clustering with small values of $\mathcal{C}(\mathcal{N}_i)$. This intuition is consistent with other work in the literature—for example, lower bounding $\Pr(\mathcal{C}(\mathcal{N}_i) = 1)$ is also the key technical ingredient of Ugander and Yin [2023].

To summarize, our results provide a flexible framework for understanding the variance of the pseudoinverse estimator under a variety of different cluster randomized designs. In the sequel, we turn to the case of complete randomization.

6 $\text{GCR}_{\text{Comp}}(\mathcal{C}, k_c)$ Design

In this section, we turn to the final remaining entry of Table 2, and analyze the pseudoinverse estimator under a $\text{GCR}_{\text{Comp}}(\mathcal{C}, k_c)$ design: a graph cluster randomization design, completely randomized. As in Section 4.2, we will limit our theoretical analysis to the case of $\beta = 1$, but reiterate

that our bounds can be computed numerically for larger β . In this design, the nodes of a graph G are first partitioned into a set of clusters \mathcal{C} , k_c of these clusters are selected, uniformly at random, and all individuals within these selected clusters are assigned to treatment. The main idea of this section is to apply the unit-to-cluster analogy of Section 5 to the analysis of complete unit randomization in Section 4.2, although there is a subtle complication.

In the same way that units with $d_i = n$ had a non-invertible design matrix and thus behaved differently under the $\text{Comp}(k)$ design — recall, e.g., the results on estimator bias in Lemma 4 — units with $|\mathcal{C}(\mathcal{N}_i)| = m$ (which is the translation of $d_i = n$ into the cluster case according to Table 3) will behave differently under a $\text{GCR}_{\text{Comp}}(\mathcal{C}, k_c)$ design than units with $|\mathcal{C}(\mathcal{N}_i)| < m$. In particular, since the design matrices for these units are not invertible, the rank decomposition argument underlying the unit-to-cluster analogy of Section 5 does not hold, and we cannot simply translate Table 3 accordingly. Instead, we make an ansatz for the form of the pseudoinverse matrix, which we verify by checking each defining property of the Moore–Penrose pseudoinverse. The resulting pseudoinverse matrix and form of $\widehat{\text{TTE}}$ are complex and not instructive, so we omit them here and proceed directly to the bias and variance analysis. Detailed expressions can be found in Appendix D, and the estimator can be implemented in practice through numerical methods.

Our results will now depend not only on the number of clusters $|\mathcal{C}(\mathcal{N}_i)|$ a node is exposed to, but on the distribution of a node’s neighbors across these clusters. To state these results, for an individual $i \in [n]$ with $|\mathcal{C}(\mathcal{N}_i)| = m$, we let $|C|_i = |\mathcal{N}_i \cap C|$ for each $C \in \mathcal{C}$. That is, $|C|_i$ is the number of i ’s neighbors belonging to cluster C . Note that each $|C|_i \geq 1$ and that $\sum_C |C|_i = d_i$.

6.1 Bias

We have the following results on the bias of $\widehat{\text{TTE}}$, which, like those of Lemma 4, are based on an application of Theorem 1.

Lemma 12. *Suppose that $\mathbf{z} \sim \text{GCR}_{\text{Comp}}(\mathcal{C}, k_c)$ and Assumption 2 holds with $\beta = 1$. Then:*

(a) *the exact bias of $\widehat{\text{TTE}}$ is*

$$\mathbb{E}[\widehat{\text{TTE}}] - \text{TTE} = \frac{m}{n} \sum_{i=1}^n \mathbb{I}(|\mathcal{C}(\mathcal{N}_i)| = m) \cdot \frac{1}{k_c^2 + \sum_{C \in \mathcal{C}} \frac{1}{|C|_i}} \cdot \left(k_c \cdot c_{i, \emptyset} - \sum_{C \in \mathcal{C}} \frac{1}{|C|_i} \sum_{j \in \mathcal{N}_i \cap C} c_{i, j} \right);$$

(b) *under Assumption 3, we have the bias bound*

$$|\mathbb{E}[\widehat{\text{TTE}}] - \text{TTE}| \leq \frac{\#\{i : |\mathcal{C}(\mathcal{N}_i)| = m\}}{n} \cdot \frac{B}{k_c/m};$$

(c) *if $|\mathcal{C}(\mathcal{N}_i)| < m$ for all i , then $\widehat{\text{TTE}}$ is unbiased.*

The difference between Lemma 4 and Lemma 12 is that the condition $d_i = n$ is replaced by the condition $|\mathcal{C}(\mathcal{N}_i)| = m$. Crucially, while units with $d_i = n$ are unlikely to exist in real-world graphs, units with $|\mathcal{C}(\mathcal{N}_i)| = m$ may arise in real settings depending on the choice of clustering — e.g., if there are only $m = 2$ or even $m = 10$ clusters — making the bias bound more relevant in this case. We see from the bound of Lemma 12 that the bias is small when there are few such units and increases as the marginal treatment probability k_c/m decreases.

6.2 Variance

Following the template of the previous sections, we now analyze the variance of $\widehat{\text{TTE}}$ under a $\text{GCR}_{\text{Comp}}(\mathcal{C}, k_c)$ design by first identifying when $\theta_i^\top \text{cov}(\widehat{\mathbf{c}}_i, \widehat{\mathbf{c}}_j) \theta_j$ is negative and then bounding γ_i . The following lemma, which characterizes the necessary condition for negative covariance terms, is a cluster-analog of Lemma 5 and can be proven identically.

Lemma 13. *Suppose that $\mathbf{z} \sim \text{GCR}_{\text{Comp}}(\mathcal{C}, k_c)$, Assumption 2 holds with $\beta = 1$, and Assumption 5 holds. Then, for two units $i, j \in [n]$ such that $\mathcal{C}(\mathcal{N}_i) \cap \mathcal{C}(\mathcal{N}_j) = \emptyset$, we have*

$$\text{cov}(\theta_i^\top \widehat{\mathbf{c}}_i, \theta_j^\top \widehat{\mathbf{c}}_j) < 0.$$

Next, as one would expect based on what has come thus far, our computation of γ_i distinguishes the cases where $|\mathcal{C}(\mathcal{N}_i)| < m$ from those where $|\mathcal{C}(\mathcal{N}_i)| = m$.

Lemma 14. *Suppose $\mathbf{z} \sim \text{GCR}_{\text{Comp}}(\mathcal{C}, k_c)$ design and Assumption 2 holds with $\beta = 1$. Then*

$$\gamma_i^2 \lesssim \begin{cases} \frac{(d_i+1)(m-1)|\mathcal{C}(\mathcal{N}_i)|}{(k_c/m)(1-k_c/m)(m-|\mathcal{C}(\mathcal{N}_i)|)} & |\mathcal{C}(\mathcal{N}_i)| < m, \\ \frac{(d_i+1)m^2 \cdot k_c^2}{(k_c^2 + \sum_{C \in \mathcal{C}} 1/|C|_i)^2} & |\mathcal{C}(\mathcal{N}_i)| = m. \end{cases} \quad (19)$$

Note that for units with $|\mathcal{C}(\mathcal{N}_i)| = m$, we have the further bound

$$\frac{m \cdot k_c \cdot \sqrt{d_i + 1}}{k_c^2 + \sum_{C \in \mathcal{C}} 1/|C|_i} \leq \frac{\sqrt{d_i + 1}}{k_c/m}. \quad (20)$$

Comparing (20) to the first case of (19), we see that (20) does not scale with $|\mathcal{C}(\mathcal{N}_i)|$ or with $(m-1)/(m-|\mathcal{C}(\mathcal{N}_i)|)$, and so we expect that γ_i will typically be smaller for units with $|\mathcal{C}(\mathcal{N}_i)| = m$ than those with $|\mathcal{C}(\mathcal{N}_i)| < m$. This means that such units present a bias-variance trade-off: they contribute to the variance less than other units do, but as we have seen in Lemma 12, they contribute to the bias, whereas units with $|\mathcal{C}(\mathcal{N}_i)| < m$ do not.

This bias-variance trade-off for $\widehat{\text{TTE}}$ under a $\text{GCR}_{\text{Comp}}(\mathcal{C}, k_c)$ design is a somewhat unusual phenomenon that differs from those previously observed in the literature. Other estimators are either unbiased for all clusterings \mathcal{C} (e.g., the Horvitz–Thompson estimator of (5)) or biased for all clusterings \mathcal{C} (e.g., the difference in means estimator). For estimators that are unbiased for all clusterings, we typically expect their variances strictly increase as the values of $|\mathcal{C}(\mathcal{N}_i)|$ increase. Here, we instead find that the variance of $\widehat{\text{TTE}}$ increases as the value of $|\mathcal{C}(\mathcal{N}_i)|$ for a node increases, until we reach the threshold $|\mathcal{C}(\mathcal{N}_i)| = m$, at which point the variance decreases and we incur bias instead. This bias-variance trade-off mediated by the quantity $\#\{i : |\mathcal{C}(\mathcal{N}_i)| = m\}$ is, to the best of our knowledge, unique to this setting and our results uncovering these properties are novel to our work. We show in Section 7.3 that the empirical bias of $\widehat{\text{TTE}}$ in simulations shows the dependence on $\#\{i : |\mathcal{C}(\mathcal{N}_i)| = m\}$ predicted by our upper bounds, indicating that our bounds correctly capture the dependence of the bias on the clustering.

Returning to the setting of Corollary 3 where we have a κ -restricted growth assumption on G , it is shown in Ugander et al. [2013] that such an assumption implies that $|\mathcal{C}(\mathcal{N}_i)| \leq \kappa^3$. Thus, a strong enough restricted growth assumption, in particular one with $\kappa^3 < m$, rules out the second case of (19), and give a variance bound like that of Corollary 3.

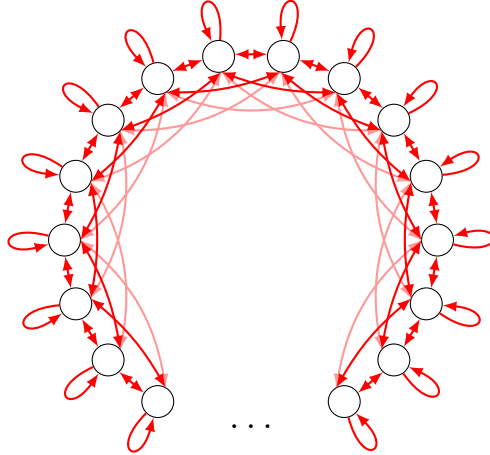


Figure 2: The graph G we consider in our experiments showing that $\widehat{\text{TTE}}$ has lower variance than the Horvitz–Thompson estimator. The graph is the third power of a cycle on $n = 840$ vertices, so that each vertex has degree 7 (3 neighbors on each side, as well as a self-loop).

Corollary 5. *Suppose that $\mathbf{z} \sim \text{GCR}_{\text{Comp}}(\mathcal{C}, k_c)$, that Assumption 2 holds with $\beta = 1$, that Assumption 3 holds for some B , and that $k_c/m < 1/2$. Suppose further that the interference graph G has restricted growth coefficient κ where $\kappa^3 < m$. If the clustering \mathcal{C} is a 3-net of G and each cluster has at most N units, then*

$$\text{var}(\widehat{\text{TTE}}) = O\left(\frac{B^2}{n} \cdot \frac{\kappa^6 N d_{\max}^2}{k_c/m} \cdot \frac{m-1}{m-\kappa^3}\right).$$

This result can be thought of as extending Corollary 3 to the case of complete cluster randomization, up to a factor of $(m-1)/(m-\kappa^3)$.

7 Experiments

In this section, we present a set of experiments to supplement our theoretical results. In Section 7.1, we consider a stylized setting in which the underlying interference graph is a cycle graph and show that the interplay between the low-order assumption and the graph clustering identified in the variance bounds of Section 5 correctly captures the variance of $\widehat{\text{TTE}}$ in simulation. Then, in Section 7.2, we move to a more realistic setting in which we use a mix of stochastic block models and real-world graphs to demonstrate the practical value of the bounds of Section 5 and 6 when choosing the clustering in a graph-cluster randomized experiment. Finally, in Section 7.3, we use one of the stochastic block models of Section 7.2 to show that our bounds on the bias of $\widehat{\text{TTE}}$ in Section 6 reflect the behavior of the bias in simulations.

Through these experiments, we find that our bounds correctly predict the behavior of $\widehat{\text{TTE}}$ in simulation and that they can be used to select a clustering with favorable results.

7.1 Interplay Between Low-Order Modeling and Cluster Randomization

In this section, we empirically verify the results of Section 5 showing that $\widehat{\text{TTE}}$ has lower variance than the Horvitz–Thompson estimator, and that the variance of $\widehat{\text{TTE}}$ depends on the stronger of



Figure 3: The family of clusterings of the cycle graph that we consider. The value of w controls the average cluster-degree $|\mathcal{C}(\mathcal{N}_i)|$. When $w = 1$, we have that $|\mathcal{C}(\mathcal{N}_i)| = d_i = 7$ for all i , while for $w = 7$, the nodes in the center of each cluster have $|\mathcal{C}(\mathcal{N}_i)| = 1$.

the low-order assumption and the graph clustering. We show that these results also hold empirically under a GCR_{Comp} design.

We take the graph G to be a power of the cycle graph on $n = 840$ nodes in which each vertex has degree $d = 7$ because it is connected to itself and the three vertices closest to it on each side; see Figure 2 for an illustration of this network.

We generate responses according to an order- β potential outcome model for $\beta \in \{1, 2, 3, 4\}$. For each choice of β , we set the coefficients $c_{i,S}$ so that

$$c_{i,S} = \binom{d_i}{|S|}^{-1} 2^{-|S|}. \quad (21)$$

With this choice of $c_{i,S}$ the baseline effects $c_{i,\emptyset} = 1$ and each non-empty subset S of size 1 has $c_{i,S} = 1/(2d_i)$, so all subsets of size 1 together contribute $1/2$ to the treatment effect. Similarly, all subsets of size 2 together contribute $1/4$ to the treatment effect, and so on for larger subsets. This response model is thus consistent with the intuition that effects from higher-order subsets should be smaller than effects from lower-order subsets.

We consider a family of clusterings in which contiguous subsets of w adjacent nodes in the cycle are assigned to the same cluster for $w \in \{1, 2, 3, 4, 5, 6, 7, 8\}$ (here w is the “width” of the cluster). Note that such clusterings only exist when w is a divisor of the sample size, hence why we use a sample size of $n = \text{lcm}(1, 2, 3, 4, 5, 6, 7, 8) = 840$ in this experiment.

The choice of w controls the cluster degree, $|\mathcal{C}(\mathcal{N}_i)|$ of each node—when $w = 1$, we have $|\mathcal{C}(\mathcal{N}_i)| = 7$ for all i , since all 7 neighbors are in different clusters. As w increases, there are more nodes with smaller values of $|\mathcal{C}(\mathcal{N}_i)|$, since nodes in the interior of the cluster will be connected to fewer other clusters. For example, when $w = 7$, there are nodes in the center of each cluster with $|\mathcal{C}(\mathcal{N}_i)| = 1$. See Figure 3 for an illustration of these clusterings with $w = 2$ and $w = 4$.

For each choice of w and β we estimate the total treatment effect using both the pseudoinverse estimator and the Horvitz–Thompson estimator with data from a $\text{GCR}_{\text{Bern}}(\mathcal{C}, 0.25)$ and $\text{GCR}_{\text{Comp}}(\mathcal{C}, \lfloor 0.25n/w \rfloor)$ design (here n/w is the number of clusters). For each estimator and each choice of parameters, we calculate the experimental root-mean-squared-error (RMSE) over 1000 trials. The results are plotted in Figure 4.

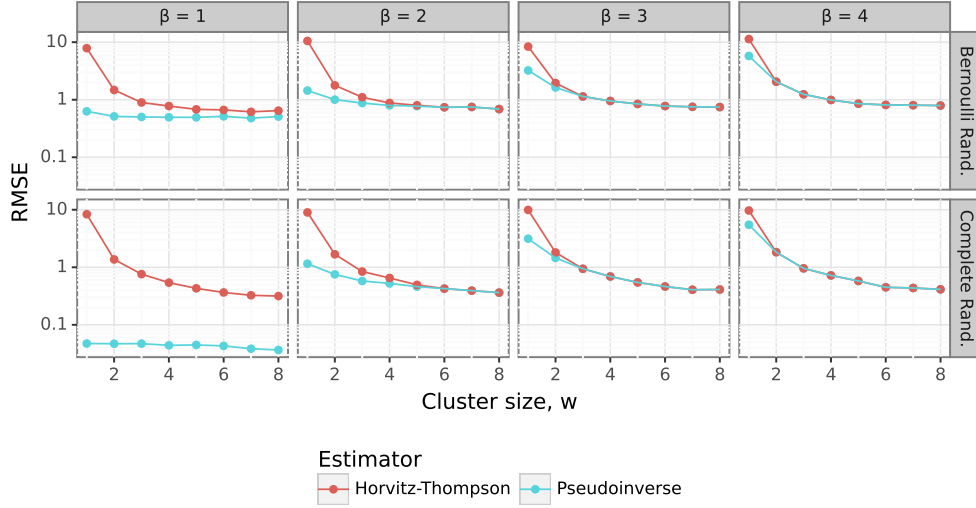


Figure 4: RMSE of the Horvitz–Thompson and pseudoinverse estimators for different values of β and w averaged over 1000 trials. Note that the number of clusters is $m = n/w$. We see across both designs that (a) the pseudoinverse estimator consistently improves on the Horvitz–Thompson estimator; (b) this improvement is largest for small values of w (which are poor clusterings of the graph); (c) the variance of the pseudoinverse is less sensitive to the quality of the clustering for small values of β .

The first row of Figure 4 corroborates both of our theoretical claims about the variance of $\widehat{\text{TTE}}$ under GCR_{Bern} designs. First, we see that across all values of w and β , the variance of $\widehat{\text{TTE}}$ is less than the variance of the Horvitz–Thompson estimator, as shown in Theorem 3. The gap between the two is largest when $\beta = 1$, in which case the low-order assumption is quite strong and offers significant variance reduction, and decreases as β increases (as the low-order assumption becomes weaker). Indeed, if we had $\beta = 7$ (the degree of each node in this graph), $\widehat{\text{TTE}}$ under the $w = 1$ design (which is unit-randomization) would coincide exactly with the Horvitz–Thompson estimator, as shown by Cortez-Rodriguez et al. [2023].

Next, Figure 4 also supports our theoretical arguments that the variance of $\widehat{\text{TTE}}$ depends on the strength of the low-order assumption and the clustering. In the left-most panel, where $\beta = 1$, the variance of $\widehat{\text{TTE}}$ is nearly constant in w . This arises since the $\beta = 1$ assumption is always stronger than any choice of clustering, and so the variance does not vary significantly with the clustering. As β increases, we see more dependence on the cluster size w , since for larger values of w there are more units with smaller values of $|\mathcal{C}(\mathcal{N}_i)|$, and in particular more units with values of $|\mathcal{C}(\mathcal{N}_i)|$ smaller than β . As shown in Lemma 11, these are the units for which the GCR_{Bern} design provides variance reduction beyond what the low-order assumption alone would.

Turning to the second row of Figure 4, we see that the behavior described above also occurs under complete randomization. This suggests that although our theoretical discussion of the relationship between the low-order parameter β and the graph clustering was only for the GCR_{Bern} design, they apply to the GCR_{Comp} design as well.

7.2 Choosing From a Set of Clusters

So far we have focused mainly on using the theory of Section 3 to provide new results on pseudoinverse estimators. In this section, we demonstrate that our bounds are also useful in practice to select cluster assignments. We consider a setting where an analyst has a fixed interference graph and a set of possible candidate clusterings and would like to choose between them without any *a priori* knowledge of the response model. We now describe each aspect of our experimental set-up in greater detail.

Graphs. We consider four graphs, two synthetic graphs and two taken from real-world data. The two synthetic graphs are drawn from a stochastic block model with $n = 500$ units divided into 20 communities. The edge probability within each community is $\pi_{ii} = 0.5$ and the edge probability between communities is $\pi_{ij} = 0$ for the first synthetic graph and $\pi_{ij} = 0.2$ for the second synthetic graph. Thus these two graphs represent a sparse graph of disconnected clusters (and thus with an obvious choice of clustering), and a denser connected graph with a less obvious choice of clustering.

The first real-world graph we consider is taken from Cai et al. [2015]. Following Viviano et al. [2023], who also use this graph in their experiments, we connected two individuals by an edge if at least one of them indicates the other as a friend. This construction can connect individuals in a given village to other individuals outside of their village, since people may indicate a person outside of their village as a friend. We take the largest connected component of this graph, which contains $n = 3677$ individuals with average degree $\bar{d} = 6.25$, suggesting that it is relatively sparse.

The second real-world graph we consider is the Caltech Facebook friendship graph from Traud et al. [2012], also previously used to study graph cluster randomized designs by Ugander and Yin [2023]. We take the largest connected component of this graph, which removes a small number of isolated individuals. This leaves $n = 762$ individuals with average degree $\bar{d} = 44.7$, suggesting that this graph is relatively dense.

Response models. We generate responses according to an order $\beta = 1$ model and use pseudoinverse estimators that (correctly) assume $\beta = 1$. We consider three response models with varying levels of interference and treatment effect sizes. To specify an order $\beta = 1$ model requires specifying the baseline effect, $c_{i,\emptyset}$, and also each of the coefficients $c_{i,\{j\}}$ for $j \in \mathcal{N}_i$. In all three of our response models, we sample $c_{i,\emptyset} \sim N(0.5, 0.1) \cdot d_i/d_{\max}$ to introduce correlation between baseline effects and graph degree, a common feature in real-world data [Basse and Airoidi, 2018b]. The three models differ in how we set $c_{i,\{j\}}$ for $j \in \mathcal{N}_i$:

- *Null model*, $\text{TTE}_i = 0$: in this model, we set $c_{i,\{j\}} = 0$ for all $j \in \mathcal{N}_i$, so the treatment has no effect and there is no interference; this is a null model. The implied form of $Y_i(\mathbf{z})$ is

$$Y_i(\mathbf{z}) = c_{i,\emptyset},$$

for all i , all \mathbf{z} .

- *Weak treatment effect model*, $\text{TTE}_i = 1$: in this model, we set $c_{i,\{j\}} = \frac{1}{2(d_i-1)}$ if $j \neq i$ and $c_{i,\{i\}} = 1/2$. Thus the total treatment effect for each individual, $c_i^\top \theta_i$, is 1, with half the effect coming when the individual is treated, and the other half from interference. The implied form of $Y_i(\mathbf{z})$ is

$$Y_i(\mathbf{z}) = c_{i,\emptyset} + \frac{1}{2}z_i + \sum_{j \in \mathcal{C}(\mathcal{N}_i), j \neq i} \frac{1}{2(d_i-1)}z_j.$$

- *Strong treatment effect model*, $\text{TTE}_i \propto d_i$: in this model, we set $c_{i,\{j\}} = 1/2$ if $j \neq i$, and $c_{i,\{i\}} = d_i/2$. Thus the total treatment effect for each individual, $c_i^\top \theta_i$, is of order d_i , with roughly half the effect coming when the individual is treated, and the other half from interference. The implied form of $Y_i(\mathbf{z})$ is

$$Y_i(\mathbf{z}) = c_{i,\emptyset} + \frac{d_i}{2} z_i + \sum_{j \in \mathcal{C}(\mathcal{N}_i), j \neq i} \frac{1}{2} z_j.$$

Clusterings. We generate the clusterings in our experiment using two different algorithms.

The first algorithm we consider is the Louvain algorithm [Blondel et al., 2008], which has previously been shown to have good performance when designing graph cluster randomized experiments [Karrer et al., 2021]. We vary the resolution parameter of the algorithm across the exponential grid $\{2^{-5}, 2^{-4}, \dots, 2^4, 2^5\}$ to generate 11 clusterings. Clusterings generated with small values of the resolution parameter tend to have one large cluster containing a majority of the nodes, and then several small clusters, while clusterings generated with larger values of the resolution parameter tend to have many small clusters of roughly equal size.

The second algorithm we consider is the METIS algorithm, a balanced partitioning algorithm [Karypis and Kumar, 1998]. This means that, unlike the Louvain algorithm, which is meant to detect communities, METIS returns m clusters of approximately equal size for a user-specified value of m . We generate 10 METIS clusterings by varying m across the grid $\{5, 10, 15, \dots, 45, 50\}$.

Our goal in this experiment is to select from the set of 11 clusterings produced by the Louvain algorithm, as well as from the set of 10 clusterings produced by METIS. Note that we consider these two tasks separately, i.e., we consider first the problem of picking from the set of Louvain clusterings and second the problem of picking from the set of METIS clusterings. Our approach can easily be used to pick from the combined set as well, but we separate the two out to highlight that our approach works well within multiple families of clusterings.

We select a clustering by computing the variance and bias bounds of Section 3 numerically for a GCR_{Bern} design for each clustering, combining these bounds to form a bound on the root-mean-squared-error (RMSE), and then selecting the clustering with the lowest bound. When computing these bounds, we numerically evaluate the quadratic form $\theta_i^\top \mathbb{E}[\tilde{\mathbf{z}}\tilde{\mathbf{z}}^\top]^\dagger \theta_i$ and then evaluate (10), rather than using the upper bounds on γ_i given in Section 5. Those bounds were necessary for our theoretical results, but are needlessly loose when selecting a clustering. We refer to the chosen clustering as $\hat{\mathcal{C}}^*$, since it approximates an oracle clustering \mathcal{C}^* defined below. Note that $\hat{\mathcal{C}}^*$ does not depend on the response model.

Then, for each response model and clustering, we simulate $N = 1000$ replications of a $\text{GCR}_{\text{Bern}}(\mathcal{C}, 0.25)$ design for each clustering \mathcal{C} to estimate the true RMSE, and identify the clustering with the true lowest RMSE, which we refer to as \mathcal{C}^* . Note that \mathcal{C}^* may vary from one response model to another since different designs will perform well under different response models. Then, we evaluate our selection by computing

$$\frac{\text{Monte Carlo RMSE of } \text{GCR}_{\text{Bern}}(\hat{\mathcal{C}}^*, 0.2)}{\text{Monte Carlo RMSE of } \text{GCR}_{\text{Bern}}(\mathcal{C}^*, 0.2)}, \quad (22)$$

for each response model. This metric will be close to 1 if we have selected a nearly optimal clustering for that response model and small if we have not.

Clustering	Graph	TTE _i = 0		TTE _i = 1		TTE ∝ d _i	
		Ber.	Comp.	Ber.	Comp.	Ber.	Comp.
Louvain	SBM(0.5, 0)	1.000	1.000	1.000	1.000	1.000	1.000
	SBM(0.5, 0.2)	1.000	0.356	1.000	0.682	1.000	1.000
	Cai et al.	1.000	1.000	0.841	0.973	0.903	1.000
	Caltech	1.000	0.512	0.986	0.385	1.000	0.433
METIS	SBM(0.5, 0)	1.000	0.618	1.000	0.969	1.000	0.966
	SBM(0.5, 0.2)	1.000	0.834	1.000	0.966	1.000	1.000
	Cai et al.	1.000	0.971	1.000	0.291	1.000	0.832
	Caltech	1.000	0.824	1.000	1.000	1.000	1.000

Table 4: Ratio of RMSE when using clustering selected by minimizing an upper bound on the RMSE to RMSE when using oracle optimal clustering for each response model, for each graph and randomization strategy. We see that the chosen clustering is consistently very close to optimal for Bernoulli randomization, and generally also good for complete randomization.

Finally, we repeat the above process for completely randomized designs by selecting a clustering based on the GCR_{Comp} RMSE bound, then running a $\text{GCR}_{\text{Comp}}(\mathcal{C}, [0.25|\mathcal{C}|])$ design for each clustering, which treats 25% of the clusters completely at random, and finally computing the same ratio as in (22).

Results. The ratios in (22) for each of the settings, as well as for the GCR_{Comp} design, are given in Table 4. We discuss the results for the Louvain clusterings first. In this case, we see that for the two sparser graphs, the SBM(0.5, 0) and the graph of Cai et al. [2015], we consistently select nearly optimal clusterings. For the denser graphs, SBM(0.5, 0.2) and the Caltech graph, we continue to select nearly optimal clusterings for the GCR_{Bern} design, but do slightly worse for the GCR_{Comp} design. In the case of the SBM(0.5, 0.2), this is a consequence of different clusterings being favorable for different response models—our chosen design is optimal for the $\text{TTE}_i \propto d_i$ response model, but not the others. This trade-off is fundamental to the problem of experimental design and is not a drawback of our particular approach. On the other hand, for the Caltech graph, the selected clustering $\hat{\mathcal{C}}^*$ has weak performance across all outcome models, suggesting that our bounds are not as informative in this case.

We also see generally similar trends in the results for the METIS clusterings. We consistently select clusterings that are optimal across all response models for the GCR_{Bern} design, while for the GCR_{Comp} design, we select clusterings that are nearly optimal for some response models, but may not perform as well under certain response models. As mentioned above, this reflects a trade-off inherent to the experimental design problem—our bounds optimize the worst-case RMSE over a class of response models, but this does not mean that the clusterings for which our bounds are small are optimal for all response models.

Next, we further visualize the results of this experiment in Figure 5, which shows the empirical RMSE and theoretical RMSE bounds in each of the two stochastic block models as a function of the resolution parameter. In the SBM(0.5, 0) graph, the Louvain algorithm identifies the correct clustering into communities for a wide range of resolution parameters, and our bounds correctly identify that this is the optimal clustering. In the SBM(0.5, 0.2) graph, the optimal clustering for the GCR_{Bern} design is obtained for a small value of the resolution parameter, and our bound also

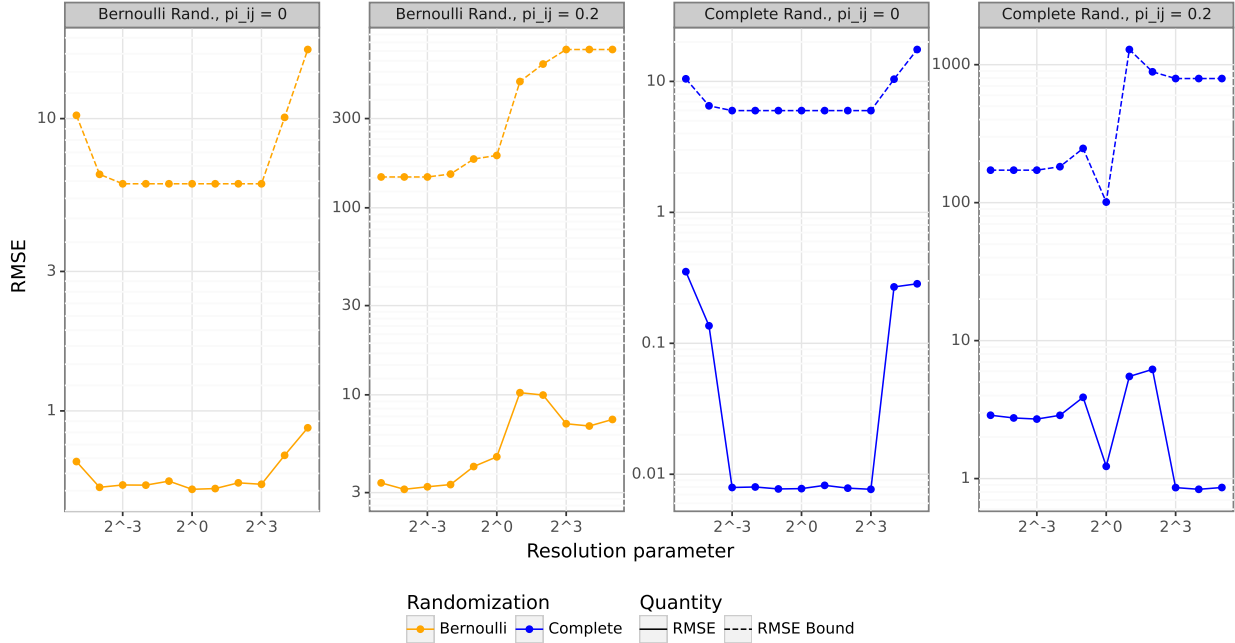


Figure 5: Visualization of our theoretical RMSE bounds (dashed) and actual RMSE in simulation (solid) across a range of Louvain algorithm resolution parameters for the SBM(0.5,0) and SBM(0.5,0.2) graphs under a GCR_{Bern} design (orange) and GCR_{Comp} design (blue) and the $\text{TTE}_i = 1$ response model. We see that the qualitative shape of our bounds correctly reflects the dependence of the RMSE on the resolution parameter.

correctly identifies this. For the GCR_{Comp} design, our bound selects a local minimum that is not the global minimum in this response model, but is the global minimum in the $\text{TTE}_i \propto d_i$ response model, as seen in the second row of Table 4.

Taken together, Table 4 and Figure 5 show that our bounds correctly capture the dependence of the RMSE when using a $\text{GCR}_{\text{Bern}}(\mathcal{C}, p)$ or $\text{GCR}_{\text{Comp}}(\mathcal{C}, k_c)$ on the clustering \mathcal{C} , and that using our bounds to select a clustering gives favorable results in practice.

7.3 Bias in the GCR_{Comp} Design

In this section, we experimentally verify the theoretical results of Section 6 on the bias-variance trade-off exhibited by $\widehat{\text{TTE}}$ under a GCR_{Comp} design. We do this by focusing on a single one of the settings considered in Section 7.2, namely the METIS clusterings of the SBM(0.5,0.2) graph, with responses generated so that $\text{TTE}_i = 1$. For each of these clusterings, we compute the number of units with $|\mathcal{C}(\mathcal{N}_i)| = m$, which is the quantity that Lemma 12 indicated would control the bias, as well as the bias, variance, and RMSE in simulation. The results are shown in Figure 6.

We see in Figure 6 that, as predicted by the bound of Lemma 12, the bias of $\widehat{\text{TTE}}$ decreases as $|\{i : |\mathcal{C}(\mathcal{N}_i)| = m\}|$ decreases, while the variance of $\widehat{\text{TTE}}$ increases. This creates a bias-variance trade-off in the RMSE, leading to a local minimum when using the METIS clustering into $m = 20$ clusters. Furthermore, we see in row six of Table 4 that our bounds select a clustering that has nearly optimal RMSE for this graph and response model, meaning that our bounds are able to effectively guide a practitioner in navigating this bias-variance trade-off.

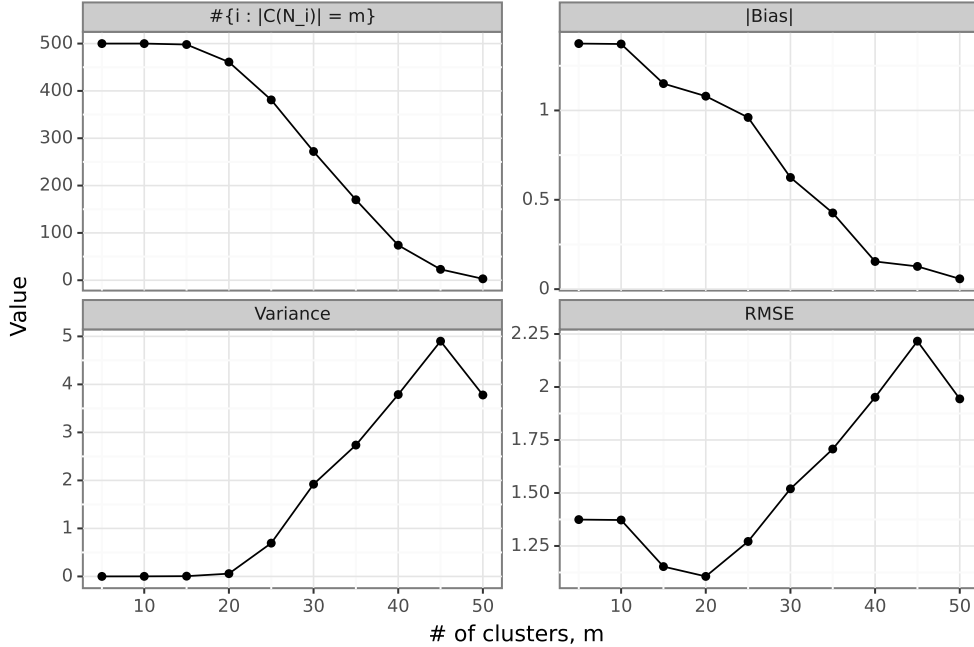


Figure 6: The value of $\{i : |\mathcal{C}(\mathcal{N}_i)| = m\}$ (i.e., the number of nodes that have a neighbor in each of the m clusters), as well as bias, variance, and RMSE in simulation for each METIS clustering of the SBM(0.5, 0.2) graph. Each cluster has size approximately n/m . As predicted by our theory, the bias decreases as $\{i : |\mathcal{C}(\mathcal{N}_i)| = m\}$ decreases, while the variance increases, leading to a bias-variance trade-off and local minimum in the RMSE.

8 Conclusion

We have presented an estimator for the total treatment effect in a low-order model, given bounds on the bias and variance of this estimator for general experimental designs, and shown how those bounds can be used to obtain new theoretical results and also inform the design of clustered experiments.

One possible future direction that builds directly on our results is to better understand the dependence of γ_i in Theorem 2 on the experimental design. The value of the quadratic form $\theta_i \mathbb{E}[\tilde{\mathbf{z}}_i \tilde{\mathbf{z}}_i^\top]^\dagger \theta_i$ will depend on the spectral properties of $\mathbb{E}[\tilde{\mathbf{z}}_i \tilde{\mathbf{z}}_i^\top]$, and further analyzing this dependence would shed further light on the variance properties of $\widehat{\text{TTE}}$ under different designs.

More generally, there are many natural extensions of the low-order model itself. For example, one could encode further constraints on the \mathbf{c}_i , such as the fact that direct effects are typically larger than indirect effects or that higher-order effects are typically smaller than lower order effects, into the estimation procedure. Taking a step further back, one could also constrain the potential outcomes $Y_i(\mathbf{z})$ to lie in a different subspace by constraining the vectors \mathbf{c}_i to be “low-order” in some other basis. We view the current work as a preliminary step in understanding the value of thinking of $Y_i(\mathbf{z})$ as a structured polynomial in \mathbf{z} and are eager to see further development of this perspective.

Acknowledgements. This work was supported in part by NSF grant #CNS-1955997, AFOSR grant #FA9550-23-1-0301, and by NSF CAREER Award #2143176.

References

- Peter M Aronow and Cyrus Samii. Estimating average causal effects under general interference, with application to a social network experiment. *Annals of Applied Statistics*, 11(4):1912–1947, 2017.
- Falco J Bargagli-Stoffi, Costanza Tortu, and Laura Forastiere. Heterogeneous treatment and spillover effects under clustered network interference. *arXiv preprint arXiv:2008.00707*, 2020.
- Guillaume W Basse and Edoardo M Airoldi. Limitations of design-based causal inference and a/b testing under arbitrary and network interference. *Sociological Methodology*, 48(1):136–151, 2018a.
- Guillaume W Basse and Edoardo M Airoldi. Model-assisted design of experiments in the presence of network-correlated outcomes. *Biometrika*, 105(4):849–858, 2018b.
- Vincent D Blondel, Jean-Loup Guillaume, Renaud Lambiotte, and Etienne Lefebvre. Fast unfolding of communities in large networks. *Journal of statistical mechanics: theory and experiment*, 2008(10):P10008, 2008.
- Jing Cai, Alain De Janvry, and Elisabeth Sadoulet. Social networks and the decision to insure. *American Economic Journal: Applied Economics*, 7(2):81–108, 2015.
- Ozan Candogan, Chen Chen, and Rad Niazadeh. Correlated cluster-based randomized experiments: Robust variance minimization. *Management Science*, 2023.
- Alex Chin. Regression adjustments for estimating the global treatment effect in experiments with interference. *Journal of Causal Inference*, 7(2), 2019.
- David Choi. Estimation of monotone treatment effects in network experiments. *Journal of the American Statistical Association*, 112(519):1147–1155, 2017.
- Mayleen Cortez, Matthew Eichhorn, and Christina Lee Yu. Graph agnostic estimators with staggered rollout designs under network interference. *Advances in Neural Information Processing Systems*, 2022.
- Mayleen Cortez-Rodriguez, Matthew Eichhorn, and Christina Lee Yu. Exploiting neighborhood interference with low-order interactions under unit randomized design. *Journal of Causal Inference*, 11(1):20220051, 2023.
- Dean Eckles, Brian Karrer, and Johan Ugander. Design and analysis of experiments in networks: Reducing bias from interference. *Journal of Causal Inference*, 5(1):20150021, 2017.
- Huan Gui, Ya Xu, Anmol Bhasin, and Jiawei Han. Network a/b testing: From sampling to estimation. In *Proceedings of the 24th International Conference on World Wide Web*, pages 399–409, 2015.
- Kevin Han and Johan Ugander. Model-based regression adjustment with model-free covariates for network interference. *Journal of Causal Inference*, 11(1):20230005, 2023.
- Christopher Harshaw, Fredrik Sävje, and Yitan Wang. A design-based riesz representation framework for randomized experiments. *arXiv preprint arXiv:2210.08698*, 2022.
- David Holtz and Sinan Aral. Limiting bias from test-control interference in online marketplace experiments. *arXiv preprint arXiv:2004.12162*, 2020.

- David Holtz, Felipe Lobel, Ruben Lobel, Inessa Liskovich, and Sinan Aral. Reducing interference bias in online marketplace experiments using cluster randomization: Evidence from a pricing meta-experiment on airbnb. *Management Science*, 2024.
- Daniel G Horvitz and Donovan J Thompson. A generalization of sampling without replacement from a finite universe. *Journal of the American Statistical Association*, 47(260):663–685, 1952.
- Yuchen Hu, Shuangning Li, and Stefan Wager. Average direct and indirect causal effects under interference. *Biometrika*, 109(4):1165–1172, 2022.
- Brian Karrer, Liang Shi, Monica Bhole, Matt Goldman, Tyrone Palmer, Charlie Gelman, Mikael Konutgan, and Feng Sun. Network experimentation at scale. In *Proceedings of the 27th acm sigkdd conference on knowledge discovery & data mining*, pages 3106–3116, 2021.
- George Karypis and Vipin Kumar. A fast and high quality multilevel scheme for partitioning irregular graphs. *SIAM Journal on scientific Computing*, 20(1):359–392, 1998.
- Michael P Leung. Causal inference under approximate neighborhood interference. *Econometrica*, 90(1):267–293, 2022a.
- Michael P Leung. Rate-optimal cluster-randomized designs for spatial interference. *The Annals of Statistics*, 50(5):3064–3087, 2022b.
- Michael P Leung. Design of cluster-randomized trials with cross-cluster interference. *arXiv preprint arXiv:2310.18836*, 2023.
- Hannah Li, Geng Zhao, Ramesh Johari, and Gabriel Y Weintraub. Interference, bias, and variance in two-sided marketplace experimentation: Guidance for platforms. In *Proceedings of the ACM Web Conference 2022*, pages 182–192, 2022.
- Shuangning Li and Stefan Wager. Random graph asymptotics for treatment effect estimation under network interference. *The Annals of Statistics*, 50(4):2334–2358, 2022.
- Charles F Manski. Identification of treatment response with social interactions. *The Econometrics Journal*, 16(1):S1–S23, 2013.
- Ben M Parker, Steven G Gilmour, and John Schormans. Optimal design of experiments on connected units with application to social networks. *Journal of the Royal Statistical Society. Series C (Applied Statistics)*, pages 455–480, 2017.
- Jean Pouget-Abadie, Vahab Mirrokni, David C Parkes, and Edoardo M Airoidi. Optimizing cluster-based randomized experiments under monotonicity. In *Proceedings of the 24th ACM SIGKDD International Conference on Knowledge Discovery & Data Mining*, pages 2090–2099, 2018.
- Daniel L Sussman and Edoardo M Airoidi. Elements of estimation theory for causal effects in the presence of network interference. *arXiv preprint arXiv:1702.03578*, 2017.
- Panos Toulis and Edward Kao. Estimation of causal peer influence effects. In *International conference on machine learning*, pages 1489–1497. PMLR, 2013.
- Amanda L Traud, Peter J Mucha, and Mason A Porter. Social structure of facebook networks. *Physica A: Statistical Mechanics and its Applications*, 391(16):4165–4180, 2012.

Johan Ugander and Hao Yin. Randomized graph cluster randomization. *Journal of Causal Inference*, 11(1):20220014, 2023.

Johan Ugander, Brian Karrer, Lars Backstrom, and Jon Kleinberg. Graph cluster randomization: Network exposure to multiple universes. In *Proceedings of the 19th ACM SIGKDD international conference on Knowledge discovery and data mining*, pages 329–337, 2013.

Davide Viviano, Lihua Lei, Guido Imbens, Brian Karrer, Okke Schrijvers, and Liang Shi. Causal clustering: design of cluster experiments under network interference. *arXiv preprint arXiv:2310.14983*, 2023.

Christina Lee Yu, Edoardo Airoldi, Christian Borgs, and Jennifer Chayes. Estimating total treatment effect in randomized experiments with unknown network structure. *Proceedings of the National Academy of Sciences*, 2022.

A Proofs from Section 3

Proof of Theorem 1

Proof. Recall that our estimate of the TTE for unit i is $\widehat{\mathbf{c}}_i^T \theta_i$ where $\widehat{\mathbf{c}}_i^T = M_i^\dagger \tilde{\mathbf{z}}_i \tilde{\mathbf{z}}_i^T \mathbf{c}_i$ and $M_i = \mathbb{E}[\tilde{\mathbf{z}}_i \tilde{\mathbf{z}}_i^T]$. Then, we write

$$\mathbb{E}[\widehat{\mathbf{c}}_i^T \theta_i] - \mathbf{c}_i^T \theta_i = (\mathbb{E}[\widehat{\mathbf{c}}_i] - \mathbf{c}_i)^T \theta_i, \quad (23)$$

$$= \left(M_i^\dagger M_i \mathbf{c}_i - \mathbf{c}_i \right)^T \theta_i, \quad (24)$$

$$= \mathbf{c}_i^T (M_i^\dagger M_i - I) \theta_i \quad (25)$$

and summing over i gives (a).

For (b), we have by Cauchy-Schwarz that $\mathbf{c}_i^T (M_i^\dagger M_i - I) \theta_i \leq \|\mathbf{c}_i\|_2 \cdot \|(M_i^\dagger M_i - I) \theta_i\|_2$ and applying Assumption 3 and summing over i gives the result. For (c), we have that $M_i^\dagger M_i \theta_i = \theta_i$ for θ_i in the column space of M_i , and the result follows. \square

Proof of Theorem 2

Proof. As noted in the main text, we have that $\text{var}(\widehat{\text{TTE}})$ is

$$= \frac{1}{n^2} \sum_{i,j=1}^n \text{cov}(\widehat{\mathbf{c}}_i^T \theta_i, \widehat{\mathbf{c}}_j^T \theta_j), \quad (26)$$

$$= \frac{1}{n^2} \sum_{i,j=1}^n \left[\text{cov}(\widehat{\mathbf{c}}_i^T \theta_i, \widehat{\mathbf{c}}_j^T \theta_j) \cdot \mathbb{I}(\text{cov}(\widehat{\mathbf{c}}_i^T \theta_i, \widehat{\mathbf{c}}_j^T \theta_j) > 0) + \text{cov}(\widehat{\mathbf{c}}_i^T \theta_i, \widehat{\mathbf{c}}_j^T \theta_j) \cdot \mathbb{I}(\text{cov}(\widehat{\mathbf{c}}_i^T \theta_i, \widehat{\mathbf{c}}_j^T \theta_j) \leq 0) \right], \quad (27)$$

$$\leq \frac{1}{n^2} \sum_{i,j=1}^n \text{cov}(\widehat{\mathbf{c}}_i^T \theta_i, \widehat{\mathbf{c}}_j^T \theta_j) \cdot \mathbb{I}(\text{cov}(\widehat{\mathbf{c}}_i^T \theta_i, \widehat{\mathbf{c}}_j^T \theta_j) > 0), \quad (28)$$

$$\leq \frac{1}{n^2} \sum_{i,j=1}^n \text{cov}(\widehat{\mathbf{c}}_i^T \theta_i, \widehat{\mathbf{c}}_j^T \theta_j) \cdot \mathbb{I}(\tilde{\mathbf{z}}_i \not\perp \tilde{\mathbf{z}}_j), \quad (29)$$

so it is sufficient to bound $\theta_i^\top \text{cov}(\widehat{\mathbf{c}}_i, \widehat{\mathbf{c}}_j) \theta_j$ for arbitrary i, j . Letting $M_i = \tilde{\mathbf{z}}_i \tilde{\mathbf{z}}_i^\top$ for convenience, we compute

$$\text{cov}(\widehat{\mathbf{c}}_i, \widehat{\mathbf{c}}_j) = \mathbb{E} \left[\mathbb{E}[M_i]^\dagger M_i \mathbf{c}_i \mathbf{c}_j^\top M_j^\top \mathbb{E}[M_j]^\dagger \right] - \mathbf{c}_i \mathbf{c}_j^\top, \quad (30)$$

so that

$$\theta_i^\top \text{cov}(\widehat{\mathbf{c}}_i, \widehat{\mathbf{c}}_j) \theta_j = \mathbb{E} \left[\theta_i^\top \mathbb{E}[M_i]^\dagger M_i \mathbf{c}_i \cdot \mathbf{c}_j^\top M_j \mathbb{E}[M_j]^\dagger \theta_j \right] - (\theta_i^\top \mathbf{c}_i)(\theta_j^\top \mathbf{c}_j), \quad (31)$$

$$\leq \mathbb{E} \left[\theta_i^\top \mathbb{E}[M_i]^\dagger M_i \mathbf{c}_i \cdot \mathbf{c}_j^\top M_j \mathbb{E}[M_j]^\dagger \theta_j \right], \quad (\text{same sign assumption})$$

$$= \mathbb{E} \left[(M_i \mathbb{E}[M_i]^\dagger \theta_i)^\top \mathbf{c}_i \cdot \mathbf{c}_j^\top M_j \mathbb{E}[M_j]^\dagger \theta_j \right], \quad (32)$$

$$\leq \mathbb{E} \left[\|M_i \mathbb{E}[M_i]^\dagger \theta_i\|_2 \|\mathbf{c}_i\|_2 \cdot \|M_j \mathbb{E}[M_j]^\dagger \theta_j\|_2 \|\mathbf{c}_j\|_2 \right], \quad (\text{Cauchy-Schwarz})$$

$$\leq \|\mathbf{c}_i\|_2 \|\mathbf{c}_j\|_2 \mathbb{E} \left[\|M_i \mathbb{E}[M_i]^\dagger \theta_i\|_2^2 \right]^{1/2} \mathbb{E} \left[\|M_j \mathbb{E}[M_j]^\dagger \theta_j\|_2^2 \right]^{1/2}, \quad (\text{Cauchy-Schwarz})$$

$$\leq B^2 \mathbb{E} \left[\|M_i \mathbb{E}[M_i]^\dagger \theta_i\|_2^2 \right]^{1/2} \mathbb{E} \left[\|M_j \mathbb{E}[M_j]^\dagger \theta_j\|_2^2 \right]^{1/2}. \quad (\text{boundedness})$$

Next, we further upper bound

$$\mathbb{E} \left[\|M_i \mathbb{E}[M_i]^\dagger \theta_i\|_2^2 \right] = \mathbb{E} \left[\|\tilde{\mathbf{z}}_i \tilde{\mathbf{z}}_i^\top \mathbb{E}[M_i]^\dagger \theta_i\|_2^2 \right], \quad (33)$$

$$= \mathbb{E} \left[\|\tilde{\mathbf{z}}_i\|_2^2 (\tilde{\mathbf{z}}_i^\top \mathbb{E}[M_i]^\dagger \theta_i)^2 \right], \quad (34)$$

$$\leq |\mathcal{S}_i| \mathbb{E} \left[\theta_i^\top \mathbb{E}[M_i]^\dagger \tilde{\mathbf{z}}_i \tilde{\mathbf{z}}_i^\top \mathbb{E}[M_i]^\dagger \theta_i \right], \quad (35)$$

$$= |\mathcal{S}_i| \cdot \theta_i^\top \mathbb{E}[M_i]^\dagger \theta_i. \quad (36)$$

Thus, with $\gamma_i = \sqrt{|\mathcal{S}_i| \cdot \theta_i^\top \mathbb{E}[M_i]^\dagger \theta_i}$, we have $\theta_i^\top \text{cov}(\widehat{\mathbf{c}}_i, \widehat{\mathbf{c}}_j) \theta_j \leq B^2 \cdot \gamma_i \gamma_j$, and substituting this bound into (29) completes the proof. \square

B Proofs from Section 4

Proof of Lemma 1

Before proving Lemma 1 we must first evaluate the quadratic form $\theta_i^\top \mathbb{E}_{\mathbf{z}} [\tilde{\mathbf{z}}_i \tilde{\mathbf{z}}_i^\top]^\dagger \theta_i$.

Lemma 15. *Suppose that $\mathbf{z} \sim \text{Bern}(p)$. Then, for a node of degree d_i ,*

$$\theta_i^\top \mathbb{E}_{\mathbf{z}} [\tilde{\mathbf{z}}_i \tilde{\mathbf{z}}_i^\top]^\dagger \theta_i = \sum_{u=1}^{\min(\beta, d_i)} \binom{d_i}{u} \left[\left(\frac{1-p}{p} \right)^u - 2(-1)^u + \left(\frac{p}{1-p} \right)^u \right].$$

Proof. Using the formula for the entries of the design matrix pseudoinverse given in (11), we may simplify this quadratic form

$$\theta_i^\top \mathbb{E}_{\mathbf{z}} [\tilde{\mathbf{z}}_i \tilde{\mathbf{z}}_i^\top]^\dagger \theta_i = \sum_{\substack{S \in \mathcal{S}_i^\beta \\ S \neq \emptyset}} \sum_{\substack{T \in \mathcal{S}_i^\beta \\ T \neq \emptyset}} \left(\frac{-1}{p} \right)^{|S|+|T|} \sum_{\substack{U \in \mathcal{S}_i^\beta \\ (S \cup T) \subseteq U}} \left(\frac{p}{1-p} \right)^{|U|}.$$

Let us define $u = |U|$, $a = |S \cap T|$, $b = |S \setminus T|$, and $c = |T \setminus S|$. Note that $a + b = |S|$ and $a + c = |T|$. Finally, for ease of notation, let us define $m = \min(\beta, d_i)$. Then, we can rewrite our quadratic form:

$$\sum_{u=1}^m \binom{d_i}{u} \left(\frac{p}{1-p}\right)^u \sum_{a=0}^u \binom{u}{a} \sum_{b=0}^{u-a} \binom{u-a}{b} \sum_{c=0}^{u-a-b} \binom{u-a-b}{c} \mathbb{I}(a+b \geq 1) \mathbb{I}(a+c \geq 1) \left(\frac{-1}{p}\right)^{2a+b+c}.$$

Now, there are two possible cases in which this indicator is non-zero.

Case 1: $a = 0$; $b, c \geq 1$

In this case, we may further simplify the quadratic form:

$$\begin{aligned} & \sum_{u=1}^m \binom{d_i}{u} \left(\frac{p}{1-p}\right)^u \sum_{b=1}^u \binom{u}{b} \left(\frac{-1}{p}\right)^b \sum_{c=1}^{u-b} \binom{u-b}{c} \left(\frac{-1}{p}\right)^c \\ &= \sum_{u=1}^m \binom{d_i}{u} \left(\frac{p}{1-p}\right)^u \sum_{b=1}^u \binom{u}{b} \left(\frac{-1}{p}\right)^b \left[\left(\frac{p-1}{p}\right)^{u-b} - 1 \right] && \text{(binomial theorem)} \\ &= \sum_{u=1}^m \binom{d_i}{u} \left(\frac{p}{1-p}\right)^u \left[\left(\frac{p-2}{p}\right)^u - 2\left(\frac{p-1}{p}\right)^u + 1 \right] && \text{(binomial theorem)} \end{aligned}$$

Case 2: $a \geq 1$

In this case, we may further simplify the quadratic form:

$$\begin{aligned} & \sum_{u=1}^m \binom{d_i}{u} \left(\frac{p}{1-p}\right)^u \sum_{a=1}^u \binom{u}{a} \left(\frac{1}{p^2}\right)^a \sum_{b=0}^{u-a} \binom{u-a}{b} \left(\frac{-1}{p}\right)^b \sum_{c=0}^{u-a-b} \binom{u-a-b}{c} \left(\frac{-1}{p}\right)^c \\ &= \sum_{u=1}^m \binom{d_i}{u} \left(\frac{p}{1-p}\right)^u \sum_{a=1}^u \binom{u}{a} \left(\frac{1}{p^2}\right)^a \sum_{b=0}^{u-a} \binom{u-a}{b} \left(\frac{-1}{p}\right)^b \left(\frac{p-1}{p}\right)^{u-a-b} && \text{(binomial theorem)} \\ &= \sum_{u=1}^m \binom{d_i}{u} \left(\frac{p}{1-p}\right)^u \sum_{a=1}^u \binom{u}{a} \left(\frac{1}{p^2}\right)^a \left(\frac{p-2}{p}\right)^{u-a} && \text{(binomial theorem)} \\ &= \sum_{u=1}^m \binom{d_i}{u} \left(\frac{p}{1-p}\right)^u \left[\left(\frac{p-1}{p}\right)^{2u} - \left(\frac{p-2}{p}\right)^u \right] && \text{(binomial theorem)} \end{aligned}$$

Combining the two cases, our quadratic form simplifies to

$$\begin{aligned} & \sum_{u=1}^m \binom{d_i}{u} \left(\frac{p}{1-p}\right)^u \left[\left(\frac{p-1}{p}\right)^{2u} - 2\left(\frac{p-1}{p}\right)^u + 1 \right] \\ &= \sum_{u=1}^m \binom{d_i}{u} \left[\left(\frac{1-p}{p}\right)^u - 2(-1)^u + \left(\frac{p}{1-p}\right)^u \right]. \end{aligned}$$

□

We will also need the following technical lemma.

Lemma 16. For any $\beta, d \in \mathbb{N}$ with $0 < \beta < d$, we have

$$\sum_{k=0}^{\beta} \binom{d}{k} \leq 2d^{\beta}.$$

Proof. We compute

$$\sum_{k=0}^{\beta} \binom{d}{k} \leq \sum_{k=0}^{\beta} d^k = \frac{d^{\beta+1} - 1}{d - 1} \leq d^{\beta} \cdot \frac{d}{d - 1} \leq 2d^{\beta}.$$

□

Now, we are ready to prove Lemma 1.

Lemma 1. Suppose that $p \leq 1/2$ and $\mathbf{z} \sim \text{Bern}(p)$. Then, for a node of degree d_i ,

$$\gamma_i^2 \leq \begin{cases} 4d_i^{\beta} \cdot p^{-d_i} & d_i \leq \beta, \\ 16d_i^{2\beta} \cdot p^{-\beta} & d_i > \beta. \end{cases} \quad (13)$$

Proof. Recall that $\gamma_i = \sqrt{|\mathcal{S}_i^{\beta}| \cdot \theta_i^{\top} \mathbb{E}[\tilde{\mathbf{z}}_i \tilde{\mathbf{z}}_i^{\top}] \dagger \theta_i}$. To bound γ_i^2 , we must bound $|\mathcal{S}_i^{\beta}|$ (which was done in Lemma 16) and $\theta_i^{\top} \mathbb{E}[\tilde{\mathbf{z}} \tilde{\mathbf{z}}^{\top}] \dagger \theta_i$.

For $\theta_i^{\top} \mathbb{E}[\tilde{\mathbf{z}} \tilde{\mathbf{z}}^{\top}] \dagger \theta_i$, we consider cases on the result of Lemma 15. When $d_i \leq \beta$, we have

$$\begin{aligned} \theta_i^{\top} \mathbb{E}[\tilde{\mathbf{z}} \tilde{\mathbf{z}}^{\top}] \dagger \theta_i &= \sum_{u=1}^{d_i} \binom{d_i}{u} \left[\left(\frac{p}{1-p} \right)^u - 2(-1)^u + \left(\frac{1-p}{p} \right)^u \right] \\ &= \left(1 + \frac{p}{1-p} \right)^{d_i} - 1 - 2(-1) + \left(1 + \frac{1-p}{p} \right)^{d_i} - 1, \\ &= \left(\frac{1}{1-p} \right)^{d_i} + \left(\frac{1}{p} \right)^{d_i} \\ &\leq 2p^{-d_i} \end{aligned} \quad (37)$$

On the other hand, when $d_i > \beta$, our assumption that $p \leq 1/2$ ensures that $p/(1-p) \leq 1$ and $(1-p)/p \geq 1$. Thus,

$$\begin{aligned} \theta_i^{\top} \mathbb{E}[\tilde{\mathbf{z}} \tilde{\mathbf{z}}^{\top}] \dagger \theta_i &= \sum_{u=1}^{\beta} \binom{d_i}{u} \left[\left(\frac{p}{1-p} \right)^u - 2(-1)^u + \left(\frac{1-p}{p} \right)^u \right] \\ &\leq \sum_{u=1}^{\beta} \binom{d_i}{u} [1 + 2 + p^{-\beta}] \\ &\leq 4p^{-\beta} \sum_{u=1}^{\beta} \binom{d_i}{u} \\ &\leq 8p^{-\beta} d_i^{\beta} \end{aligned} \quad (38)$$

Combining (37) and (38) with the fact that $|\mathcal{S}_i^{\beta}| \leq 2d_i^{\beta}$ from Lemma 16 completes the proof. □

Proof of Corollary 1

Proof. For each i there are at most d_{\max}^2 non-zero terms in the bound of (10). Furthermore, we can uniformly upper bound the value of each γ_i by $d_{\max}^{2\beta} p^{-\beta}$. Plugging into (10), we find that

$$\text{var}(\widehat{\text{TTE}}) = O\left(\frac{B^2}{n^2} \cdot n \cdot d_{\max}^2 \cdot d_{\max}^{2\beta} p^{-\beta}\right) = O\left(\frac{B^2 d_{\max}^{2\beta+2}}{n p^\beta}\right).$$

□

Proof of Lemma 2

Proof. We carry out a cofactor expansion of this determinant. Throughout the proof, we let $\mathbf{1}_{x \times y}$ denote the $x \times y$ (sub)matrix of all 1s, and \mathbf{I}_x denote the $x \times x$ identity (sub)matrix. For each $x \in \mathbb{N}$, we also recursively define the $x \times x$ matrices

$$\mathbf{A}_x = \underbrace{\begin{bmatrix} 1 & \frac{k-1}{n-1} \cdot \mathbf{1}_{1 \times (x-1)} \\ \frac{k-1}{n-1} \cdot \mathbf{1}_{(x-1) \times 1} & \mathbf{A}_{x-1} \end{bmatrix}}_{\frac{k-1}{n-1} \cdot \mathbf{1}_{x \times x} + \frac{n-k}{n-1} \cdot \mathbf{I}_x}, \quad \mathbf{B}_x = \begin{bmatrix} 1 & \frac{k-1}{n-1} \cdot \mathbf{1}_{1 \times (x-1)} \\ \mathbf{1}_{(x-1) \times 1} & \mathbf{A}_{x-1} \end{bmatrix}.$$

Note that

$$\mathbb{E}_{\mathbf{z}} [\tilde{\mathbf{z}}_i \tilde{\mathbf{z}}_i^\top] = \begin{bmatrix} 1 & \frac{k}{n} \cdot \mathbf{1}_{1 \times d_i} \\ \frac{k}{n} \cdot \mathbf{1}_{d_i \times 1} & \frac{k}{n} \cdot \mathbf{A}_{d_i} \end{bmatrix} \Rightarrow \det\left(\mathbb{E}_{\mathbf{z}} [\tilde{\mathbf{z}}_i \tilde{\mathbf{z}}_i^\top]\right) = \frac{k^{d_i}}{n^{d_i}} \cdot \det\left(\begin{bmatrix} 1 & \frac{k}{n} \cdot \mathbf{1}_{1 \times d_i} \\ \mathbf{1}_{d_i \times 1} & \mathbf{A}_{d_i} \end{bmatrix}\right).$$

Performing a cofactor expansion of the latter matrix along its first row, we have

$$\det\left(\mathbb{E}_{\mathbf{z}} [\tilde{\mathbf{z}}_i \tilde{\mathbf{z}}_i^\top]\right) = \frac{k^{d_i}}{n^{d_i}} \left[\det(\mathbf{A}_{d_i}) - d_i \cdot \frac{k}{n} \cdot \det(\mathbf{B}_{d_i}) \right]. \quad (39)$$

Observe that the second cofactor in this expansion is exactly \mathbf{B}_{d_i} , and each successive cofactor can be obtained from the previous one via a single row transposition. Hence, it suffices to reason about the determinants of the \mathbf{A}_x and \mathbf{B}_x matrices.

We compute the determinant of \mathbf{A}_x as the product of its eigenvalues. Note that $\mathbf{1}_{x \times x}$ has eigenvalue x with multiplicity 1 and 0 with multiplicity $x-1$. Hence, $\mathbf{A}_x = \frac{k-1}{n-1} \cdot \mathbf{1}_{x \times x} + \frac{n-k}{n-1} \cdot \mathbf{I}_x$ has determinant

$$\det(\mathbf{A}_x) = \left(x \cdot \frac{k-1}{n-1} + \frac{n-k}{n-1}\right) \cdot \left(\frac{n-k}{n-1}\right)^{x-1}.$$

Next, we argue by induction on x that $\det(\mathbf{B}_x) = \left(\frac{n-k}{n-1}\right)^{x-1}$. The base case is immediate, as $\mathbf{B}_1 = [1]$. Given $x \geq 2$, we performing a cofactor expansion along the first row of \mathbf{B}_x to obtain,

$$\det(\mathbf{B}_x) = \det(\mathbf{A}_{x-1}) - (x-1) \cdot \frac{k-1}{n-1} \cdot \det(\mathbf{B}_{x-1}).$$

Observe that the second cofactor in this expansion is exactly \mathbf{B}_{x-1} , and each successive cofactor can be obtained from the previous one via a single row transposition. Applying our formula for

\mathbf{A}_{x-1} and the inductive hypothesis, we have

$$\begin{aligned}
\det(\mathbf{B}_x) &= \left((x-1) \cdot \frac{k-1}{n-1} + \frac{n-k}{n-1} \right) \cdot \left(\frac{n-k}{n-1} \right)^{x-2} - (x-1) \cdot \frac{k-1}{n-1} \cdot \left(\frac{n-k}{n-1} \right)^{x-2} \\
&= \left(\frac{n-k}{n-1} \right)^{x-2} \cdot \left[\left((x-1) \cdot \frac{k-1}{n-1} + \frac{n-k}{n-1} \right) - (x-1) \cdot \frac{k-1}{n-1} \right] \\
&= \left(\frac{n-k}{n-1} \right)^{x-2} \cdot \frac{n-k}{n-1} \\
&= \left(\frac{n-k}{n-1} \right)^{x-1},
\end{aligned}$$

completing the induction. Finally, plugging into (39), we have

$$\begin{aligned}
\det\left(\mathbb{E}_{\mathbf{z}} [\tilde{\mathbf{z}}_i \tilde{\mathbf{z}}_i^\top]\right) &= \frac{k^{d_i}}{n^{d_i}} \left[\left(d_i \cdot \frac{k-1}{n-1} + \frac{n-k}{n-1} \right) \cdot \left(\frac{n-k}{n-1} \right)^{d_i-1} - d_i \cdot \frac{k}{n} \cdot \left(\frac{n-k}{n-1} \right)^{d_i-1} \right] \\
&= \frac{k^{d_i} \cdot (n-k)^{(d_i-1)}}{n^{d_i} \cdot (n-1)^{(d_i-1)}} \left[d_i \cdot \left(\frac{k-1}{n-1} - \frac{k}{n} \right) + \frac{n-k}{n-1} \right] \\
&= \frac{k^{d_i} \cdot (n-k)^{d_i} \cdot (n-d_i)}{n^{(d_i+1)} \cdot (n-1)^{d_i}}.
\end{aligned}$$

□

Proof of Lemma 3

Proof. We must first pseudoinvert the design matrices, which, as discussed in the main text, we do separately for the invertible and non-invertible cases.

First, if $d_i < n$, then Lemma 2 ensures that $\mathbb{E}_{\mathbf{z}} [\tilde{\mathbf{z}}_i \tilde{\mathbf{z}}_i^\top]$ is invertible, and the (pesudo)inverse is given by the formula:

$$\mathbb{E}_{\mathbf{z}} [\tilde{\mathbf{z}}_i \tilde{\mathbf{z}}_i^\top]^\dagger = \frac{n(n-1)}{k(n-k)(n-d_i)} \begin{bmatrix} \frac{k(n+d_i(k-1)-k)}{n-1} & -k & -k & \dots & -k \\ -k & n-(d_i-1) & 1 & \dots & 1 \\ -k & 1 & n-(d_i-1) & \ddots & \vdots \\ \vdots & \vdots & \ddots & \ddots & 1 \\ -k & 1 & \dots & 1 & n-(d_i-1) \end{bmatrix},$$

which can be verified by direct multiplication.

Multiplying this by θ_i gives

$$\mathbb{E}_{\mathbf{z}} [\tilde{\mathbf{z}}_i \tilde{\mathbf{z}}_i^\top]^\dagger \theta_i = \frac{n(n-1)}{k(n-k)(n-d_i)} \begin{bmatrix} -d_i \cdot k \\ n \\ \vdots \\ n \end{bmatrix},$$

which in turn gives the inner product

$$\left\langle \mathbb{E}_{\mathbf{z}} [\tilde{\mathbf{z}}_i \tilde{\mathbf{z}}_i^\top]^\dagger \theta_i, \tilde{\mathbf{z}}_i \right\rangle = \frac{n^2(n-1)}{k(n-k)(n-d_i)} \sum_{j \in \mathcal{N}_i} \left(z_j - \frac{k}{n} \right)$$

Next, if $d_i = n$, then the pseudoinverse of the design matrix is given by the formula:

$$\mathbb{E}_{\mathbf{z}} [\tilde{\mathbf{z}}_i \tilde{\mathbf{z}}_i^\top]^\dagger = \frac{1}{k(n-k)(k^2+n)^2} \begin{bmatrix} nk^2(n-k) & nk^2(n-k) & nk^2(n-k) & \dots & nk^2(n-k) \\ nk^2(n-k) & \star & \diamond & \dots & \diamond \\ nk^2(n-k) & \diamond & \star & \ddots & \vdots \\ \vdots & \vdots & \ddots & \ddots & \diamond \\ nk^2(n-k) & \diamond & \dots & \diamond & \star \end{bmatrix},$$

where

$$\begin{aligned} \star &= n \left((n-2)k^4 + k^3 + 2(n-1)^2k^2 + n(n-1)^2 \right), \\ \diamond &= -n \left(k^4 - k^3 + 2(n-1)k^2 + n(n-1) \right). \end{aligned}$$

This can again be verified by matrix multiplication.

Multiplying this by θ_i gives

$$\mathbb{E}_{\mathbf{z}} [\tilde{\mathbf{z}}_i \tilde{\mathbf{z}}_i^\top]^\dagger \theta_i = \frac{nk}{(k^2+n)^2} \begin{bmatrix} n \\ k \\ \vdots \\ k \end{bmatrix},$$

which in turn gives the inner product

$$\left\langle \mathbb{E}_{\mathbf{z}} [\tilde{\mathbf{z}}_i \tilde{\mathbf{z}}_i^\top]^\dagger \theta_i, \tilde{\mathbf{z}}_i \right\rangle = \frac{nk^2}{(k^2+n)^2} \sum_{j \in \mathcal{N}_i} \left(z_j + \frac{1}{k} \right).$$

Plugging into (7) gives the desired formula. □

Proof of Lemma 4

Proof. To apply Theorem 1, we must calculate the vector $(M_i^\dagger M_i - I)\theta_i$ where $M_i = \mathbb{E} [\tilde{\mathbf{z}}_i \tilde{\mathbf{z}}_i^\top]$ for each $i \in [n]$. We do this in two cases. First, when $d_i < n$, Lemma 2 ensures that M_i is invertible, meaning $M_i^\dagger = M_i^{-1}$; these nodes do not contribute to the bias (verifying part (c) of the lemma). On the other hand, if $d_i = n$, then we can use the explicit form of the pseudoinverse matrix given in the proof of Lemma 3 to calculate:

$$M_i^\dagger M_i = \frac{1}{k^2+n} \begin{bmatrix} n & k & k & \dots & k \\ k & k^2+n-1 & -1 & \dots & -1 \\ k & -1 & k^2+n-1 & \ddots & \vdots \\ \vdots & \vdots & \ddots & \ddots & -1 \\ k & -1 & \dots & -1 & k^2+n-1 \end{bmatrix},$$

which gives

$$(M_i^\dagger M_i - I)\theta = \frac{n}{k^2+n} \begin{bmatrix} k \\ -1 \\ \vdots \\ -1 \end{bmatrix}$$

Now, from Theorem 1(a), we obtain the exact bias

$$\mathbb{E} [\widehat{\text{TTE}}] - \text{TTE} = \frac{1}{k^2+n} \sum_{i=1}^n \mathbb{I}(d_i = n) \cdot \left(k \cdot c_{i,\emptyset} - \sum_{j=1}^n c_{i,j} \right).$$

Similarly from Theorem 1(b), we obtain the bias upper bound

$$|\mathbb{E} [\widehat{\text{TTE}}] - \text{TTE}| \leq \frac{B}{k^2+n} \sum_{i=1}^n \mathbb{I}(d_i = n) \cdot \sqrt{k^2+n} = \frac{\#\{i: d_i = n\}}{n} \cdot \frac{Bn}{\sqrt{k^2+n}} \leq \frac{\#\{i: d_i = n\}}{n} \cdot \frac{B}{k/n}.$$

□

Proof of Lemma 5

Proof. Substituting the definition of $\widehat{\mathbf{c}}_i$ and $\widehat{\mathbf{c}}_{i'}$, we have,

$$\begin{aligned} \text{cov}(\theta_i^\top \widehat{\mathbf{c}}_i, \theta_{i'}^\top \widehat{\mathbf{c}}_{i'}) &= \text{cov} \left(Y_i(\mathbf{z}) \left\langle \mathbb{E} [\tilde{\mathbf{z}}_i \tilde{\mathbf{z}}_i^\top] \theta_i, \tilde{\mathbf{z}}_i \right\rangle, Y_{i'}(\mathbf{z}) \left\langle \mathbb{E} [\tilde{\mathbf{z}}_{i'} \tilde{\mathbf{z}}_{i'}^\top] \theta_{i'}, \tilde{\mathbf{z}}_{i'} \right\rangle \right) \\ &= \mathbb{E} \left[Y_i(\mathbf{z}) \left\langle \mathbb{E} [\tilde{\mathbf{z}}_i \tilde{\mathbf{z}}_i^\top] \theta_i, \tilde{\mathbf{z}}_i \right\rangle \cdot Y_{i'}(\mathbf{z}) \left\langle \mathbb{E} [\tilde{\mathbf{z}}_{i'} \tilde{\mathbf{z}}_{i'}^\top] \theta_{i'}, \tilde{\mathbf{z}}_{i'} \right\rangle \right] \\ &\quad - \mathbb{E} \left[Y_i(\mathbf{z}) \left\langle \mathbb{E} [\tilde{\mathbf{z}}_i \tilde{\mathbf{z}}_i^\top] \theta_i, \tilde{\mathbf{z}}_i \right\rangle \right] \cdot \mathbb{E} \left[Y_{i'}(\mathbf{z}) \left\langle \mathbb{E} [\tilde{\mathbf{z}}_{i'} \tilde{\mathbf{z}}_{i'}^\top] \theta_{i'}, \tilde{\mathbf{z}}_{i'} \right\rangle \right] \end{aligned}$$

Since $i \in \mathcal{N}_i$ and $\mathcal{N}_i \cap \mathcal{N}_{i'} = \emptyset$, we know that $i \notin \mathcal{N}_{i'}$, so $d_i < n$. Similarly, $d_{i'} < n$. Hence, we can use our calculation from the proof of Lemma 3 to rewrite this

$$\frac{n^4(n-1)^2}{k^2(n-k)^2(n-d_i)(n-d_{i'})} \left(\mathbb{E} \left[Y_i(\mathbf{z}) \cdot Y_{i'}(\mathbf{z}) \sum_{j \in \mathcal{N}_i} \left(z_j - \frac{k}{n} \right) \sum_{j' \in \mathcal{N}_{i'}} \left(z_{j'} - \frac{k}{n} \right) \right] \right) \quad (40)$$

$$- \mathbb{E} \left[Y_i(\mathbf{z}) \sum_{j \in \mathcal{N}_i} \left(z_j - \frac{k}{n} \right) \right] \mathbb{E} \left[Y_{i'}(\mathbf{z}) \sum_{j' \in \mathcal{N}_{i'}} \left(z_{j'} - \frac{k}{n} \right) \right] \Bigg)$$

$$= \frac{n^4(n-1)^2}{k^2(n-k)^2(n-d_i)(n-d_{i'})} \mathbb{E} \left[Y_i(\mathbf{z}) \cdot Y_{i'}(\mathbf{z}) \sum_{j \in \mathcal{N}_i} \left(z_j - \frac{k}{n} \right) \sum_{j' \in \mathcal{N}_{i'}} \left(z_{j'} - \frac{k}{n} \right) \right] - \sum_{j \in \mathcal{N}_i} c_{i,j} \sum_{j' \in \mathcal{N}_{i'}} c_{i',j'}. \quad (41)$$

Here, the second line uses an expectation calculation from the proof of Lemma 4. Next, let us focus our attention on the expectation in the latter expression. By substituting in the definitions of $Y_i(\mathbf{z})$ and $Y_{i'}(\mathbf{z})$ (under our assumed $\beta = 1$ order potential outcomes model), we can rewrite this expectation

$$\begin{aligned} &\mathbb{E} \left[\left(c_{i,\emptyset} + \sum_{h \in \mathcal{N}_i} c_{i,h} \right) \left(c_{i',\emptyset} + \sum_{h' \in \mathcal{N}_{i'}} c_{i',h'} \right) \sum_{j \in \mathcal{N}_i} \left(z_j - \frac{k}{n} \right) \sum_{j' \in \mathcal{N}_{i'}} \left(z_{j'} - \frac{k}{n} \right) \right] \\ &= c_{i,\emptyset} \cdot c_{i',\emptyset} \sum_{j \in \mathcal{N}_i} \sum_{j' \in \mathcal{N}_{i'}} \mathbb{E} \left[\left(z_j - \frac{k}{n} \right) \left(z_{j'} - \frac{k}{n} \right) \right] \quad (\star) \end{aligned}$$

$$+ c_{i,\emptyset} \sum_{h' \in \mathcal{N}_{i'}} c_{i',h'} \sum_{j \in \mathcal{N}_i} \sum_{j' \in \mathcal{N}_{i'}} \mathbb{E} \left[z_{h'} \left(z_j - \frac{k}{n} \right) \left(z_{j'} - \frac{k}{n} \right) \right] \quad (\star\star)$$

$$+ c_{i',\emptyset} \sum_{h \in \mathcal{N}_i} c_{i,h} \sum_{j \in \mathcal{N}_i} \sum_{j' \in \mathcal{N}_{i'}} \mathbb{E} \left[z_h \left(z_j - \frac{k}{n} \right) \left(z_{j'} - \frac{k}{n} \right) \right]$$

$$+ \sum_{h \in \mathcal{N}_i} c_{i,h} \sum_{h' \in \mathcal{N}_{i'}} c_{i',h'} \sum_{j \in \mathcal{N}_i} \sum_{j' \in \mathcal{N}_{i'}} \mathbb{E} \left[z_h z_{h'} \left(z_j - \frac{k}{n} \right) \left(z_{j'} - \frac{k}{n} \right) \right].$$

Now, let us separately consider the expectations in (\star) and $(\star\star)$; the following line has the same form, so it is handled analogously. In all of these expressions, note that our assumption that $\mathcal{N}_i \cap \mathcal{N}_{i'} = \emptyset$ ensures that $z_j \neq z'_j$ (and also $z_h \neq z_{j'}$ and $z_{h'} \neq z_j$). Thus, in (\star) ,

$$\mathbb{E} \left[\left(z_j - \frac{k}{n} \right) \left(z_{j'} - \frac{k}{n} \right) \right] = \frac{k(k-1)}{n(n-1)} - \frac{k^2}{n^2} = \frac{-k(n-k)}{n^2(n-1)}.$$

This is always negative, and our same-signs assumption ensures that $c_{i,\emptyset} \cdot c_{i',\emptyset} \geq 0$, so the entire expression (\star) is ≤ 0 .

In $(\star\star)$, there are two possibilities for $z_{j'}$ which we must handle separately. First, if $z_{j'} = z_{h'}$, then

$$\mathbb{E} \left[z_{h'} \left(z_j - \frac{k}{n} \right) \left(z_{j'} - \frac{k}{n} \right) \right] = \frac{k(k-1)}{n(n-1)} - \frac{k^2}{n^2} - \frac{k^2(k-1)}{n^2(n-1)} + \frac{k^3}{n^3} = \frac{-k(n-k)^2}{n^3(n-1)}.$$

Next, if $z_{j'} \neq z_{h'}$, then

$$\mathbb{E} \left[z_{h'} \left(z_j - \frac{k}{n} \right) \left(z_{j'} - \frac{k}{n} \right) \right] = \frac{k(k-1)(k-2)}{n(n-1)(n-2)} - \frac{2k^2(k-1)}{n^2(n-1)} + \frac{k^3}{n^3} = \frac{-k(n-k)(nk-2n+2k)}{n^3(n-1)(n-2)}.$$

Together, this allows us to simplify $(\star\star)$ to

$$c_{i,\emptyset} \sum_{h' \in \mathcal{N}_{i'}} c_{i',h'} \cdot d_i \cdot \left(\frac{-k(n-k)}{n^2(n-1)} + (d_{i'} - 1) \cdot \frac{-k(n-k)(nk-2n+2k)}{n^3(n-1)(n-2)} \right).$$

Within the large parentheses, note that the first traction is always negative, and the second fraction is negative when $k \geq 2$, as this makes $nk - 2n + 2k > 0$. If $k = 1$, then this parenthesized expression simplifies to $\frac{d_{i'} - 1 - n}{n^3} < 0$. Again, appealing to our same-signs assumption, we find that the entire expression $(\star\star)$ is ≤ 0 .

These observations allow us to bound (41),

$$(41) \leq \sum_{h \in \mathcal{N}_i} c_{i,h} \sum_{h' \in \mathcal{N}_{i'}} c_{i',h'} \left(\frac{n^4(n-1)^2}{k^2(n-k)^2(n-d_i)(n-d_{i'})} \sum_{j \in \mathcal{N}_i} \sum_{j' \in \mathcal{N}_{i'}} \mathbb{E} \left[z_h z_{h'} \left(z_j - \frac{k}{n} \right) \left(z_{j'} - \frac{k}{n} \right) \right] - 1 \right).$$

Let us simplify this expectation. Here, there are three possibilities for z_j and $z_{j'}$ which we must handle separately. First, if $z_j = z_h$ and $z_{j'} = z_{h'}$, then

$$\mathbb{E} \left[z_h z_{h'} \left(z_j - \frac{k}{n} \right) \left(z_{j'} - \frac{k}{n} \right) \right] = \frac{k(k-1)}{n(n-1)} - \frac{2k^2(k-1)}{n^2(n-1)} + \frac{k^3(k-1)}{n^3(n-1)} = \frac{k(k-1)(n-k)^2}{n^3(n-1)}.$$

Next, if either $z_j = z_h$ or $z_{j'} = z_{h'}$, but not both, then

$$\mathbb{E} \left[z_h z_{h'} \left(z_j - \frac{k}{n} \right) \left(z_{j'} - \frac{k}{n} \right) \right] = \frac{k(k-1)(k-2)}{n(n-1)(n-2)} - \frac{k^2(k-1)(k-2)}{n^2(n-1)(n-2)} - \frac{k^2(k-1)}{n^2(n-1)} + \frac{k^3(k-1)}{n^3(n-1)} = \frac{-2k(k-1)(n-k)^2}{n^3(n-1)(n-2)}.$$

Finally, if $z_j \neq z_h$ and $z_{j'} \neq z_{h'}$, then

$$\mathbb{E} \left[z_h z_{h'} \left(z_j - \frac{k}{n} \right) \left(z_{j'} - \frac{k}{n} \right) \right] = \frac{k(k-1)(k-2)(k-3)}{n(n-1)(n-2)(n-3)} - \frac{2k^2(k-1)(k-2)}{n^2(n-1)(n-2)} + \frac{k^3(k-1)}{n^3(n-1)} = \frac{-k(k-1)(n-k)(nk-6n+6k)}{n^3(n-1)(n-2)(n-3)}.$$

Together, this allows us to rewrite our bound on (41) as

$$(41) \leq \sum_{h \in \mathcal{N}_i} c_{i,h} \sum_{h' \in \mathcal{N}_{i'}} c_{i',h'} \left(-1 + \frac{n^4(n-1)^2}{k^2(n-k)^2(n-d_i)(n-d_{i'})} \cdot \left[\frac{k(k-1)(n-k)^2}{n^3(n-1)} - (d_i + d_{i'} - 2) \frac{2k(k-1)(n-k)^2}{n^3(n-1)(n-2)} - (d_i - 1)(d_{i'} - 1) \frac{k(k-1)(n-k)(nk-6n+6k)}{n^3(n-1)(n-2)(n-3)} \right] \right) \\ = \sum_{h \in \mathcal{N}_i} c_{i,h} \sum_{h' \in \mathcal{N}_{i'}} c_{i',h'} \left(-1 + \frac{n(n-1)(k-1)(n-2d_i-2d_{i'}+2)}{k(n-2)(n-d_i)(n-d_{i'})} - \frac{n(n-1)(k-1)(nk-6n+6k)(d_i-1)(d_{i'}-1)}{k(n-k)(n-2)(n-3)(n-d_i)(n-d_{i'})} \right).$$

By our same-signs assumption, our proof will be complete once we argue that the parenthesized expression in the last expression is negative, which we do via a case analysis.

Case 1: $k = 1$

Both fractions in the parenthesized expression zero out, and we are left with $-1 < 0$.

Case 2: $k = 2$

The parenthesized expression simplifies to $-1 + \frac{n(n-1)(n-2d_i)(n-2d_{i'})}{2(n-2)^2(n-d_i)(n-d_{i'})}$. If $(n-2d_{i'}) < 0$, since $d_i + d_{i'} \leq n$, we must have that $n - 2d_i > 0$. In this case, the parenthesized fraction is negative. Thus, we are left to consider the possibility where $n - 2d_{i'} > 0$. Since $d_i > 1$, we have,

$$\frac{(n-1)(n-2d_i)}{(n-2)(n-d_i)} \leq \frac{(n-1)(n-d_i-1)}{(n-2)(n-d_i)} = \frac{n^2 - nd_i - 2n + d_i + 1}{n^2 - nd_i - 2n + 2d_i} \leq 1.$$

Thus, we can upper-bound the parenthesized expression by $-1 + \frac{n(n-2d_{i'})}{2(n-2)(n-d_{i'})}$. Noting that $d_{i'} \geq 1$, we can bound this fraction,

$$\frac{n(n-2d_{i'})}{n(n-2d_{i'}) + (n^2 - 4n + 4d_{i'}^2)} \leq \frac{n(n-2d_{i'})}{n(n-2d_{i'}) + (n^2 - 4n + 4)} = \frac{n(n-2d_{i'})}{n(n-2d_{i'}) + (n-2)^2} \leq \frac{n(n-2d_{i'})}{n(n-2d_{i'}) + (n-2)^2} < 1.$$

Again, we find that the parenthesized expression must be negative.

Case 3: $d_i = 1$ (analogously, $d_{i'} = 1$), $k \geq 2$

Note that the factor of $d_i - 1$ in the second fraction makes it assume value 0 in this case. Thus, we can simplify the expression to $-1 + \frac{n(k-1)(n-2d_{i'})}{k(n-2)(n-d_{i'})}$. Taking the derivative with respect to $d_{i'}$, we obtain $\frac{-n^2(k-1)}{k(n-2)(n-d_{i'})^2} < 0$. Thus, the parenthesized expression is maximized when $d_{i'} = 1$, with value $-1 + \frac{n(k-1)}{k(n-1)} = \frac{-(n-k)}{k(n-1)} < 0$.

Case 4: $k \geq 6$

Here, the factor $nk - 6n + 6k \geq 6k$ is positive, as is every other factor in the second fraction. Thus, we can upper-bound the parenthesized expression by $-1 + \frac{n(n-1)(k-1)(n-2d_i-2d_{i'}+2)}{k(n-2)(n-d_i)(n-d_{i'})}$. Note that the factor $\frac{(n-1)(k-1)}{k(n-2)} = \frac{nk-2k-(n-1-k)}{nk-2k} \leq 1$ since $k \leq n-1$. Thus, we may further upper bound the expression by $-1 + \frac{n(n-2d_i-2d_{i'}+2)}{(n-d_i)(n-d_{i'})}$. Since $d_i, d_{i'} \geq 1$, we can again upper bound this by

$$-1 + \frac{n(n-d_i-d_{i'})}{(n-d_i)(n-d_{i'})} = \frac{-d_i d_{i'}}{(n-d_i)(n-d_{i'})} < 0.$$

Case 5: $k \in \{3, 4, 5\}$, $d_i, d_{i'} \geq 2$

Taking the derivative of the parenthesized expression with respect to d_i , we obtain

$$\begin{aligned} & \frac{n(n-1)(k-1)}{k(n-2)(n-d_{i'})} \cdot \frac{\partial}{\partial d_i} \left[\frac{(n-2d_i-2d_{i'}+2)}{(n-d_i)} - \frac{(nk-6n+6k)(d_i-1)(d_{i'}-1)}{(n-k)(n-3)(n-d_i)} \right] \\ &= \frac{n(n-1)(k-1)}{k(n-2)(n-d_{i'})} \cdot \left[\frac{-n-2d_{i'}+2}{(n-d_i)^2} - \frac{(nk-6n+6k)(d_{i'}-1)}{(n-k)(n-3)} \cdot \frac{n-1}{(n-d_i)^2} \right] \\ &= \frac{n(n-1)(k-1)}{k(n-2)(n-3)(n-k)(n-d_{i'})(n-d_i)^2} \cdot \left[(n-k)(n-3)(-n-2d_{i'}+2) - (n-1)(nk-6n+6k)(d_{i'}-1) \right] \end{aligned}$$

In this last expression, the outer fraction is positive, so we can restrict to understanding the sign of the bracketed expression. We do this separately for each value of k .

$k = 3$: The expression simplifies to $-n^3 + n^2d_{i'} + 5n^2 - 9nd_{i'}$. If $n = 4$, this further simplifies to $16 - 20d_{i'} < 0$. Otherwise, if $n \geq 5$, we can rewrite it $-n(n - 5)(n - d_{i'}) - 4nd_{i'} < 0$.

$k = 4$: The expression simplifies to $-n(n^2 - 7n + 12d_{i'})$. Under our assumption that $d_{i'} \geq 2$, we can upper bound this by $-n(n^2 - 7n + 24) < 0$.

$k = 5$: The expression simplifies to $-n(n^2 - 9n + d_{i'}n + 15d_{i'})$. Under our assumption that $d_{i'} \geq 2$, we can upper bound this by $-n(n^2 - 7n + 30) < 0$. \square

Proof of Lemma 6

Proof. Using the intermediary calculations from the proof of Lemma 3, we find that for any i with $d_i < n$,

$$\theta_i^\top \mathbb{E}[\tilde{\mathbf{z}}_i \tilde{\mathbf{z}}_i^\top]^\dagger \theta_i = \frac{n(n-1)}{k(n-k)(n-d_i)} [0 \quad 1 \quad \dots \quad 1] \begin{bmatrix} -d_i \cdot k \\ n \\ \vdots \\ n \end{bmatrix} = \frac{n^2 d_i (n-1)}{k(n-k)(n-d_i)} = \frac{d_i (n-1)}{k/n(1-k/n)(n-d_i)}.$$

Similarly, for any i with $d_i = n$,

$$\theta_i^\top \mathbb{E}[\tilde{\mathbf{z}}_i \tilde{\mathbf{z}}_i^\top]^\dagger \theta_i = \frac{nk}{(k^2+n)^2} [0 \quad 1 \quad \dots \quad 1] \begin{bmatrix} n \\ k \\ \vdots \\ k \end{bmatrix} = \frac{n^2 k^2}{(k^2+n)^2}.$$

Plugging these expressions into the formula $\gamma_i = \sqrt{|\mathcal{S}_i^\beta| \cdot \theta_i^\top \mathbb{E}[\tilde{\mathbf{z}}_i \tilde{\mathbf{z}}_i^\top]^\dagger \theta_i}$, and noting that $|\mathcal{S}_i^\beta| = (d_i + 1)$ when $\beta = 1$ gives the expression from the lemma. \square

Proof of Corollary 2

Proof. Lemma 5 implies that, in the bound of Theorem 2, there will be at most d_{\max}^2 values of j for which $\mathbb{I}(\theta_i^\top \text{cov}(\hat{\mathbf{c}}_i, \hat{\mathbf{c}}_j) \theta_j > 0) > 0$. The calculation above implies that each of these non-zero $\gamma_i \gamma_j$ terms will be at most $nd_{\max}^2 / ((k/n)(1-k/n)(n-d_{\max}))$, for a total contribution of $nd_{\max}^4 / ((k/n)(1-k/n)(n-d_{\max}))$ for each of the n units. Substituting this into the bound of Theorem 2 gives the result. \square

C Proofs from Section 5

Proof of Lemma 7

Proof. Recall that \mathcal{C}_i^β refers to all subsets of clusters $\mathcal{S} \subseteq \mathcal{C}(\mathcal{N}_i)$ with $|\mathcal{S}| \leq \beta$. Let us enumerate these subsets $\mathcal{C}_i^\beta = \{\mathcal{S}_1, \dots, \mathcal{S}_\ell\}$. From Section 5, the design matrix $\mathbb{E}_{\mathbf{z}} [\tilde{\mathbf{z}}_i \tilde{\mathbf{z}}_i^\top]$ has a block structure with blocks corresponding to pairs of subsets $\mathcal{S}, \mathcal{T} \in \mathcal{C}_i^\beta$. The $(\mathcal{S}, \mathcal{T})$ blocks have dimension $M_i^\beta(\mathcal{S}) \times M_i^\beta(\mathcal{T})$ and entry $\left[\mathbb{E}_{\mathbf{w}} [\tilde{\mathbf{w}}_i \tilde{\mathbf{w}}_i^\top] \right]_{\mathcal{S}, \mathcal{T}}$. Thus, we can factor the design matrix:

$$\mathbb{E}_{\mathbf{z}} [\tilde{\mathbf{z}}_i \tilde{\mathbf{z}}_i^\top] = \underbrace{\begin{bmatrix} \mathbf{1}_{M_i^\beta(\mathcal{S}_1) \times 1} & & 0 \\ & \ddots & \\ 0 & & \mathbf{1}_{M_i^\beta(\mathcal{S}_\ell) \times 1} \end{bmatrix}}_{D_i \in \mathbb{R}^{|\mathcal{S}_i^\beta| \times |\mathcal{C}_i^\beta|}} \mathbb{E}_{\mathbf{w}} [\tilde{\mathbf{w}}_i \tilde{\mathbf{w}}_i^\top] \underbrace{\begin{bmatrix} \mathbf{1}_{1 \times M_i^\beta(\mathcal{S}_1)} & & 0 \\ & \ddots & \\ 0 & & \mathbf{1}_{1 \times M_i^\beta(\mathcal{S}_\ell)} \end{bmatrix}}_{D_i^\top}.$$

Here, we use the notation $\mathbf{1}_{a \times b}$ to refer to the $a \times b$ submatrix of all ones. Thus D_i is a tall and narrow block diagonal matrix that maps the standard basis vectors in $\mathbb{R}^{\mathcal{S}_i^\beta}$ identifying a subset $S \subseteq \mathcal{N}_i$ to the standard basis vector in $\mathbb{R}^{\mathcal{C}_i^\beta}$ identifying the subset $\mathcal{C}(S) \subseteq \mathcal{C}(\mathcal{N}_i)$.

As the matrix D_i has full (column) rank, this factorization $\mathbb{E}_{\mathbf{z}} [\tilde{\mathbf{z}}_i \tilde{\mathbf{z}}_i^\top] = D_i \cdot \mathbb{E}_{\mathbf{w}} [\tilde{\mathbf{w}}_i \tilde{\mathbf{w}}_i^\top] D_i^\top$ is a rank decomposition. Thus, we can apply properties of the pseudoinverse to obtain

$$\mathbb{E}_{\mathbf{z}} [\tilde{\mathbf{z}}_i \tilde{\mathbf{z}}_i^\top]^\dagger = (D_i^\top)^\dagger \mathbb{E}_{\mathbf{w}} [\tilde{\mathbf{w}}_i \tilde{\mathbf{w}}_i^\top]^\dagger D_i^\dagger = D_i \left(D_i^\top D_i \right)^{-1} \mathbb{E}_{\mathbf{w}} [\tilde{\mathbf{w}}_i \tilde{\mathbf{w}}_i^\top]^\dagger \left(D_i^\top D_i \right)^{-1} D_i^\top.$$

Noting that $D_i^\top D_i = \text{diag}\left(M_i^\beta(\mathcal{S}_1), \dots, M_i^\beta(\mathcal{S}_\ell)\right)$, we have

$$\left[\mathbb{E}_{\mathbf{z}} [\tilde{\mathbf{z}}_i \tilde{\mathbf{z}}_i^\top]^\dagger \right]_{S,T} = \frac{1}{M_i^\beta(\mathcal{C}(S))} \cdot \left[\mathbb{E}_{\mathbf{w}} [\tilde{\mathbf{w}}_i \tilde{\mathbf{w}}_i^\top]^\dagger \right]_{\mathcal{C}(S), \mathcal{C}(T)} \cdot \frac{1}{M_i^\beta(\mathcal{C}(T))}.$$

□

Proof of Lemma 8

Lemma 8. *Fix a clustering \mathcal{C} and suppose that $\mathbf{z} \sim \text{GCR}_{\text{Bern}}(\mathcal{C}, p)$. Then, the pseudoinverse estimator for the TTE is*

$$\widehat{\text{TTE}} = \frac{1}{n} \sum_{i=1}^n Y_i(\mathbf{z}) \sum_{u \in \mathcal{C}_i^\beta} \left(\prod_{C \in \mathcal{U}} \frac{w_C - p}{p} - \prod_{C \in \mathcal{U}} \frac{w_C - p}{p - 1} \right). \quad (17)$$

Proof. Appealing to (7), it suffices to argue that

$$\left\langle \mathbb{E}_{\mathbf{z}} [\tilde{\mathbf{z}}_i \tilde{\mathbf{z}}_i^\top]^\dagger \theta_i, \tilde{\mathbf{z}}_i \right\rangle = \sum_{u \in \mathcal{C}_i^\beta} \left[(1-p)^{|u|} - (-p)^{|u|} \right] \prod_{C \in \mathcal{U}} \frac{w_C - p}{p(1-p)}$$

for each $i \in [n]$. Plugging in (16), we can expand this inner product

$$\begin{aligned}
\left\langle \mathbb{E}_{\mathbf{z}} [\tilde{\mathbf{z}}_i \tilde{\mathbf{z}}_i^\top]^\dagger \theta_i, \tilde{\mathbf{z}}_i \right\rangle &= \sum_{S \in \mathcal{S}_i^\beta} [\tilde{\mathbf{z}}_i]_S \sum_{T \in \mathcal{S}_i^\beta} \left[\mathbb{E}_{\mathbf{z}} [\tilde{\mathbf{z}}_i \tilde{\mathbf{z}}_i^\top]^\dagger \right]_{S,T} \cdot [\theta_i]_T \\
&= \sum_{S \in \mathcal{C}_i^\beta} \prod_{C \in \mathcal{S}} \left(\frac{-w_C}{p} \right) \sum_{\substack{\mathcal{T} \in \mathcal{C}_i^\beta \\ \mathcal{T} \neq \emptyset}} \left(\frac{-1}{p} \right)^{|\mathcal{T}|} \sum_{\substack{\mathcal{U} \in \mathcal{C}_i^\beta \\ (\mathcal{S} \cup \mathcal{T}) \subseteq \mathcal{U}}} \left(\frac{p}{1-p} \right)^{|\mathcal{U}|} \\
&= \sum_{S \in \mathcal{C}_i^\beta} \prod_{C \in \mathcal{S}} \left(\frac{-w_C}{p} \right) \sum_{\substack{\mathcal{U} \in \mathcal{C}_i^\beta \\ S \subseteq \mathcal{U}}} \left(\frac{p}{1-p} \right)^{|\mathcal{U}|} \sum_{\substack{\mathcal{T} \subseteq \mathcal{U} \\ \mathcal{T} \neq \emptyset}} \left(\frac{-1}{p} \right)^{|\mathcal{T}|} && \text{(reorder sum)} \\
&= \sum_{S \in \mathcal{C}_i^\beta} \prod_{C \in \mathcal{S}} \left(\frac{-w_C}{p} \right) \sum_{\substack{\mathcal{U} \in \mathcal{C}_i^\beta \\ S \subseteq \mathcal{U}}} \left(\frac{p}{1-p} \right)^{|\mathcal{U}|} \left[\left(\frac{p-1}{p} \right)^{|\mathcal{U}|} - 1 \right] && \text{(distributivity)} \\
&= \sum_{\mathcal{U} \in \mathcal{C}_i^\beta} \left[(-1)^{|\mathcal{U}|} - \left(\frac{p}{1-p} \right)^{|\mathcal{U}|} \right] \sum_{S \subseteq \mathcal{U}} \prod_{C \in \mathcal{S}} \left(\frac{-w_C}{p} \right) && \text{(reorder sum)} \\
&= \sum_{\mathcal{U} \in \mathcal{C}_i^\beta} \left[(-1)^{|\mathcal{U}|} - \left(\frac{p}{1-p} \right)^{|\mathcal{U}|} \right] \prod_{C \in \mathcal{U}} \frac{p-w_C}{p} && \text{(distributivity)} \\
&= \sum_{\mathcal{U} \in \mathcal{C}_i^\beta} \left[(1-p)^{|\mathcal{U}|} - (-p)^{|\mathcal{U}|} \right] \prod_{C \in \mathcal{U}} \frac{w_C-p}{p(1-p)}. && \text{(distributivity)}
\end{aligned}$$

□

Proof of Theorem 3

Next, we turn to proving Theorem 3, which requires first deriving the closed form of the Horvitz–Thompson estimators under a GCR_{Bern} design.

Lemma 17. *Given an interference network on n individuals and a clustering \mathcal{C} of these individuals, suppose that we sample treatment assignments according to a graph cluster randomized design $\mathbf{z} \sim \text{GCR}(\mathcal{C}, p)$. Then, the Horvitz–Thompson estimator for TTE is given by the formula*

$$\widehat{\text{TTE}}_{\text{HT}} = \frac{1}{n} \sum_{i=1}^n Y_i(\mathbf{z}) \sum_{\mathcal{U} \subseteq \mathcal{C}(\mathcal{N}_i)} \left[(1-p)^{|\mathcal{U}|} - (-p)^{|\mathcal{U}|} \right] \prod_{C \in \mathcal{U}} \frac{w_C-p}{p(1-p)}.$$

Proof. We have,

$$\begin{aligned}
& \sum_{\mathcal{U} \subseteq \mathcal{C}(\mathcal{N}_i)} \left[(1-p)^{|\mathcal{U}|} - (-p)^{|\mathcal{U}|} \right] \prod_{C \in \mathcal{U}} \frac{w_C - p}{p(1-p)} \\
&= \sum_{\mathcal{U} \subseteq \mathcal{C}(\mathcal{N}_i)} \prod_{C \in \mathcal{U}} \frac{w_C - p}{p} - \sum_{\mathcal{U} \subseteq \mathcal{C}(\mathcal{N}_i)} \prod_{C \in \mathcal{U}} \frac{p - w_C}{1-p} \\
&= \prod_{C \in \mathcal{C}(\mathcal{N}_i)} \frac{w_C}{p} - \prod_{C \in \mathcal{C}(\mathcal{N}_i)} \frac{1 - w_C}{1-p} \quad (\text{distributivity}) \\
&= \frac{\mathbb{I}(\mathcal{N}_i \text{ entirely treated})}{\Pr(\mathcal{N}_i \text{ entirely treated})} - \frac{\mathbb{I}(\mathcal{N}_i \text{ entirely untreated})}{\Pr(\mathcal{N}_i \text{ entirely untreated})}.
\end{aligned}$$

□

With this closed form in hand, we can prove Theorem 3.

Theorem 3. Fix a clustering \mathcal{C} and suppose that $\mathbf{z} \sim \text{GCR}(\mathcal{C}, p)$ with $p \leq \frac{1}{2}$ and that Assumption 5 holds, so that each $c_{i,S}$ has the same sign. Then, writing $\widehat{\text{TTE}}$ for the pseudoinverse estimator and $\widehat{\text{TTE}}_{\text{HT}}$ for Horvitz-Thompson estimator, we have

$$\text{var}(\widehat{\text{TTE}}) \leq \text{var}(\widehat{\text{TTE}}_{\text{HT}}).$$

Proof. For ease of notation, let us define the function $g: \mathbb{N} \rightarrow [0, 1]$ with $g(n) = (1-p)^n - (-p)^n$. Note that $0 \leq g(n) \leq 1$ for all $n \in \mathbb{N}$ and all $0 \leq p \leq \frac{1}{2}$. By 8 and 17, we may represent

$$\widehat{\text{TTE}} = \frac{1}{n} \sum_{i=1}^n Y_i(\mathbf{z}) \sum_{\mathcal{U} \in \mathcal{C}_i^\beta} g(|\mathcal{U}|) \prod_{C \in \mathcal{U}} \frac{w_C - p}{p(1-p)}, \quad \widehat{\text{TTE}}_{\text{HT}} = \frac{1}{n} \sum_{i=1}^n Y_i(\mathbf{z}) \sum_{\mathcal{U} \in \mathcal{C}(\mathcal{N}_i)} g(|\mathcal{U}|) \prod_{C \in \mathcal{U}} \frac{w_C - p}{p(1-p)}.$$

Next, for each $i \in [n]$, let us define cluster-scale effect coefficients

$$\mathbf{c}_{i,S} = \sum_{\substack{S \in \mathcal{S}_i^\beta \\ \mathcal{C}(S) = \mathcal{S}}} c_{i,S}$$

for each $S \in \mathcal{C}_i^\beta$, which allows us to re-express

$$Y_i(\mathbf{z}) = \sum_{S \in \mathcal{C}_i^\beta} \mathbf{c}_{i,S} \prod_{C \in S} w_C.$$

Our assumption that each $c_{i,S}$ has the same sign implies that each $\mathbf{c}_{i,S}$ also has the same sign. Now, we are ready to expand the variance of the Horvitz-Thompson estimator. We have,

$$\begin{aligned}
\text{var}(\widehat{\text{TTE}}_{\text{HT}}) &= \frac{1}{n^2} \sum_{i=1}^n \sum_{i'=1}^n \sum_{S \in \mathcal{C}_i^\beta} \mathbf{c}_{i,S} \sum_{S' \in \mathcal{C}_{i'}^\beta} \mathbf{c}_{i',S'} \sum_{\mathcal{U} \in \mathcal{C}(\mathcal{N}_i)} g(|\mathcal{U}|) \sum_{\mathcal{U}' \in \mathcal{C}(\mathcal{N}_{i'})} g(|\mathcal{U}'|) \\
&\quad \cdot \text{cov} \left(\prod_{C_1 \in S} w_{C_1} \prod_{C_2 \in \mathcal{U}} \frac{w_{C_2} - p}{p(1-p)}, \prod_{C_3 \in S'} w_{C_3} \prod_{C_4 \in \mathcal{U}'} \frac{w_{C_4} - p}{p(1-p)} \right). \quad (42)
\end{aligned}$$

By an analogous calculation to that from Lemma 4 of Cortez-Rodriguez et al. [2023], we may simplify this covariance to

$$\text{cov} = \mathbb{I}\left(\begin{matrix} \mathcal{U} \subseteq (\mathcal{S} \cup \mathcal{S}' \cup \mathcal{U}') \\ \mathcal{U}' \subseteq (\mathcal{S} \cup \mathcal{U} \cup \mathcal{S}') \end{matrix}\right) \cdot p^{|\mathcal{S} \cup \mathcal{S}' \setminus (\mathcal{U} \cup \mathcal{U}')| - |\mathcal{U} \cup \mathcal{U}'|} \cdot \left(\frac{1}{1-p}\right)^{|\mathcal{U} \cap \mathcal{U}' \setminus (\mathcal{S} \cup \mathcal{S}')|} - \mathbb{I}\left(\begin{matrix} \mathcal{U} \subseteq \mathcal{S} \\ \mathcal{U}' \subseteq \mathcal{S}' \end{matrix}\right) \cdot p^{|\mathcal{S} \setminus \mathcal{U}| + |\mathcal{S}' \setminus \mathcal{U}'|}.$$

Note that if $\mathcal{U} \not\subseteq \mathcal{S}$ or $\mathcal{U}' \not\subseteq \mathcal{S}'$, then the second term of this covariance is 0, ensuring that the entire covariance expression is non-negative. Otherwise, if $\mathcal{U} \subseteq \mathcal{S}$ and $\mathcal{U}' \subseteq \mathcal{S}'$, then we may further simplify this covariance expressions to

$$\text{cov} = p^{|\mathcal{S} \cup \mathcal{S}' \setminus (\mathcal{U} \cup \mathcal{U}')| - |\mathcal{U} \cup \mathcal{U}'|} - p^{|\mathcal{S} \setminus \mathcal{U}| + |\mathcal{S}' \setminus \mathcal{U}'|} = p^{|\mathcal{S} \cup \mathcal{S}' \setminus (\mathcal{U} \cup \mathcal{U}')| - |\mathcal{U} \cup \mathcal{U}'|} \left(1 - p^{|\mathcal{S} \cap \mathcal{S}'|}\right) \geq 0.$$

Thus, the covariance is always non-negative. Our same-sign assumption on the $c_{i,S}$ coefficients and our definition of g ensure that each coefficient in the sextuple sum in (42) is non-negative. Hence, we may lower bound the variance of the Horvitz-Thompson estimator by removing some of these terms. In particular, we may remove all of the terms with $|\mathcal{U}| > \beta$ or $|\mathcal{U}'| \geq \beta$, giving us

$$\begin{aligned} \text{var}\left(\widehat{\text{TTE}}_{\text{HT}}\right) &\geq \frac{1}{n^2} \sum_{i=1}^n \sum_{i'=1}^n \sum_{\mathcal{S} \in \mathcal{C}_i^\beta} c_{i,S} \sum_{\mathcal{S}' \in \mathcal{C}_{i'}^\beta} c_{i',S'} \sum_{\mathcal{U} \in \mathcal{C}_i^\beta} g(|\mathcal{U}|) \sum_{\mathcal{U}' \in \mathcal{C}^\beta} g(|\mathcal{U}'|) \\ &\quad \cdot \text{cov}\left(\prod_{\mathcal{C}_1 \in \mathcal{S}} w_{\mathcal{C}_1} \prod_{\mathcal{C}_2 \in \mathcal{U}} \frac{w_{\mathcal{C}_2} - p}{p(1-p)}, \prod_{\mathcal{C}_3 \in \mathcal{S}} w_{\mathcal{C}_3} \prod_{\mathcal{C}_4 \in \mathcal{U}} \frac{w_{\mathcal{C}_4} - p}{p(1-p)}\right) \\ &= \text{var}\left(\widehat{\text{TTE}}\right). \end{aligned}$$

□

Proof of Lemma 9

Proof. By the result of Theorem 1(c), it suffices to verify that θ_i lies in the column space of the design matrix $\mathbb{E}_{\mathbf{z}} [\tilde{\mathbf{z}}_i \tilde{\mathbf{z}}_i^\top]$ for graph cluster randomization. To do this, we leverage the factorization of the design matrix given in the proof of Lemma 7.

By our choice of canonical ordering, $\mathcal{S}_1 = \emptyset$, so $M_i^\beta(\mathcal{S}_1) = 1$. Therefore, $\theta_i = D_i \psi_i$, where ψ_i is the $|\mathcal{C}_i^\beta|$ -length column vector with 0 in its first entry and 1s in all other entries. This means that θ_i lies in the column space of D_i . As $\mathbb{E}_{\mathbf{w}} [\tilde{\mathbf{w}}_i \tilde{\mathbf{w}}_i^\top] D_i^\top$ has full (row) rank, θ_i also lies in the column space of $\mathbb{E}_{\mathbf{z}} [\tilde{\mathbf{z}}_i \tilde{\mathbf{z}}_i^\top] = D_i \mathbb{E}_{\mathbf{w}} [\tilde{\mathbf{w}}_i \tilde{\mathbf{w}}_i^\top] D_i^\top$. □

Proof of Lemma 10

Proof. Recall that \tilde{z}_i is a function of W_ℓ for $\ell \in \mathcal{C}(\mathcal{N}_i)$ and that \tilde{z}_j is a function of $W_{\ell'}$ for $\ell' \in \mathcal{C}(\mathcal{N}_j)$. If $\mathcal{C}(\mathcal{N}_i) \cap \mathcal{C}(\mathcal{N}_j) = \emptyset$, since W_1, \dots, W_k are independent, we have that \tilde{z}_i and \tilde{z}_j are functions of independent random variables and thus are themselves independent. □

Proof of Lemma 11

This proof proceeds analogously to the proof of Lemma 1. First, we evaluate the quadratic form $\theta_i^\top \mathbb{E}_{\mathbf{z}} [\tilde{\mathbf{z}}_i \tilde{\mathbf{z}}_i^\top] \dagger \theta_i$.

Lemma 18. *We have*

$$\theta_i^\top \mathbb{E}_{\mathbf{z}} [\tilde{\mathbf{z}}_i \tilde{\mathbf{z}}_i^\top]^\dagger \theta_i = \sum_{u=1}^{\min(\beta, |\mathcal{C}(\mathcal{N}_i)|)} \binom{|\mathcal{C}(\mathcal{N}_i)|}{u} \left[\left(\frac{1-p}{p} \right)^u - 2(-1)^u + \left(\frac{p}{1-p} \right)^u \right]. \quad (43)$$

Proof. Using the decomposition of $\mathbb{E}_{\mathbf{z}} [\tilde{\mathbf{z}}_i \tilde{\mathbf{z}}_i^\top]^\dagger$ from the proof of Lemma 7, we have

$$\theta_i^\top \mathbb{E}_{\mathbf{z}} [\tilde{\mathbf{z}}_i \tilde{\mathbf{z}}_i^\top]^\dagger \theta_i = \theta_i^\top D (D^\top D)^{-1} \mathbb{E}_{\tilde{\mathbf{w}}} [\tilde{\mathbf{w}}_i \tilde{\mathbf{w}}_i^\top]^\dagger (D^\top D)^{-1} D^\top \theta_i.$$

Letting ψ_i is the $|\mathcal{C}_i^\beta|$ -length column vector with 0 in its first entry and 1s in all other entries, we may simplify

$$\theta_i^\top \mathbb{E}_{\mathbf{z}} [\tilde{\mathbf{z}}_i \tilde{\mathbf{z}}_i^\top]^\dagger \theta_i = \psi_i^\top \mathbb{E}_{\tilde{\mathbf{w}}} [\tilde{\mathbf{w}}_i \tilde{\mathbf{w}}_i^\top]^\dagger \psi_i.$$

Note that this latter quadratic form has the exact form of that from Lemma 1, with $\theta_i = \psi_i$, $\mathbf{z} = \tilde{\mathbf{w}}$, and $d_i = |\mathcal{C}(\mathcal{N}_i)|$. Invoking this lemma with these parameters completes the proof. \square

We are now ready to prove Lemma 11, which is done analogously to Lemma 1.

Lemma 11. *Suppose that $p \leq 1/2$ and $\mathbf{z} \sim \text{GCR}_{\text{Bern}}(\mathcal{C}, p)$. Then, for a node of degree d_i ,*

$$\gamma_i^2 \leq \begin{cases} 4d_i^\beta \cdot p^{-|\mathcal{C}(\mathcal{N}_i)|} & |\mathcal{C}(\mathcal{N}_i)| < \beta, \\ 16d_i^\beta \cdot |\mathcal{C}(\mathcal{N}_i)|^\beta p^{-\beta} & |\mathcal{C}(\mathcal{N}_i)| \geq \beta. \end{cases} \quad (18)$$

Proof of Lemma 11. To bound γ_i^2 , we must bound $|\mathcal{S}_i^\beta|$ (which was done in Lemma 16) and $\theta_i^\top \mathbb{E}[\tilde{\mathbf{z}}\tilde{\mathbf{z}}^\top]^\dagger \theta_i$.

For $\theta_i^\top \mathbb{E}[\tilde{\mathbf{z}}\tilde{\mathbf{z}}^\top]^\dagger \theta_i$, we consider cases on the result of Lemma 18. When $|\mathcal{C}(\mathcal{N}_i)| \leq \beta$, we have

$$\begin{aligned} \theta_i^\top \mathbb{E}[\tilde{\mathbf{z}}\tilde{\mathbf{z}}^\top]^\dagger \theta_i &= \sum_{u=1}^{|\mathcal{C}(\mathcal{N}_i)|} \binom{|\mathcal{C}(\mathcal{N}_i)|}{u} \left[\left(\frac{p}{1-p} \right)^u - 2(-1)^u + \left(\frac{1-p}{p} \right)^u \right] \\ &= \left(1 + \frac{p}{1-p} \right)^{|\mathcal{C}(\mathcal{N}_i)|} - 1 - 2(-1) + \left(1 + \frac{1-p}{p} \right)^{|\mathcal{C}(\mathcal{N}_i)|} - 1 \\ &= \left(\frac{1}{1-p} \right)^{|\mathcal{C}(\mathcal{N}_i)|} + \left(\frac{1}{p} \right)^{|\mathcal{C}(\mathcal{N}_i)|} \\ &\leq 2p^{-|\mathcal{C}(\mathcal{N}_i)|} \end{aligned} \quad (44)$$

On the other hand, when $|\mathcal{C}(\mathcal{N}_i)| > \beta$, our assumption that $p \leq 1/2$ ensures that $p/(1-p) \leq 1$ and $(1-p)/p \geq 1$. Thus,

$$\begin{aligned} \theta_i^\top \mathbb{E}[\tilde{\mathbf{z}}\tilde{\mathbf{z}}^\top]^\dagger \theta_i &= \sum_{u=1}^{\beta} \binom{|\mathcal{C}(\mathcal{N}_i)|}{u} \left[\left(\frac{p}{1-p} \right)^u - 2(-1)^u + \left(\frac{1-p}{p} \right)^u \right] \\ &\leq \sum_{u=1}^{\beta} \binom{|\mathcal{C}(\mathcal{N}_i)|}{u} [1 + 2 + p^{-\beta}] \end{aligned} \quad (45)$$

$$\begin{aligned} &\leq 4p^{-\beta} \sum_{u=1}^{\beta} \binom{|\mathcal{C}(\mathcal{N}_i)|}{u} \\ &\leq 8p^{-\beta} |\mathcal{C}(\mathcal{N}_i)|^\beta \end{aligned} \quad (46)$$

Finally, combining (44) and (46) with the fact that $|\mathcal{S}_i^\beta| \leq 2d_i^\beta$ from Lemma 16 completes the proof. \square

Proof of Corollary 3

Proof. It is shown in Ugander et al. [2013] that $|\mathcal{C}(\mathcal{N}_i)| \leq \kappa^3$. This means that unit i is connected to at most κ^3 clusters, and since each of those κ^3 clusters has at most N units, each of which has at most d_{\max} neighbors, there are at most $n\kappa^3Nd$ non-zero terms in (10). Furthermore, since $|\mathcal{C}(\mathcal{N}_i)| \geq 1$ always, we have $\gamma_i^2 \leq 2d_{\max}\kappa^3p^{-1}$. Combining these two gives the result. \square

Proof of Corollary 4

Proof. For a fixed unit i , we consider two cases: either $\mathcal{C}(\mathcal{N}_i) = 1$ or $\mathcal{C}(\mathcal{N}_i) > 1$. If $\mathcal{C}(\mathcal{N}_i) = 1$, we have $\gamma_i^2 \leq 2d^2p^{-1}$ and there are at most Nd units j for which $\tilde{\mathbf{z}}_i \not\perp \tilde{\mathbf{z}}_j$. If $\mathcal{C}(\mathcal{N}_i) > 1$, we have $\gamma_i^2 \leq 2d^4p^{-2}$ and there are at most Nd^2 units j for which $\tilde{\mathbf{z}}_i \not\perp \tilde{\mathbf{z}}_j$, where we naively use the bound that $|\mathcal{C}(\mathcal{N}_i)| \leq d$.

Then, the bound of Theorem 2 is

$$\frac{B^2}{n^2} \sum_{i=1}^n \gamma_i \sum_{j=1}^n \gamma_j \cdot \mathbb{I}(\tilde{\mathbf{z}}_i \not\perp \tilde{\mathbf{z}}_j), \quad (47)$$

$$\leq \frac{\sqrt{2}B^2d_{\max}^2p^{-1}}{n^2} \sum_{i=1}^n \gamma_i \sum_{j=1}^n \mathbb{I}(\tilde{\mathbf{z}}_i \not\perp \tilde{\mathbf{z}}_j). \quad (48)$$

There are n_1 units for which $\gamma_i \leq \sqrt{2}d_{\max}p^{-1/2}$ and the inner sum is at most Nd ; these units contribute a total of $\sqrt{2}n_1d_{\max}^2p^{-1/2}N$. There are $n_{>1}$ units for which $\gamma_i \leq \sqrt{2}d_{\max}^2p^{-1}$ and the inner sum is at most Nd^2 ; these units contribute a total of $\sqrt{2}n_{>1}d_{\max}^4p^{-1}N$. Substituting these into (48) gives the result. \square

D Proofs from Section 6

The Form of the Design Matrix

We first present the form of the pseudoinverse matrix for the $\text{GCR}_{\text{Comp}}(\mathcal{C}, k_c)$ design, where \mathcal{C} is a clustering of G into m clusters. For a node i with $|\mathcal{C}(\mathcal{N}_i)| < m$, the entries of the pseudoinverse matrix can be found by combining Lemma 7 with Lemma 3. For a node i with $|\mathcal{C}(\mathcal{N}_i)| = m$, Lemma 7 does not apply, and we give the form of the pseudoinverse matrix for these nodes in the following lemma.

Lemma 19. *Suppose that $\mathbf{z} \sim \text{GCR}_{\text{Comp}}(\mathcal{C}, k_c)$, where $|\mathcal{C}| = m$. Suppose that i such that $|\mathcal{C}(\mathcal{N}_i)| = m$, and for each $C \in \mathcal{C}$ let $|\mathcal{C}|_i := |\mathcal{C} \cap \mathcal{N}_i|$, and let us define*

$$\delta = \frac{m}{k_c(k_c - m) \left(k_c^2 + \sum_{C \in \mathcal{C}} \frac{1}{|\mathcal{C}|_i} \right)^2}.$$

Then, the pseudoinverse matrix $M_i^\dagger = \mathbb{E} [\tilde{\mathbf{z}}_i \tilde{\mathbf{z}}_i^\top]^\dagger$ is symmetric, and its entries are given by the

formulas:

$$\begin{aligned}
[M_i^\dagger]_{\emptyset, \emptyset} &= \delta \left[\left(\sum_{C \in \mathcal{C}} \frac{1}{|C|_i} \right)^2 - (m-1) \sum_{C \in \mathcal{C}} \frac{1}{|C|_i^2} \right] k_c^2 - \left(\sum_{C \in \mathcal{C}} \frac{1}{|C|_i} \right)^2 k_c \\
[M_i^\dagger]_{\emptyset, C} &= \frac{\delta}{|C|_i} \left[\left(\sum_{C' \neq C} \frac{1}{|C'|_i} - \frac{m-2}{|C|_i} \right) k_c^3 - \left(\sum_{C' \in \mathcal{C}} \frac{1}{|C'|_i} \right) k_c^2 + (m-1) \left(\sum_{C' \neq C} \left(\frac{1}{|C'|_i^2} - \frac{1}{|C'|_i |C|_i} \right) \right) k_c \right] \\
[M_i^\dagger]_{C, C} &= \frac{\delta}{|C|_i^2} \left[-(m-2) k_c^4 - k_c^3 - 2(m-1) \left(\sum_{C' \in \mathcal{C}} \frac{1}{|C'|_i} \right) k_c^2 - (m-1) \left[\left(\sum_{C' \neq C} \frac{1}{|C'|_i} \right)^2 + \sum_{C' \neq C} \frac{1}{|C'|_i^2} \right] \right] \\
[M_i^\dagger]_{C, C'} &= \frac{\delta}{|C|_i |C'|_i} \left[k_c^4 - k_c^3 + (m-1) \left(\frac{1}{|C|_i} + \frac{1}{|C'|_i} \right) k_c^2 + (m-1) \left[\sum_{C'' \in \mathcal{C}} \left(\frac{1}{|C|_i |C''|_i} + \frac{1}{|C'|_i |C''|_i} - \frac{1}{|C''|_i^2} \right) \right] \right]
\end{aligned}$$

Proof. We must verify that the matrix M^\dagger satisfies the four properties of a Moore–Penrose pseudoinverse. Letting $M_i = \mathbb{E} [\tilde{\mathbf{z}}_i \tilde{\mathbf{z}}_i^\top]$, we compute the block matrix

$$M_i^\dagger M_i = \frac{1}{k_c^2 + \sum_{C \in \mathcal{C}} \frac{1}{|C|_i}} \begin{array}{c} \left[\begin{array}{cccc} \sum_{C \in \mathcal{C}} \frac{1}{|C|_i} & & & \\ & \frac{k_c}{|C_1|_i} & & \\ & & \frac{k_c}{|C_2|_i} & \\ & & & \cdots \end{array} \right] & \left. \vphantom{\begin{array}{c} \sum_{C \in \mathcal{C}} \frac{1}{|C|_i} \\ \frac{k_c}{|C_1|_i} \\ \frac{k_c}{|C_2|_i} \\ \vdots \end{array}} \right\} 1 \\ \left[\begin{array}{cccc} \frac{k_c}{|C_1|_i} & & & \\ & \frac{k_c^2}{|C_1|_i} + \frac{1}{|C_1|_i} \sum_{C \neq C_1} \frac{1}{|C|_i} & & \\ & & \frac{-1}{|C_1|_i |C_2|_i} & \\ & & & \cdots \end{array} \right] & \left. \vphantom{\begin{array}{c} \frac{k_c}{|C_1|_i} \\ \frac{k_c^2}{|C_1|_i} + \frac{1}{|C_1|_i} \sum_{C \neq C_1} \frac{1}{|C|_i} \\ \frac{-1}{|C_1|_i |C_2|_i} \\ \vdots \end{array}} \right\} |C_1|_i \\ \left[\begin{array}{cccc} \frac{k_c}{|C_2|_i} & & & \\ & \frac{-1}{|C_1|_i |C_2|_i} & & \\ & & \frac{k_c^2}{|C_2|_i} + \frac{1}{|C_2|_i} \sum_{C \neq C_2} \frac{1}{|C|_i} & \\ & & & \cdots \end{array} \right] & \left. \vphantom{\begin{array}{c} \frac{k_c}{|C_2|_i} \\ \frac{-1}{|C_1|_i |C_2|_i} \\ \frac{k_c^2}{|C_2|_i} + \frac{1}{|C_2|_i} \sum_{C \neq C_2} \frac{1}{|C|_i} \\ \vdots \end{array}} \right\} |C_2|_i \\ \left[\begin{array}{cccc} \vdots & & & \\ & \vdots & & \\ & & \vdots & \\ & & & \ddots \end{array} \right] & \left. \vphantom{\begin{array}{c} \vdots \\ \vdots \\ \vdots \\ \ddots \end{array}} \right\} \end{array}$$

by direct multiplication. Note that this matrix is symmetric, so $M_i^\dagger M_i = M_i M_i^\dagger$ and the Hermitian conditions of the pseudoinverse are satisfied. It remains to check that $M_i M_i^\dagger M_i = M_i$ and $M_i^\dagger M_i M_i^\dagger = M_i^\dagger$. This can be verified through direct computation, which we omit here for the sake of brevity. \square

Proof of Lemma 12

Proof. This proof proceeds similarly to that of Lemma 4. We start by computing the vector $(M_i^\dagger M_i - I)\theta_i$ where $M_i = \mathbb{E} [\tilde{\mathbf{z}}_i \tilde{\mathbf{z}}_i^\top]$ for each $i \in [n]$. We do this in two cases. First, when $|\mathcal{C}(\mathcal{N}_i)| < m$ we can use the reasoning in the proof of Lemma 9 to conclude that θ_i lies in the column space of M_i . Thus, these nodes do not contribute to the bias (verifying part (c) of the lemma). On the other hand, if $|\mathcal{C}(\mathcal{N}_i)| = m$, then we can use the explicit form of $M_i^\dagger M_i$ given in the proof of Lemma 19 to calculate:

$$(M_i^\dagger M_i - I)\theta = \frac{m}{k_c^2 + \sum_{C \in \mathcal{C}} \frac{1}{|C|_i}} \left. \begin{array}{c} \left. \begin{array}{c} k_c \\ \hline -\frac{1}{|C_1|_i} \\ \hline -\frac{1}{|C_2|_i} \\ \hline \vdots \end{array} \right\} \begin{array}{l} 1 \\ |C_1|_i \\ |C_2|_i \\ \end{array} \end{array} \right\}$$

Then, using Theorem 1(a), we obtain the exact bias

$$\mathbb{E} [\widehat{\text{TTE}}] - \text{TTE} = \sum_{i=1}^n \mathbb{I}(|\mathcal{C}(\mathcal{N}_i)| = m) \cdot \frac{1}{k_c^2 + \sum_{C \in \mathcal{C}} \frac{1}{|C|_i}} \left(k_c \cdot c_{i,\emptyset} - \sum_{C \in \mathcal{C}} \frac{1}{|C|_i} \sum_{j \in \mathcal{N}_i \cap C} c_{i,j} \right).$$

Similarly, using Theorem 1(b), we obtain the bias upper bound

$$|\mathbb{E} [\widehat{\text{TTE}}] - \text{TTE}| \leq \frac{Bm}{n} \sum_{i=1}^n \mathbb{I}(|\mathcal{C}(\mathcal{N}_i)| = m) \cdot \sqrt{\frac{1}{k_c^2 + \sum_{C \in \mathcal{C}} \frac{1}{|C|_i}}} \leq \frac{\#\{i: |\mathcal{C}(\mathcal{N}_i)| = m\}}{n} \cdot \frac{B}{k_c/m}.$$

□

Proof of Lemma 14

To reason about nodes i with $|\mathcal{C}(\mathcal{N}_i)| = m$, we will use the following lemma.

Lemma 20. *Suppose that $\mathbf{z} \sim \text{GCR}_{\text{Comp}}(\mathcal{C}, k_c)$ and that unit i has $|\mathcal{C}(\mathcal{N}_i)| = m$. Then*

$$\theta_i^\top \mathbb{E} [\tilde{\mathbf{z}}_i \tilde{\mathbf{z}}_i^\top]^\dagger \theta_i = \delta \left[mk_c^4 - m^2 k_c^3 + m(m-1) \sum_{C' \in \mathcal{C}} \frac{1}{|C'|_i} \sum_{C \neq C'} \left(\frac{1}{|C|_i} - \frac{1}{|C'|_i} \right) \right].$$

Proof. First, let us compute the entries of the vector $\mathbb{E} [\tilde{\mathbf{z}}_i \tilde{\mathbf{z}}_i^\top]^\dagger \theta_i$ corresponding to clusters $C \in \mathcal{C}$ (the entry corresponding to \emptyset is zeroed out in the final quadratic form). We have,

$$\begin{aligned} & \left[\mathbb{E} [\tilde{\mathbf{z}}_i \tilde{\mathbf{z}}_i^\top]^\dagger \theta_i \right]_C \\ &= \frac{\delta}{|C|_i} \left[- (m-2)k_c^4 - k_c^3 - 2(m-1) \left(\sum_{C' \in \mathcal{C}} \frac{1}{|C'|_i} \right) k_c^2 - (m-1) \left[\left(\sum_{C' \neq C} \frac{1}{|C'|_i} \right)^2 + \sum_{C' \neq C} \frac{1}{|C'|_i^2} \right] \right] \\ & \quad + \frac{\delta}{|C|_i} \sum_{C' \neq C} \left[k_c^4 - k_c^3 + (m-1) \left(\frac{1}{|C|_i} + \frac{1}{|C'|_i} \right) k_c^2 + (m-1) \left[\sum_{C'' \in \mathcal{C}} \left(\frac{1}{|C|_i |C''|_i} + \frac{1}{|C'|_i |C''|_i} - \frac{1}{|C''|_i^2} \right) \right] \right] \\ &= \frac{\delta}{|C|_i} \left[k_c^4 - mk_c^3 + (m-1) \sum_{C' \neq C} \left(\frac{1}{|C|_i} - \frac{1}{|C'|_i} \right) k_c^2 + m(m-1) \sum_{C' \neq C} \left(\frac{1}{|C|_i |C'|_i} - \frac{1}{|C'|_i^2} \right) \right] \end{aligned}$$

Summing up these entries gives us the value of the quadratic form:

$$\begin{aligned}
& \theta_i^\top \mathbb{E} [\tilde{\mathbf{z}}_i \tilde{\mathbf{z}}_i^\top]^\dagger \theta_i \\
&= \delta \sum_{C \in \mathcal{C}} \left[k_c^4 - m k_c^3 + (m-1) \sum_{C' \neq C} \left(\frac{1}{|C|_i} - \frac{1}{|C'|_i} \right) k_c^2 + m(m-1) \sum_{C' \neq C} \left(\frac{1}{|C|_i |C'|_i} - \frac{1}{|C'|_i^2} \right) \right] \\
&= \delta \left[m k_c^4 - m^2 k_c^3 + \underbrace{(m-1) \sum_{C \in \mathcal{C}} \sum_{C' \neq C} \left(\frac{1}{|C|_i} - \frac{1}{|C'|_i} \right) k_c^2}_{0 \text{ by symmetry}} + m(m-1) \sum_{C \in \mathcal{C}} \sum_{C' \neq C} \left(\frac{1}{|C|_i |C'|_i} - \frac{1}{|C'|_i^2} \right) \right] \\
&= \delta \left[m k_c^4 - m^2 k_c^3 + m(m-1) \sum_{C' \in \mathcal{C}} \frac{1}{|C'|_i} \sum_{C \neq C'} \left(\frac{1}{|C|_i} - \frac{1}{|C'|_i} \right) \right].
\end{aligned}$$

□

We are ready to prove the main lemma.

Proof of Lemma 14. For the case of $|\mathcal{C}(\mathcal{N}_i)| < m$, since the design matrix is invertible, the same argument as in Lemma 7 allow us obtain the result by translating Lemma 6 to the clustered setting. If $|\mathcal{C}(\mathcal{N}_i)| = m$, we may observe that

$$\sum_{C' \in \mathcal{C}} \frac{1}{|C'|_i} \sum_{C \neq C'} \left(\frac{1}{|C|_i} - \frac{1}{|C'|_i} \right) = \left(\sum_{C \in \mathcal{C}} \frac{1}{|C|_i} \right)^2 - m \sum_{C \in \mathcal{C}} \frac{1}{|C|_i^2} \leq 0,$$

where this inequality is an application of Cauchy-Schwarz. Thus, we can upper bound the quadratic form from Lemma 20 by

$$\theta_i^\top \mathbb{E} [\tilde{\mathbf{z}}_i \tilde{\mathbf{z}}_i^\top]^\dagger \theta_i \leq \delta \left[m k_c^4 - m^2 k_c^3 \right] = \frac{m^2 k_c^2}{\left(k_c^2 + \sum_{C \in \mathcal{C}} \frac{1}{|C|_i} \right)^2},$$

which allows us to bound

$$\gamma_i = \sqrt{|\mathcal{S}_i^1| \cdot \theta_i^\top \mathbb{E} [\tilde{\mathbf{z}}_i \tilde{\mathbf{z}}_i^\top]^\dagger \theta_i} \leq \frac{m \cdot k_c \cdot \sqrt{d_i + 1}}{k_c^2 + \sum_{C \in \mathcal{C}} \frac{1}{|C|_i}}.$$

□

Proof of Corollary 5

Proof. For a fixed unit i , we have from Ugander et al. [2013] that $|\mathcal{C}(\mathcal{N}_i)| \leq \kappa^3$. This means that unit i is connected to at most κ^3 clusters, each of which has at most N units, each of which has at most d_{\max} neighbors, so there are most $\kappa^3 N d_{\max}$ non-zero terms in (10).

Furthermore, since we have assumed that $\kappa^3 < m$, all units i fall into the first case of Lemma 14, and so each non-zero term is at most

$$\frac{(m-1)|\mathcal{C}(\mathcal{N}_i)|(d_i+1)}{(k_c/m)(1-k_c/m)(m-|\mathcal{C}(\mathcal{N}_i)|)} \lesssim \frac{\kappa^3 d_{\max}}{(k_c/m)(1-k_c/m)} \cdot \frac{m-1}{m-\kappa^3}.$$

Combining these two observations with Theorem 2 gives the result. □

E Monte Carlo Estimation of the Design Matrix

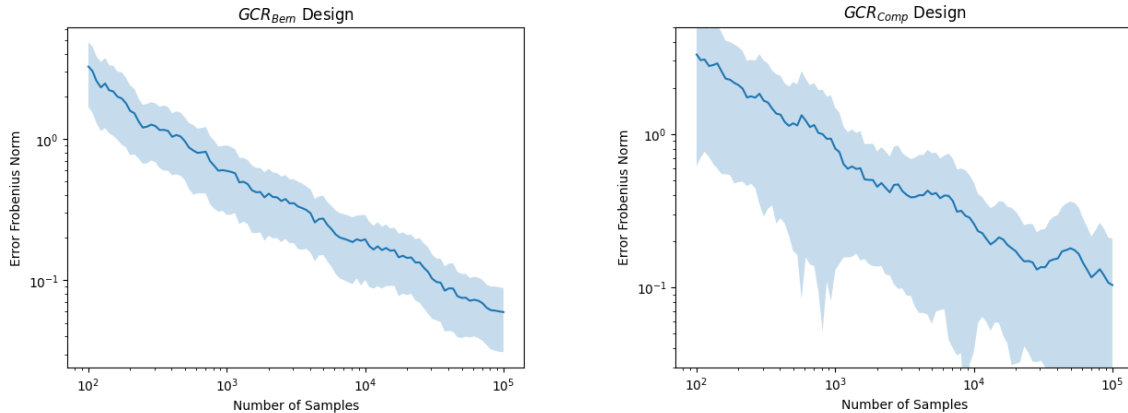
Throughout our work, we leverage analytic expressions for the design matrices to carry out our theoretical analysis. Here we demonstrate that these closed-form expressions are not necessary to use pseudoinverse estimation in practice. Rather, it is sufficient to have sampling access to the randomized designs, which we can leverage to construct Monte Carlo estimates of the necessary joint treatment probabilities. This insight will be crucial for analyzing more sophisticated randomized designs, such as the randomized GCR designs of Ugander and Yin [2023], where it is unclear whether the design matrix entries, let alone the entries of the pseudoinverse, have a tractable closed form.

Suppose that \mathcal{D} denotes the joint distribution over the treatment assignment vectors for a randomized design of interest. Then, given R independent samples $\mathbf{z}^1, \dots, \mathbf{z}^R \stackrel{iid}{\sim} \mathcal{D}$, and given any $S \subseteq [n]$, we may estimate

$$\Pr_{\mathcal{D}}(S \text{ fully treated}) \approx \frac{1}{R} \sum_{r=1}^R \prod_{j \in S} z_j^r.$$

The Law of Large Numbers ensures the convergence of these estimates as $R \rightarrow \infty$. By carrying out this process for each entry of each design matrix $\mathbb{E}[\tilde{\mathbf{z}}_i \tilde{\mathbf{z}}_i^T]$, we obtain an estimate matrix, which we may pseudoinvert numerically to obtain an approximation to our desired matrix.

The following plots demonstrate the convergence of this Monte Carlo estimation. Here, we consider both the GCR_{Bern} and GCR_{Comp} randomized designs on the Caltech Facebook friendship graph from Traud et al. [2012]. We use the METIS clustering with $m = 10$ clusters, and we set the marginal treatment probability to $p = 0.2$ (so we treat $k_c = 2$ cluster in the completely randomized design). The plots visualize the Frobenius norm of the error between the true design matrix pseudoinverse and the pseudoinverse calculated by the Monte Carlo procedure described above. We vary the number of samples R used for the Monte Carlo calculations. In both plots, the blue line depicts the average Frobenius norm across the 762 vertices, and the shading depicts the standard deviation. The axes of these plots use a logarithmic scale.



The plots demonstrate the decrease in approximation error as more samples are used in the Monte Carlo probability calculations. This suggests that with sufficient samples, these probabilities can be computed to an arbitrary precision. In the case of the completely randomized cluster design, the discrepancies in the error magnitude do not appear to be correlated with the vertices connected to all clusters (which corresponds to a discontinuity in the analytic pseudoinverse formulas).